

UNCLASSIFIED

---

AD 402 589

*Reproduced  
by the*

DEFENSE DOCUMENTATION CENTER

FOR

SCIENTIFIC AND TECHNICAL INFORMATION

CAMERON STATION, ALEXANDRIA, VIRGINIA



---

UNCLASSIFIED

NOTICE: When government or other drawings, specifications or other data are used for any purpose other than in connection with a definitely related government procurement operation, the U. S. Government thereby incurs no responsibility, nor any obligation whatsoever; and the fact that the Government may have formulated, furnished, or in any way supplied the said drawings, specifications, or other data is not to be regarded by implication or otherwise as in any manner licensing the holder or any other person or corporation, or conveying any rights or permission to manufacture, use or sell any patented invention that may in any way be related thereto.

AD 402589

FTD-TT-62-1423/1+2

## UNEDITED ROUGH DRAFT TRANSLATION

RADAR METHODS OF METEOROLOGICAL OBSERVATIONS

BY: V. S. Nelepets and V. D. Stepanenko

English Pages: 220

THIS TRANSLATION IS A RENDITION OF THE ORIGINAL FOREIGN TEXT WITHOUT ANY ANALYTICAL OR EDITORIAL COMMENT. STATEMENTS OR THEORIES ADVOCATED OR IMPLIED ARE THOSE OF THE SOURCE AND DO NOT NECESSARILY REFLECT THE POSITION OR OPINION OF THE FOREIGN TECHNOLOGY DIVISION.

PREPARED BY:

TRANSLATION SERVICES BRANCH  
FOREIGN TECHNOLOGY DIVISION  
WP-APB, OND.

FTD-TT-62-1423/1+2

Date 11 April 1963

V. S. Nelepets, V. D. Stepanenko

RADIOPOKATIONNYE METODY METEOROLOGICHESKIKH NABPYUDENIY

Gidrometeorologicheskoye Izdatel'stvo  
Leningrad - 1961

Pages: 1-175

FTD-62-1423/1+2



## TABLE OF CONTENTS

Abstract . . . . .	1
Foreword . . . . .	2
Chapter 1. Introduction . . . . .	3
1. Brief Information on the Development of Radar Observations in Meteorology . . . . .	3
2. Features and Advantages of Radar Observation Methods . . . . .	7
Chapter 2. Principles of Radar . . . . .	10
1. General Information . . . . .	10
2. Physical Characteristics and Preliminary Technical Data on Radar Systems . . . . .	12
3. Direction of Radiation and Reception of Electromagnetic Waves . . . . .	37
4. Radar Systems and Stations . . . . .	44
5. Quantitative Relations . . . . .	52
Chapter 3. Theory of Radar Detection of Meteorological Targets . . . . .	55
1. Radar Formula for Meteorological Targets . . . . .	55
2. Analysis of the Radar Formula for Meteorological Targets . . . . .	59
3. Effective Radar Scattering Area of Clouds and Precipitation . . . . .	61
4. Attenuation of Electromagnetic Waves . . . . .	69
5. Choice of Wavelength for Radars for Meteorological Purposes . . . . .	76
Chapter 4. Practice of Radar Detection of Atmospheric Formations . . . . .	88
1. Use of Radar for the Detection and Investigation of Cloudiness and Precipitation . . . . .	88
2. Radar Images and Their Physical Interpretation . . . . .	92
3. Errors in Radar Observations of Clouds and Precipitations . . . . .	103
4. Measurement of Intensity of Precipitation and Water Content of Clouds by Radar Methods . . . . .	114
5. Quantitative Estimate of the Water Content of Clouds and of Icing of Airplanes by Radar Methods . . . . .	125
6. Estimate of Turbulence by the Radar Methods . . . . .	145
7. Effectiveness of Detection of Cloudiness and Precipitation Zones by Radar Stations . . . . .	148
8. Radar Observations of Precipitation Zones from Artificial Satellites . . . . .	157

Chapter 5. Use of Radiotechnical Stations for Wind and Temperature Sounding of the Atmosphere . . . . .	162
1. Radio Direction Finding Method of Determining the Wind . . . . .	162
2. Radar Method of Determining the Wind Velocity and Direction . . . . .	167
3. Organization of Radio Direction Finding and Radar Wind Measurements . . . . .	173
4. Accuracy of Wind Measurement . . . . .	174
Chapter 6. Review of Radar Methods . . . . .	178
1. Determination of Distance . . . . .	178
2. Measurement of Angular Coordinates . . . . .	181
3. Methods of Scanning the Space . . . . .	184
4. Indication Methods and Indicator Systems. . . . .	186
Chapter 7. Radar Apparatus . . . . .	193
1. Interrogator-Responder Systems . . . . .	193
2. Radar Stations for Temperature-Wind Sounding . . . . .	198
3. Radar Station for the Observation of Precipitation Zones and Atmospheric Formations . . . . .	201
4. Auxiliary Equipment . . . . .	203
Conclusion . . . . .	207
References . . . . .	211

# ABSTRACT

The book deals with the use of radar methods in meteorology, some general problems in radar, the theory of radar sounding of atmospheric formations, and many practical problems in this field.

It is designed for workers in the meteorological service, can be used by teachers and students specializing in meteorology, and is also of certain interest to radio specialists who engage in the introduction of radar techniques into the national economy.

Best Available Copy

## FOREWORD

The use of radar techniques in meteorology has now become a firmly established daily practice, and the methods developed during the recent years continue to be improved, a fact contributed to the work by domestic and foreign scientists, and also work by practicing meteorologists. This circumstance has stimulated the authors in writing the present book.

The book is intended for a broad circle of meteorologists. The material is developed in it under the assumption that the reader has sufficient knowledge of both the general methods used to investigate the atmosphere and meteorological terminology. At the same time, to make full use of the material on radar measurement methods contained in the book, the authors deemed it useful to present the reader with information (in limited volume) on the principles of radar and the construction of radar stations used for meteorological measurements.

The work on the book was divided by the authors in the following manner. Chapter 1 and the conclusion were written by the authors jointly. Chapters 2, 6, and 7 were written by Candidate of Technical Sciences Lecturer V.S. Nelepets, while Chapters 3, 4, and 5 were written by Candidate of Physical-Mathematical Sciences Lecturer V.D. Step-  
anenko.

The bibliography for this book was essentially compiled by O.A. Nelepets of the cataloging division of the State Public Library imeni M.Ye. Saltykov-Shchedrin.

## Chapter 1

### INTRODUCTION

#### 1. BRIEF INFORMATION ON THE DEVELOPMENT OF RADAR OBSERVATIONS IN METEOROLOGY

The direct utilization of radar observation methods in meteorology was preceded by the introduction of radio technique into meteorological practice. The first instrument of this type was the radiosonde of P.A. Molchanov (1930).

The start of the use of radio methods in meteorological research began in 1932 with the work of M.A. Bonch-Bruyevich. In subsequent years methods were developed in the Pavlova (Slutsk) Observatory for the observation of the motion of radiosondes by using direction finders, and later, in 1943, the ground apparatus used for this purpose was a pulsed radar.

The difference in the use of a radio direction finder and a radar for the observation of a moving target lies essentially in the fact that the direction finder can respond only to radio signals produced by the target, whereas a radar transmits its own radio signals to the target. Consequently, in the latter case the target does not have to contain a radio transmitter, and consequently it is called a passive target, while for the radio direction finding method an active target with a transmitter is necessary.

An active target affords the possibility of using a method of all-inclusive sounding of the atmosphere, in which the signals of the transmitter are controlled by the receivers of the meteorological ele-

ments comprising the radiosonde (the target).

Further improvements in the target circuitry have led to the use of a system of so-called responders, which respond to inquiries from the ground installation. Technical data concerning these methods will be considered below.

During the course of development of radar before the second world war, relatively long radio waves were used. As the techniques improved, the wavelengths on which the radar stations operated became shorter; at the same time it became clear that radar signals are reflected not only by the so-called targets (airplanes, ships, etc.), but also by water drops and ice crystals suspended in the air. An analysis of extensive experimental material discovered, on the one hand, a connection between the propagation of the shortest radio waves and the meteorological conditions, something demonstrated in many works [39, 40], and disclosed on the other hand real capabilities of observing phenomena in the atmosphere with the aid of radar stations. This has handed the meteorologist a new and sufficiently perfected research method.

... The advantages of this method compared with analogous optical and acoustical methods are considered in Section 2 below. They are essentially manifest in the fact that the use of radar apparatus has greater operating flexibility. It is possible in any weather, during any time of the day or the year. The data obtained pertain to the instant of observation and can be directly determined by visual means. The latter provides the exceptional possibility of observing various processes in the atmosphere, and furthermore at any distance within a radius up to hundreds of Kilometers.

Without complicating the apparatus, it is possible to observe simultaneously several objects located in a single direction, within the confines of a certain sector or circle, in the center of which the

radar station is situated.

Specialized radars are used in meteorology to carry out the following observations: measurement of wind velocity and direction at high altitudes, detection of atmospheric fronts and regions with electric inhomogeneities of the atmosphere, and also detection and investigation of clouds and precipitation, turbulent and convective formations of the atmosphere; the latter investigation became possible after centimeter-wave and subsequently also millimeter-wave techniques were mastered. The coordinates, dimensions, shape, displacement direction and velocity, and also the tendency in the development of the observed precipitation regions are determined with accuracy adequate for practical purposes.

Investigations of the material obtained by radar observations of precipitation help to a considerable degree to clarify the mechanisms of their formation in various cloud shapes, which are at different stages of their development. In particular, the so-called thaw layer, the upper limit of which almost coincides with the zero-isotherm level, was detected; the influence of the solid phase on the formation of precipitation was determined; the main attributes distinguishing thunderstorms from showers were clarified, etc.

In synoptic practice, data from the radio stations help make more precise the position of atmospheric fronts, their direction of motion, their rate of displacement, and their development tendency, by detecting the precipitation zones connected with these fronts.

Recently there have been developed radar stations capable of detecting not only precipitation but also clouds and dielectric inhomogeneities in the atmosphere in the form of inversions and convective and turbulent formations. These stations operate on wavelengths from 3 cm to several millimeters. They are frequently called cloud meters.

since they make it possible to determine the heights of the cloud layers. If quantitative methods are used to measure the power of the reflected signals, these stations make it also possible to determine the water content and the distribution of the drops in the clouds.

Together with development of qualitative observations, investigations were made on the possibility of quantitative remote measurements of rain intensity. Special surface and airborne stations were developed for the observation of precipitation zones.

Radar observations and measurements turned out to be quite valuable in the study of the radiowave propagation conditions, and also for the development of the theory of their scattering and absorption.

At the present time there exist in the USSR and other countries, along with points for temperature and wind sounding of the atmosphere, also radar points for storm forecasting and warning. These points are equipped with standard radar stations, specially adapted for better use in meteorology.

According to data in the foreign press, the use of radar methods for the meteorological service has greatly expanded in recent years; in particular, a project has been proposed [46] to equip 35 meteorological stations with radars for the observation of precipitation within a radius of several times ten kilometers and for the observations of clouds; millimeter-band radars are used for this purpose. The USA Weather Bureau had in 1954 22 radars for meteorological purposes [47], and a doubling of this network was planned for the nearest future.

Radar posts for storm warning are operated also by the Tactical Air Command of the US Air Force [49]. According to the literature sources [52], the US Air Force has radars which can detect storms at distances exceeding 600 km.

Many US companies, for example Raytheon [48], Bendix [50], and



also the British firm Marconi [54] have built radar stations specially developed for use in meteorology. The British firm Decca constructed a radar for the detection of storm fronts [54].

Recently the first station in a special network of hurricane-warning stations was constructed in the British territories in Africa [51]. It was planned to construct in Australia [53] 15 radars for meteorological services.

In the USSR there is also much work done on the introduction of perfected radar apparatus into the practice of meteorological and aerological observations.

## 2. FEATURES AND ADVANTAGES OF RADAR OBSERVATION METHODS

The rapid development and introduction of radar methods into the practice of meteorological and aerological observations are due to the following reasons:

- 1) the observation range and the volumes of space covered by the radar station are much larger than the visible range and volumes;

- 2) the time required to obtain the over-all pattern of the distribution of observed meteorological objects within the operating radius of the radar is very short and does not exceed several times ten seconds;

- 3) within the operating range of the station one can obtain both horizontal and vertical sections through the atmosphere;

- 4) during a prolonged time it is possible to carry out continuous observations and measurements of the characteristics of meteorological objects, including thunderstorm and shower regions; flights in modern aircraft under such conditions are either impossible or very dangerous;

- 5) radar observations and measurements can be carried out during any time of the day, since they do not depend on the visibility conditions, which limit the use of optical instruments;

6) radar measurements of the characteristics of atmospheric formations such as the intensity of precipitation, water content of the clouds, distribution of drop dimensions and crystal dimensions, and also turbulence and inversion layers do not disturb the natural state of the fields of these characteristics, as would occur in the case of airplane, balloon, or radio sounding.

Actually, ordinary meteorological and aerological instruments make it possible to carry out observations and measurements in small volumes compared with all of space. As a result the general pattern of the atmospheric processes can be obtained only from data of a large number of observations and measurements, carried out at many points. Even when the organization of these observations is highly perfected, immediate acquisition of some data over appreciable regions is practically impossible, since time must be consumed in their gathering and processing. Yet in meteorological service the time factor is frequently exceedingly important, and the timely acquisition of at least the general picture of the phenomenon can be much more valuable than delayed but very precise and detailed information.

Radar methods are particularly valuable in shore regions under conditions when ordinary meteorological and aerological data above the sea and above unilluminated regions of the dry land are missing.

Of great significance is the remote character of the measurement of microphysical characteristics of precipitation and clouds of different shapes. It is further expanded by the possibility of carrying out continuous registration of the measurement results, which make it possible to determine from a single point the space-time variation of these meteorological characteristics with such detail as would be inaccessible to any of the existing aerological methods.

Knowledge of these characteristics is essential not only for re-

liable forecasting of clouds and the phenomena associated with them, but also for exerting positive action on them.

Finally, the use of radar stations has made it possible to determine with accuracy sufficient for practical purposes the velocity and direction of wind in the free atmosphere under all weather conditions, day and night, and to much greater altitudes than in the case of optical theodolite observations of a pilot balloon.

## Chapter 2

### PRINCIPLES OF RADAR

#### 1. GENERAL INFORMATION

The processes occurring during the use of radar consist of transmission by the radio antenna of electromagnetic energy in the form of radio waves in some direction. These radio waves reach a certain object (target) from which they are reflected. In most cases the reflected energy propagates from the object also in all directions in the form of radio waves. Some part, usually very small, of the energy initially radiated by the antenna of the radio station returns to the antenna and can be detected with a receiver. This process is accompanied by measurement of the direction and of the time.

In the simplest case one determines the direction in which the antenna radiated the electromagnetic energy or, what is the same, the direction of the object (target) reflecting the radio waves. Thus, the position of the radius vector OM is established in three-dimensional space (Fig. 1). The length of OM is determined by measuring the time consumed by the radio waves in covering this distance. Knowing the radiowave propagation velocity  $c$ , it is easy to determine the distance R from the relation

$$R = ct/2,$$

where  $t$  is the time.

Inasmuch as the time is measured between the instant of radiation of energy from the antenna and the instant of return of the reflected energy, i.e., the time consumed in covering the distance 2R is meas-

ured, the time employed in this equation is  $t/2$ .

Thus, radar is based on the use of reflection of radio waves from the observed objects.

The determination of the spatial coordinates of an object is carried out in the following manner:

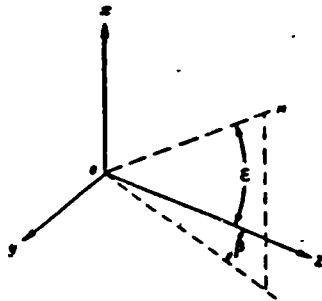


Fig. 1. Three-dimensional system for the determination of the coordinates of a point M in space.

- a) distance – by measuring the time,
- b) angular coordinates – by using directional transmission and reception of the radio waves.

All radar methods are divided into two principal classes:

- 1) systems with continuous transmission,
- 2) systems with pulsed transmission.

The characteristic features of these systems are considered in Section 4.

All radar systems can be divided into one-position and two-position types.

The first type includes systems in which one and the same antenna or two approximated antennas are used for transmission and reception. Two-position systems are those in which the antennas are separated by considerable distances; interest in such systems has increased considerably in recent times.

The use of two-position and multiposition systems in the meteorological services uncovers the prospects of creating a single radar transmitter in the center of the observation system and many (several) peripheral radar receivers, each of which carries out all-inclusive reception of the reflected signals in its own sector. In such a system it is possible to carry out specialized observation, in which some radar receivers observe the running development of various meteorolog-

ical processes influencing the weather forecasting, whereas others, belonging for example to specialized meteorological stations, carry out the functions of storm warning.

Such a system is above all economical. The only technical difficulty in this system (using pulsed transmission) is the synchronization of the receiver operation with the transmitter equipment. To effect such synchronization it is possible to transmit from the central transmitting station, in addition to the sounding pulses, also timing synchronizing signals, as is done in television systems.

## 2. PHYSICAL CHARACTERISTICS AND PRELIMINARY TECHNICAL DATA ON RADAR SYSTEMS

Radar technology employs a wide range of wavelengths (frequencies), which encompasses in accordance with the existing classification (Table 1) meter, decimeter, centimeter, and millimeter waves, or short and ultrashort wave bands.

The concept of wavelike propagation of electromagnetic energy is connected with the notion of an alternating electromagnetic field. This field (as well as other fields of the same type) is determined in accordance with modern science as an objective reality, as a special form of matter, and is included along with gravitational, meson, and other fields in the class of physical fields.

The electromagnetic field is the intermediary effecting interaction between charged bodies (electric charges) located a certain distance from each other in space.

The space in which the radio waves are propagated can be regarded as a medium having complicated properties; this medium is at the same time a conductor and a dielectric. It has the following properties: conductivity  $\sigma'$ , dielectric constant  $\epsilon'$ , and magnetic permeability  $\mu'$ .

Under the influence of the electric field component  $E$ , complicated

TABLE 1

1. Диапазон радиоволн	2. Длина волны $\lambda$	3. Частота $f$
4. Длинные . . . . .	30 000—3 000 м	10—100 кГц 14
5. Средние . . . . .	3 000—200 м	100—1 500 кГц
6. Промежуточные . . . . .	200—50 м	500—6 000 кГц
7. Короткие . . . . .	50—10 м	6—30 мГц 15
8. Ультракороткие . . . . .	13. короче 10 м	
9. Метровые . . . . .	10—1 м	30—300 мГц
10. Дециметровые . . . . .	100—10 см	300—3 000 мГц
11. Сантиметровые . . . . .	10—1 см	3 000—30 000 мГц
12. Миллиметровые . . . . .	10—1 мм	3·10 <sup>10</sup> —3·10 <sup>11</sup> ц 16

1) Radio band; 2) wavelength; 3) frequency; 4) long; 5) medium; 6) intermediate; 7) short; 8) ultrashort; 9) meter; 10) decimeter; 11) centimeter; 12) millimeter; 13) shorter than; 14) kilocycles; 15) megacycles; 16) cps.

motion of electricity takes place in such a medium; namely the motion of free charges produces a conduction current  $J_{pr}$  and the displacement of bound charges forms the displacement current  $J_{sm}$ . As will be shown below, the quantitative relationship between these currents in space is determined by the properties of the medium.

The total current density in each volume of the medium can be represented by the expression

$$J = E\sigma' + \frac{E}{4\pi} \frac{dE}{dt}.$$

From the physical point of view, the simplest type of electromagnetic field can be represented as a combination of its electric component  $E$  and the magnetic component  $H$ , which vary harmonically in time and which are related by the following equation:

$$\frac{E}{H} = \sqrt{\frac{\mu}{\epsilon}}.$$

This quantity is called the equivalent (characteristic) impedance of free space and is denoted  $Z_0$ .

The possibility of determining the field intensity  $E$  in the atmosphere by measurements with the aid of spheres, probes, etc. was first pointed out by the inventor of radio, A.S. Popov [16], as long ago as in 1902.

If the electric field component  $E$  varies sinusoidally, the conduction current is in phase with it, while the displacement is shifted  $90^\circ$  in phase. The higher the frequency of the field (the shorter the wavelength) and the smaller the conductivity  $\sigma'$ , the more the displacement current exceeds the conduction current.

The general premises pertaining to the physical and mathematical interpretation of the problems considered here are discussed in the scientific literature (for example, [32]), while special problems on reflection are given in the work of Academician V.A. Fok [15]. We present below information on the propagation of electromagnetic energy as applied to the topic under consideration.

From the quantitative point of view, all the properties of the electromagnetic field (we are referring to the macroscopic field) are uniquely determined by classical electrodynamics with the aid of Maxwell's system of equations. These equations simplify the treatment of some of the problems touched upon in this book, and we therefore present them here (in canonical form):

$$\operatorname{rot} H = \frac{1}{c} \frac{\partial D}{\partial t} + \frac{4\pi}{c} J, \quad (\text{I})$$

$$\operatorname{rot} E = -\frac{1}{c} \frac{\partial B}{\partial t}, \quad (\text{II})$$

$$\operatorname{div} D = 4\pi\rho, \quad (\text{III})$$

$$\operatorname{div} B = 0, \quad (\text{IV})$$

with

$$\left. \begin{array}{l} D = \epsilon' E \\ B = \mu' H \end{array} \right\} \quad (\text{V})$$

Here the vectors  $E$  and  $D$  characterize the electric field, while the vectors  $H$  and  $B$  characterize the magnetic field. The sources that excite the field are characterized by the density of the free electric charge  $\rho$  and by the current density  $J$ , as shown above. Equations (I) and (III) contain in the right half the quantities  $J$  and  $\rho$ , and this



emphasizes the connection between the field sources and the field characterized by the vectors H and D which are contained in the left halves of these equations.

Examining Eqs. (I) and (II) simultaneously, we verify that an alternating magnetic field causes the appearance of an alternating electric field, which in turn generates an alternating magnetic field. A continuous series of energy transformations takes place, in which the energy changes from one form to another. It is important to take it into account here that in such transitions the magnetic energy is produced not only in the place where the electric field generating it was located hitherto, but also somewhat in advance of this place, so that the energy, on changing from one form into another, propagates in addition around the place where the field is perturbed, in the form of a traveling wave moving in space.

The Maxwell equations presented above in vector form can be represented in differential form.

We break up the equations into the following three groups.

The first group shows the connection between the magnetic field intensity at some point of the medium and the current density at this point [similar to Eq. (I) given above]:

$$\frac{4\pi E_x}{\rho} + \epsilon \frac{dE_x}{dt} = \frac{\partial H_z}{\partial y} + \frac{\partial H_y}{\partial z},$$

$$\frac{4\pi E_y}{\rho} + \epsilon \frac{dE_y}{dt} = \frac{\partial H_x}{\partial z} - \frac{\partial H_z}{\partial x},$$

$$\frac{4\pi E_z}{\rho} + \epsilon \frac{dE_z}{dt} = \frac{\partial H_y}{\partial x} - \frac{\partial H_x}{\partial y}.$$

The second group in conjunction with the first indicates, like the foregoing simultaneous examination of Eqs. (I) and (II), the connection between the electric and magnetic forces, from which it fol-

laws that any time variation of the magnetic component generates a variation of the electric component:

$$\mu \frac{dH_x}{dt} = \frac{\partial E_y}{\partial z} - \frac{\partial E_z}{\partial y},$$

$$\mu \frac{dH_y}{dt} = \frac{\partial E_z}{\partial x} - \frac{\partial E_x}{\partial z},$$

$$\mu \frac{dH_z}{dt} = \frac{\partial E_x}{\partial y} - \frac{\partial E_y}{\partial x}.$$

The third group includes the so-called continuity equations, which express the idea that the increase in the number of force lines contained in some volume bounded by a closed surface is equal to the increase in the number of force lines leaving this volume:

$$\frac{\partial H_x}{\partial x} + \frac{\partial H_y}{\partial y} + \frac{\partial H_z}{\partial z} = 0,$$

$$\frac{\partial E_x}{\partial x} + \frac{\partial E_y}{\partial y} + \frac{\partial E_z}{\partial z} = 0.$$

Since the use of the field essentially reduces to the extraction of certain energy from the field, distributed over a volume V where the given field acts, one can speak of a volume density, which is expressed by the volume integral

$$W = \frac{1}{8\pi} \int_V (\epsilon E^2 + \mu H^2) dV.$$

The variations of the energy W can occur either inside the volume V, for example, in the form of transition to some other form of energy, say heat (this includes in practice the case of energy dissipation in the medium or in the inclusions suspended in it), or outside the volume V by flow out of the given volume, with conservation of its electromagnetic form.

In the former case the energy converted into a different form per unit time forms the loss power

$$P_s = \int_V j E dV,$$

which is expressed in watts.

In the latter case useful radiation power is produced.

If we imagine a certain surface  $a$ , bounding the volume under consideration, then at each instant for each square centimeter of the surface there will exist a definite power flux  $S$ ; it can be expressed in Gaussian units in terms of ergs per second per square centimeter. It is obvious that the product of this flux by the area of the surface  $a$  under consideration expresses the power passing at each instant of time through the entire surface  $a$ , with  $S$  being a vector quantity determined quantitatively in the following manner:

$$\oint S da = - \frac{\partial}{\partial t} \frac{1}{8\pi} \int (\mu H^2 + \epsilon E^2) dV,$$

which yields ultimately

$$S_0 = \frac{c}{4\pi} [EH].$$

The vector  $S_0$  is called the Umov-Poynting vector. Its value changes with change in the vectors  $E$  and  $H$ , and when the latter have their maximum positive or negative values, the vector  $S_0$  has a maximum; it is equal to zero when  $E$  and  $H$  are equal to zero.

The flux of electromagnetic energy (the amount of energy flowing per unit time through a unit surface perpendicular to the direction of the flux) is expressed with the aid of the Umov-Poynting vector both in magnitude and in direction. The direction of the Umov-Poynting vector is perpendicular to the hypothetical plane that can be drawn through the vectors  $E$  and  $H$ . The length of the vector  $S_0$  is proportional in the graphic representation to the energy flux density.

The velocity of propagation of radio waves of any length depends on the properties of the media in which they propagate. In a space that has no conductivity  $\sigma'$ , the propagation velocity  $c$  is determined from the expression

$$c = \frac{1}{\sqrt{\epsilon \mu}}.$$

In most practical cases the propagation velocity is assumed to be  $c = 300,000 \text{ km/sec.}$

It is known that in free space the propagation velocity is  $2.99796 \cdot 10^8 \text{ m/sec.}$  In order to increase the accuracy with which distances are determined by measuring time, it is necessary to introduce a correction for the refractive index  $n$  as a function of the meteorological conditions.

For radio waves in the band employed for radar, the refractive index  $n$ , which depends on the density and humidity of the atmosphere, can be determined from the following expression:

$$n = \frac{80}{T} \left( p + \frac{4800e}{T} \right) 10^{-6} + 1;$$

where  $p$  is the atmospheric pressure in millibars,  $e$  is the partial pressure of water vapor in millibars, and  $T$  is the absolute temperature.

According to Yamada [57], the refractive index  $n$  of the atmosphere changes with the altitude. Inasmuch as the refractive index decreases with increasing altitude, it is necessary, if appreciable altitudes are used, to determine the curvature of the path of the waves resulting from the influence of the gradient of the refractive index in a vertical direction. The net result is that the radiowave propagation velocity becomes larger with increasing altitude.

According to the classical theory of electromagnetic phenomena, the radiowave propagation velocity does not depend on the wavelength, but the conditions under which radio waves of different length propagate are different.

As they propagate in the space surrounding the earth, electromagnetic waves can be reflected, refracted, and diffracted. Depending on

the character of the propagation, a distinction is made between radio waves which bend around the concave surface of the earth as they propagate and are called ground (or surface) waves, and space (or sky) waves, which propagate linearly around the earth's sphere as a result of single or multiple reflection from the upper layers of the atmosphere — the ionosphere.

Diffraction is a term applied to bending of propagating radio waves around obstacles which have dimensions commensurate with the wavelength. Because of diffraction, the surface waves, starting with the longest waves of the short-wave band (and longer ones), can propagate over distances of hundreds of kilometers.

An important role was played in the development of the theory of diffraction by Soviet scientists. These include primarily the works of Academician V.A. Fok, and also of the Corresponding Members of the USSR Academy of Sciences A.A. Pistol'kors and Ya.N. Fel'd.

An interesting book on diffraction as applied to radar was written by J.R. Mentser [78], who solved several specific problems both rigorously and by approximate methods. In connection with the equation for the maximum radar range, which we present below (in Section 5), Mentser shows that for a single-position system this equation relates the maximum range with the scattering properties of radar targets, which are completely characterized by a quantity  $\sigma$ , called the effective reflecting surface of the target, or the radar cross section. Quantitatively this quantity is defined by the expression

$$\sigma = \lim_{R \rightarrow \infty} 4\pi R^2 \left| \frac{W_r}{W_i} \right|,$$

where  $W_r$  is the flux density of the power dissipated in space, and  $W_i$  is the power flux density of the field of the incoming plane wave.

The quantity  $\sigma$  defined with the aid of the last expression is pro-

portional to the power dissipated per unit solid angle divided by the power incident on a unit area. For a single-position system  $\sigma$  is a function of the position of the receiving-transmitting antenna relative to the target, inasmuch as the radar cross section has different values for different polarization planes of the incident wave.

Waves shorter than 10 meters are subject to atmospheric refraction, which is manifest in the deflection of the beam of radio waves propagating in the lower layers of the atmosphere from straight-line propagation. The latter circumstance can give rise to errors in radar measurements. Fennin and Jen [64] investigated errors of this type, due to atmospheric refraction (the daily variation of the refraction index).

Of considerable interest is the propagation of radio waves (predominantly the shortest ones) in the troposphere. As is well known, the dielectric constant of air in the troposphere is not constant, and this gives rise to inhomogeneities. Such inhomogeneities are due to variations in the temperature and humidity, and under the influence of the underlying surface and the earth's gravitation these inhomogeneities acquire a stratified character, which in turn creates conditions for considerable reflection and scattering of radio waves.

The observed variability of the dielectric constant of the troposphere, as shown by Wheelon [46], influences the propagation of the radio waves. To an equal degree, the attenuation and fluctuations influence the propagation of millimeter waves, according to Tolbert and Strepton [56].

Problems involving the propagation of radio waves in the troposphere were the subject of many papers in a scientific conference held in Moscow in January 1957 [12] concerning problems of long-distance propagation of radio waves, as well as individual works of domestic

and foreign authors. Thus, V.N. Troitskiy [13] has shown that quantitative connections exist between the increase in the dielectric constant of air within the confines of the inhomogeneity and the increase in the humidity and in the temperature. Kitchen and Richmond [58] considered the question of tropospheric scattering of radio waves by a troposphere containing inhomogeneities. Scattering of radio waves in the troposphere (the Booker and Gordon theory of 1950) is the subject of a paper by W. Gordon [60].

A quantitative determination of the dependence of the field on the altitude in tropospheric propagation of meter waves was made by Sexton, Kreylsheymer, and Laskomb [59] using telemetering apparatus raised by a balloon under anticyclone conditions with pronounced temperature inversion. It was observed that as altitude varied from 15 to 180 meters, the field variation was within 10 db. At altitudes above 60 meters, the correlation between the fading of the field at high altitude and at the surface of the earth disappears.

The already mentioned reflection of radio waves can be connected with multiple scattering within a volume having a large number of scattering inhomogeneities. D.M. Vysokovskiy [2] made an approximate estimate of the influence of multiple scattering in diffuse propagation of radio waves in the troposphere. The results of this investigation show that the energy scattered in one meter of path amounts to  $3.5 \cdot 10^{-9}$  of the incident energy. Say for a path 300 km long, the energy scattered at a wavelength  $\lambda = 10$  cm may reach 25% of the initial (incident) energy. Consequently, one can hardly neglect the attenuation of the direct wave due to multiple scattering occurring in the troposphere.

If temperature inversion exists and with it a sharp decrease in the water-vapor pressure, then conditions are created for super refraction of radio waves. The latter is manifest in such a bending of the

radio beam trajectory, at which this bending is equal (or almost equal) to the curvature of the earth's surface; because of super refraction, the radio waves propagate in parallel to the earth's surface. Under these conditions, owing to the already noted layered structure of the atmosphere there are formed up to altitudes of several times ten meters so-called atmospheric wave ducts, and under such circumstances the range of propagation of ultrashort waves can in individual cases reach 2000 km and more.

Favorable conditions for the formation of the atmospheric wave-ducts occur when the upper layers of the atmosphere are exceedingly dry and warm. Because of this, the density of the upper layers decreases, and at the same time the refractive index  $n$  decreases, and consequently anomalous propagation effects are produced.

The normal range of a radar extends to the horizon and consequently depends on the height  $h_a$  of the antenna. The distance to the horizon is equal to

$$D_{\text{km}} = 3,58 \sqrt{h_a \text{ m.}}$$

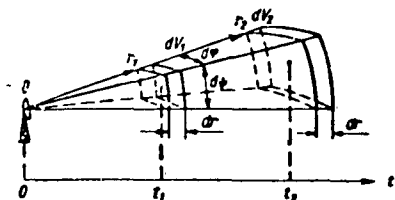


Fig. 2. Decrease in intensity of electromagnetic field with increasing distance from the point  $o$ .

However, anomalous propagation of radio waves makes it possible for the radar to "see" much farther. For example, at a wavelength  $\lambda = 10$  cm, when the direct visibility range is about 70 km, it is possible to detect by radar over distances exceeding 250 km. Such cases are frequently described in the literature. For example,

a radar in Bombay, located at an altitude  $h_a = 80$  meters, had a normal range of 34 km, while during the hot season the range increases to 320 and sometimes to even 1120 km. A. Klement [41] cites an example wherein this effect was used on the shore of England. A shore radar station of



the type AN/MPQ-1 operating on  $\lambda = 3$  cm with a normal range of 25 km detected ships at sea at distances up to 96 km. A method for calculating the transmission of radio waves in the atmospheric waveguide is given in a paper by Macfarlane [71], which compares the results obtained with the experimental data.

The intensity of electromagnetic energy is determined quantitatively by the intensity of the electric field of the wave  $E$  and is given in volts per meter, while when expressed in terms of power  $P_\Sigma$  it is given in watts.

Any propagation of radio waves in space is accompanied by a decrease in the propagating energy density (a decrease in intensity) from point to point in space, reminiscent of attenuation. We must understand here, however, not some loss of energy, but only its spatial distribution, as a result of which the field intensity decreases. This decrease is in inverse proportion to the distance, something that can be explained in the following manner.

Assume that a source producing the radiation field is located at the point  $O$  (Fig. 2). At constant propagation velocity  $c$ , the energy  $W$  is transported within a time  $t_1$  over a distance  $r_1$ , where the element  $dV_1$  of the radiation field will occupy a certain volume. In determining the latter, in view of the small values of the angles  $\varphi$  and  $\psi$ , we replace the sine by its argument, and obtain

$$dV_1 = r_1 d\varphi r_1 d\psi dr = r_1^2 d\varphi d\psi dr.$$

Quantitatively the field energy in this volume will be

$$dW_1 = E_1^2 r_1^2 d\varphi d\psi dr.$$

Obviously by the instant of time  $t_2$  the radiation field moves further, to a distance  $r_2$ , where the element of the radiation field occupies a volume  $dV_2$ . The field energy assumes here the value

$$dW_2 = E_2^2 r_2^2 d\varphi d\psi dr.$$

Assuming that the space between the volume elements  $dV_1$  and  $dV_2$  does not contain any media in which energy can be lost, we can put

$$dW_2 = dW_1,$$

from which it follows that

$$E_2/E_1 = r_1/r_2.$$

The intensity of the electromagnetic field of the radiation decreases in proportion to the first power of the distance from the source O. The field energy per unit volume (just as in the case, for example, of propagation of light oscillations), decreases in proportion to the square of the distance from the given point of space to the radiation source.

In addition to the cause indicated above for the decrease in the field intensity with distance, under natural conditions there is also attenuation (weakening) of the intensity in the atmosphere. This is caused by absorption and dissipation of energy [14], occurring during the propagation. These phenomena are caused by the composition of the atmosphere and by the inclusions suspended in it, for example hydrometeors.

In the general case the absorption  $\alpha$  of electromagnetic waves propagating in a humid medium, expressed in decibels, is approximately equal to

$$\alpha = 0.3Q/\lambda^2,$$

where  $Q$  is the rate of precipitation in millimeters per hour, and  $\lambda$  is the wavelength in meters.

Compared with the longer waves, radio waves in the centimeter and particularly the millimeter band are subject to large absorption. This absorption is made up of molecular absorption by the oxygen and water vapor contained in the medium and of absorption and reflection by hydrometeor elements, predominantly drops of water.

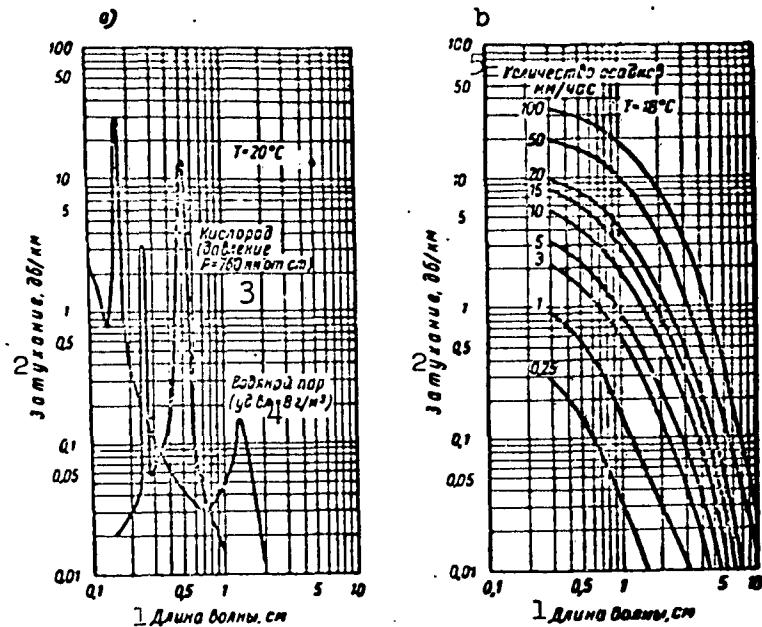


Fig. 3. Dependence of the attenuation of radio waves in the centimeter band on the wavelength, due to the influence of oxygen in air and water vapor (a), and also due to absorption in rain of varying intensity (b). 1) Wavelength, cm; 2) attenuation, db/km; 3) oxygen (pressure  $p = 760$  mm Hg); 4) water vapor (specific humidity =  $8 \text{ g/m}^3$ ); 5) amount of precipitation, mm/hr.

The quantitative influence of these factors [43] is illustrated by Fig. 3, which shows the damping of radio waves of the centimeter band under the influence of the oxygen in the air and water vapor, and also absorption in rain of varying intensity.

For the band under consideration, the variation of the attenuation [44] as a function of wavelength, expressed in decibels per kilometer, is shown in Table 2.

TABLE 2

$\lambda$ cm	1	2	3	4	5	6	8	10
$\alpha$	0,20	0,075	0,032	0,014	0,007	0,0034	0,001	0,003

Decimeter, centimeter, and millimeter waves are subject to scattering as a result of the inhomogeneity of the troposphere as the

propagation medium. Waves up to 1.5 cm are absorbed more in summer than in winter, while the opposite holds for longer waves.

The question of attenuation (joint scattering and absorption) of centimeter waves in gases, and also by liquid and solid particles contained in the atmosphere, was considered in sufficient detail by J. Ryde [75]. The author of the article characterizes the attenuation, in decibels per kilometer of path, by the following expression:

$$4,343 \cdot 10^3 N \left( \frac{\pi D^2}{4} \right) f_a \left( \frac{D}{\lambda} : M \right),$$

where  $N$  is the number of drops per cubic centimeter of air,  $D$  the drop diameter,  $f_a$  a function of  $D/\lambda$  and  $M$  as the ratio of the energy absorbed and scattered by one drop to the energy of the wave front per area of the drop projection; for the interval  $0.005 < D/\lambda < 1$  the function  $f_a$  ranges between 0.001 and 5.  $M$  is a parameter determined by the coefficient of refraction and by the coefficient of absorption.

Ryde believes that the intensity of a parallel beam crossing an absorbing and scattering medium decreases exponentially. The article makes use of the law of random distribution of the scattering particles, so that the electromagnetic energy radiation scattered by these particles is assumed to be perfectly noncoherent.

Analyzing the question of the intensity of the reflected signal, Ryde defines in his paper the equivalent reflecting surface of the target as the projection of an ideally reflecting sphere, and gives for an equivalent surface in the form of a gale an expression

$$A = 0,9 \tau^2 \theta^2 N S \cdot 10^3 \varphi \text{ m}^2,$$

where  $\tau$  is the duration of the pulse in  $\mu\text{sec}$ ,  $r$  the distance to the gale in km,  $\theta$  the aperture angle of the directivity pattern (in terms of power) in degrees,  $N$  the number of drops in one cubic centimeter,  $S$  the scattering function of a single drop,  $\varphi$  part of the wave-front en-

energy incident on the front of the gale, and  $\psi$  a coefficient which takes into account the attenuation in the gale itself. Averaged values are used for  $NS$ ,  $\varphi$  and  $\psi$ .

The factors considered here, which cause attenuation of the electromagnetic field in space, depend on the properties of the medium in which the electromagnetic energy propagates. In the case of radar these factors influence the intensity twice, when the sounding pulse travels from the radar antenna to the target and then when the energy reflected from the target returns to the radar antenna.

There are reasons for the attenuation of the received signals, depending on the laws governing the propagation of the electromagnetic energy and the structure of the radiowave field. These include, for example, changes in the polarization of the radio waves.

It is known that electromagnetic waves have two components, electric and magnetic. When the radio waves propagate in free space, these components are in mutually perpendicular planes, and the vectors  $E$  and  $H$  of the electric and magnetic components, respectively, are perpendicular to the direction of motion of the wave. The polarization plane of the wave is defined as the plane passing through the vector  $E$  in the direction of motion of the wave.

The influence of polarization on the reception strength was investigated by many researchers, and the results obtained can be found in the book by V.N. Kessenikh [25]. An interesting study as applied to radar problems was carried out by W. Sharpless [74] who carried out investigations at a wavelength  $\lambda = 3$  cm. The author of the article observed the propagation of the waves under normal and anomalous conditions and made a comparison of vertically and horizontally polarized waves. He observed a decrease in the intensity of the signal by more than 20 db, and showed that there is no essential difference in the

propagation conditions of vertically and horizontally polarized waves. In addition, it was established that antennas that have sharper directivity ensure smaller fading of the received reflected signals.

In the general case polarization manifests itself as follows: if the position of a linear receiving antenna in space is such that its axis coincides with the direction of the vector of the electric component  $E$  of the radio wave, then, other conditions being equal, maximum reception takes place. During the process of radiowave propagation (in particular the shortest waves), under certain conditions a change takes place in the position of their polarization plane under the influence of various factors, which include the existence of two or more beams in the plane, and their plane of polarization rotates with different velocities. Inasmuch as the components of such a wave are not mutually parallel in individual points of space along the direction of the propagation of the wave, their interaction occurs at various angles. Under these conditions, owing to the interference, the resultant vector describes a circle or an ellipse, and thus electromagnetic fields are produced in space with circular or elliptical polarization.

During the time of magnetic storms [34], rapid rotations of the plane of the polarization are possible and are caused by strong changes in the earth's magnetic field. Changes in the plane of polarization influence the intensity of the received signals.

Losses in free space, in the case of variable microwave-frequency fields, are due to the fact that the polar molecules\* of the substance (in this case the gas) attempt to follow the variations of the field. Opposing this motion are the forces of mutual attraction between the molecules, so that such motion lags behind the variations of the electric high-frequency fields, and this is manifest in the occurrence of energy losses in the substance.

However, the process of radio-wave propagation is accompanied not only by energy losses. Let us imagine two regions in space with different values of the parameters  $\epsilon'$  and  $\mu'$ ; this case corresponds to different values of the radio-wave propagation velocity in these two media. If the front of the radio wave during the course of its displacement encloses in part (not with the entire front) a region with different values of  $\epsilon'$  and  $\mu'$  than the values of these parameters for the remaining portion of the front of the wave, then the portion of the wave front under consideration will propagate more rapidly (or more slowly) than the remaining portions. The result will be a change in the front position and, as a consequence, a change in the direction of motion of the electromagnetic energy in space.

When we mentioned above the properties of the electromagnetic field in connection with Maxwell's system of equations (Eq. V) we noted that the vectors  $D$  and  $B$ , and also the current density  $J$ , depend on the properties of the medium (on the values of  $\epsilon'$ ,  $\mu'$ , and  $\sigma'$ ). In their propagation, the electromagnetic waves may encounter on their path regions (volumes of space) which have not only smooth but also abrupt changes in the values of these parameters, and in particular one observes an abrupt change in the dielectric constant  $\epsilon'$ , which gives rise to reflection of the electromagnetic energy from the boundary of the media.

A. Stickland showed in his paper [72] that a change in the dielectric constant  $\epsilon$  by merely about  $10^{-5}$  is sufficient for the occurrence of the reflection effect. Such conditions can be observed when the water vapor pressure changes abruptly by 1 mb, something possible when the relative humidity changes by 45% under conditions of a temperature inversion of  $2^{\circ}$ .

As follows from the foregoing equations of the electromagnetic

field, a change in the parameters of the medium gives rise to a redistribution of the balance of energy between the electric and magnetic components of the field. It must be noted, however, that such a redistribution on passing through the aforementioned boundary between two media cannot be effected at the expense of adding energy from the medium to the energy of the wave, but is the result only of the reflection of part of the incoming (incident) energy. This explains, in particular, the possibility of radar detection of dielectric inhomogeneities of the atmosphere and in other meteorological objects.

In radar location of single and group targets (airplanes, ships, etc.), there are methods for calculating [28] the reflecting properties of such objects, which make it possible to establish with some degree of accuracy the effective reflection areas; there are unified data for the simplest reflectors.

The similar problem for radar objects of meteorological character is made difficult by the fact that an account of the reflecting properties of such objects must include a large number of components, many of which cannot be established for each case with satisfactory accuracy. In calculations of this kind one must take into consideration, for example, such quantities as the mean effective area of the drop and the number of drops per unit volume, and also the dielectric constant of the medium and the coefficient of energy absorption at a given frequency. The last two parameters vary over a wide range. As was shown by J. Sexton [59], who carried out measurements at wavelengths  $\lambda = 1.6, 3.2, \text{ and } 9 \text{ cm}$ , the dielectric constant varies from  $1.0051 \pm 0.0001$  to  $1.0056 \pm 0.00005$  as compared with the static value  $1.00587$ . The foregoing makes it difficult to establish unified values for the effective area of meteorological objects.

Let us become acquainted with general considerations pertaining



to the effect of reflection.

The majority of ordinary radar targets are metallic surfaces, for example airplanes, ships, etc. In this case the surface of the object behaves for the incident wave like a dissipative medium, which lets the field of the incident wave penetrate to a depth of a very thin layer with very small resistance, where the power factor is close to unity. As the wave penetrates further in this thin layer, the intensity of the wave decreases exponentially. The reflection coefficient over a wide range of frequency, up to the highest ones, is close to unity; intense reflection takes place in the presence of such a medium.

The angle of incidence at which the energy arrives at the irradiated surface does not exert a decisive influence on the character of the phenomena under consideration.

When touching upon an estimate of objects (media) which do not have the character of metallic surfaces, we note that, as was indicated above, the ratio of the conduction current to the displacement current may be different in different media. Quantitatively they are determined by the values of the conductivities  $\sigma$  and  $\omega\epsilon$ , and for the majority of meteorological objects of interest to us

$$\sigma \ll \omega\epsilon,$$

which enables us (as will be shown below) to classify these objects as dielectric media.

For the case when

$$\sigma/\omega\epsilon = 1,$$

i.e., the impedances are matched, the energy of the incident wave is completely transferred from the first medium to the second, and by the same token no reflection will occur from the separating surface.

The boundary between two zones with different values of the parameters  $\epsilon'$ ,  $\mu'$ , and  $\sigma'$  is regarded as a discontinuity. Here, in addition

to the foregoing, a change takes place in the value of the characteristic impedance  $Z_0$  and consequently conditions are produced for reflection, which in this case is equivalent to backward radiation of part of the incident energy.

Radar signals can be reflected by artificial objects on land, sea, and in air (airplanes, radar beacons, radio targets of meteorological pilot balloons) and also natural objects such as meteorological objects (precipitation, clouds, etc.) and special layers of the atmosphere.

From the point of view of physics, the processes involving reflection of electromagnetic waves are represented in the following form.

Assume that on a plane surface, say a boundary between two media, there is incident an electromagnetic wave in which the components of the electric field  $E$  and of the magnetic field  $H$  are in phase. In accordance with the principles of electrodynamics, the summary (resultant) electric field in the reflecting plane should be equal to zero. Therefore the field component  $E$  is reflected with the phase inverted, i.e., reverses sign. At the same time, the intensity of the magnetic field (the field component  $H$ ) is reflected without change in phase, and consequently the resultant amplitude of the component  $H$  is doubled, i.e., it has a nonvanishing value directly at the surface, in a layer of infinitesimally small thickness. In this connection, an unlimited current flows through this layer, the density of which is infinite, inasmuch as on the surface we have

$$\text{rot } H = \infty.$$

In the case of total reflections, the components  $E$  and  $H$  in the reflected wave are shifted in phase  $180^\circ$  relative to each other.

The quantitative relationships in the case of irradiation of an object can be represented in the following fashion.

The incident plane wave, which moves in a direction  $\underline{z}$ , i.e., nor-

mal to the surface of the irradiated object, has a horizontal plane of polarization, in which lies the vector of the electric component E. The vector of the magnetic component H of the incident wave is directed parallel to the surface of the reflecting object. Physically, when the direct wave strikes the surface of the object, two processes occur: part of the energy can be reflected, and another part can penetrate inside the object. These processes are characterized from the quantitative point of view by a reflection coefficient  $p_{otr}$  and by a transmission coefficient  $p_{pr}$ .

Were there to exist only one direct (incident) wave, then the boundary condition, namely that the intensity of the electric field component E must vanish for any instant of time, would not be satisfied. If there exists another wave, then the resultant field, equal to the sum of these two components, is sufficient to satisfy the boundary condition.

Denoting the propagation constant by  $\gamma'$ , the damping by  $\alpha'$ , the phase factor by  $\beta'$ , and the wave resistance by  $\rho'$ , we write the value of the resultant field for the boundary surface of the reflecting object; in accordance with the statements made above this value consists of the values of the amplitudes of the incident and reflected waves:

$$\begin{aligned} E_{rp} &= E_{nas} \exp(\gamma'z) + E_{orp} \exp(-\gamma'z), \\ H_{rp} &= \frac{E_{nas}}{\rho'} \exp(\gamma'z) - \frac{E_{orp}}{\rho'} \exp(-\gamma'z), \end{aligned}$$

where

$$\gamma' = \alpha' + i\beta'.$$

The reflection coefficient  $p_{otr}$  is equal to the ratio of the complex amplitude of the reflected wave to the amplitude of the incident wave on the separation boundary between the two media

$$p_{orp} = \frac{E_{orp}}{E_{nas}} = \frac{\rho_2 - \rho_1}{\rho_2 + \rho_1},$$

where  $\rho'_1$  is the wave resistance of the first medium, and  $\rho'_2$  is the wave resistance of the second medium. The coefficient  $p_{otr}$  assumes values between 0 and 1.

Let us consider the limiting cases, which depend on the properties of the medium. If the wave resistances of the first and second media are equal to each other and consequently the tangential components of the vectors E and H are equal on both sides of the separation between the media, then  $p_{otr} = 0$ , i.e., there will be no physical reflection process and the entire incident energy will go over into the other medium. At the same time, as noted above, the change of the impedance  $Z_0$  of the individual portions of the medium, without influencing the value of the wave impedance of the medium as a whole, serves nevertheless as a cause of reflection of electromagnetic energy.

At the start of the section it was indicated that the representation of the total current density is made up of the concepts of the conduction and displacement currents of which it is made up. The quantitative relationships between these currents make it possible to classify the medium as a conductor or as a dielectric.

If the medium has properties expressed by the inequality

$$\sigma \gg \epsilon\omega,$$

it approaches an ideal conductor with conductivity

$$\sigma \approx \infty$$

and consequently with wave resistance

$$\rho' \approx 0.$$

In this case total reflection takes place ( $p_{otr} = -1$ ) and the energy passing to the second medium is quantitatively equal to zero.

Inasmuch as the energy flux cannot penetrate under these conditions through the boundary separating the media (for example between the free space and the irradiated object), and the vector E is equal

to zero, the component of the Umov-Poynting vector

$$S_0 = \frac{c}{4\pi} |EH|,$$

normal to the surface of the irradiated object is also equal to zero.

It follows from the foregoing that the entire energy carried by the incident wave should be reflected if the medium does not contain any inclusions on which the energy can be dissipated (absorbed) at least in part.

If the properties of the medium are expressed by the inequality

$$\sigma \ll \epsilon\omega,$$

then such a medium should be regarded as a dielectric.

The expression

$$\sigma = \epsilon\omega_{gr},$$

which is evidence of the equality of the conduction current to the displacement current, makes it possible to establish the limiting frequency

$$f_{gr} = \frac{\omega_{gr}}{2\pi}.$$

above which the predominant role is played by the displacement current; consequently, the medium should be classified as having dielectric properties. At frequencies below  $f_{gr}$ , the predominant role is played by the conduction current, pointing to the "conductor" character of the properties of the medium. At radio frequencies the conduction current exceeds, in practice, the displacement current by millions of times.

Summarizing the foregoing, we shall use the expressions derived above for the determination of  $f_{gr}$  of meteorological objects. We assume  $\epsilon = 80\epsilon_0$  (where  $\epsilon_0$  is the dielectric constant of vacuum); allowing for inclusions,  $\sigma = 3-5$  mho (reciprocal ohms). For these data, the limiting frequency will equal approximately several thousand megacycles,

which corresponds to the centimeter wavelength band. Consequently, at the shortest waves of this band and at waves of the millimeter band the meteorological objects observed by the radar method must be regarded in the general case as dielectrics.

Radar objects are characterized by a reflecting ability which determines the amount of electromagnetic energy returning after reflection from the object to the antenna of the radar station. The reflecting ability depends on the form and dimensions of the objects and to a considerable degree on the character of the substance (material) of which the reflecting object is made up, and also on the extent to which its surface is "smooth."

In analogy with light rays reflected by different surfaces, one can say that irregularities on the reflecting surface exert an influence on the position of the front of the reflected wave. Surface irregularities break up the front of the reflected waves if these irregularities exceed  $\lambda/8$  in height and in depth. Thus, say, a coarsely ground glass plate, which does not reflect visible light, reflects well the rays of the longer-wave infrared light. Reflection from rough surfaces was investigated by V. Twersky [65].

Radar reflection depends among other things also on the smoothness or roughness of the reflecting surface in the respect that in the case of a smooth surface the incident energy experiences specular reflection; this process is explained in Fig. 4a. In the case of a rough and uneven surface diffused scattering of energy takes place, similar to that shown in Fig. 4b. The foregoing pertains predominantly to surface targets.

Radar detection of three-dimensional targets has its own specific nature. Many three-dimensional observation objects (three-dimensional targets), among which are included aerological objects, consist of a

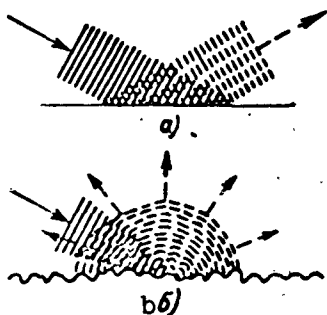


Fig. 4. Specular reflection (a) and diffuse scattering (b).

large number of independent single scattering particles, so that statistical laws can be applied with respect to such targets.

The problem of radar detection and observation of atmospheric formations (rain, snow, cloudiness, fog) and the associated problems of absorption of microwaves, as well as the quantitative relationships in this field has been developed by D.M. Vysokovskiy

[1]. Chapter 4 is devoted to these questions.

The intensity of the reflected radar signal is determined within known limits by the area of the projection of the object on a plane perpendicular to the direction of propagation of the radio waves incident on the object; it is understood here that for a given range the linear dimensions of the object do not exceed the width of the beam of radio waves incident on the object. For a quantitative estimate of the intensity of the reflected signal, of great importance is the angle formed by the plane of polarization of the incident wave and the plane in which the reflecting object is situated. The maximum intensity of reflection is observed when the vector  $E$  of the incident wave is oriented normal to the reflecting plane.

### 3. DIRECTION OF RADIATION AND RECEPTION OF ELECTROMAGNETIC WAVES

As was mentioned in Section 1, the determination of the angular coordinates of radar objects is made by using directional transmission and reception of radio waves; this directivity is realized by means of special antenna devices in the radar stations.

Relegating the study of the directional properties of antennas to the specialized divisions of radio engineering, we present here only brief information necessary for the exposition that follows, and the

readers desiring to become acquainted in greater detail with this problem as applied to the given case are referred to the series "Radar Engineering" [4, 5].

A specified maximum operating range of a radar station is attained with the aid of directional antennas by concentrating (focusing) the radiation in a given direction. Such a concentration of the energy is the result of a suitable decrease in the radiation intensity in all other directions except the one specified. The directional action of antennas is thus a function of the direction.

The field intensity produced by a directional antenna in a given direction depends on two factors: first, on the efficiency, quantitatively determined by the relation

$$\eta = \frac{P_z}{P_0},$$

where  $P_z$  is the power radiated by the antenna and  $P_0$  is the power fed to the antenna; second, on the directivity coefficient. The latter is defined quantitatively for each individual direction as the ratio

$$D = \frac{E_0^2}{E_{cp}^2}.$$

where  $E_0$  is the field intensity in the given direction and  $E_{sr}$  is the value of the field intensity produced in the case of isotropic radiation, averaged over all directions.

The characteristic value of  $D$  is usually taken to be the value of this parameter taken for the direction of the principal maximum of the radiation.

If we take into consideration the fact that the square of the field intensity is directly proportional to the radiated power causing it, we can characterize the directional action of a transmitting antenna by a ratio which shows by how many times the power directed by a nondirectional antenna must exceed the power radiated by the direc-



tional antenna under consideration in a given direction in order that both compared antennas produce at a certain distance from the transmitting antenna, at the reception point, a field of equal intensity. In other words, we are speaking here of the power advantage resulting from the use of the directional antenna.

As the standard antenna with which the comparison of the antenna under consideration is made we can use an isotropic (pointlike) radiator in free space, a Hertz dipole, i.e., an infinitesimally small radiator with uniform current distribution, the radiation of which is received in the equatorial plane, or else a real half-wave antenna. The latter type of standard antenna is much easier to realize in practice than, say, an isotropic radiator, inasmuch as an inherent property of all simple antennas is not to have any radiation in certain directions. Therefore an isotropic radiator is used predominantly only in theoretical calculations.

Quantitatively, the concept of advantage referred to above is characterized by the value of the gain, which depends on the directional properties as well as on the efficiency of the antenna, i.e.,

$$\text{gain} = \text{directivity} \times \text{efficiency}.$$

The directional antennas used in radar devices can be broken up into the following groups:

- a) antennas made up of elements, namely of half-wave dipoles,
- b) reflecting antennas, which make use of reflectors (mirrors) in the form of paraboloids of revolution and parabolic cylinders,
- c) antennas using other optical methods, such as lens antennas,
- d) dielectric rod, slot, and other microwave antennas.

The directivity of antennas can be represented graphically with the aid of directivity patterns, which characterize the radiation (reception) of the antenna in the horizontal and vertical planes. Direc-

tivity patterns in the horizontal plane are constructed in polar and rectangular coordinates (Fig. 5). Diagrams in polar coordinates are more illustrative, in that they represent in a certain scale the pattern of radiation distribution (or reception distribution) over the terrain.

In both types of diagrams it is advantageous to express the intensity (for example the field intensity) in relative units, assuming, say, the maximum value of the field to be 100%.

A directivity pattern in polar coordinates is essentially the geometric locus of the points formed by the end of the radius vectors drawn from the origin in the specified directions, indicated by the given radius vectors; the lengths of the latter are proportional to the field intensity at a definite distance.

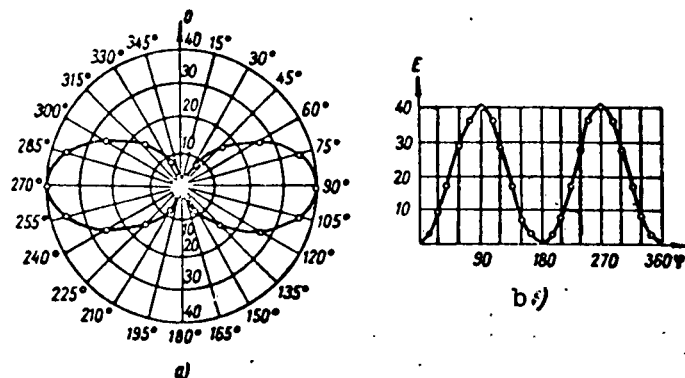


Fig. 5. Radiation characteristics of a directional antenna in polar (a) and rectangular (b) coordinates.

From the directivity pattern in the horizontal plane it is also possible to determine one of the essential characteristics of a directional antenna, namely the aperture angle  $\Phi$  of the diagram. The aperture angle of the directivity pattern, plotted in terms of power, is measured at the points corresponding to half the power (Fig. 6a), while for the diagram plotted in terms of the field it is measured at

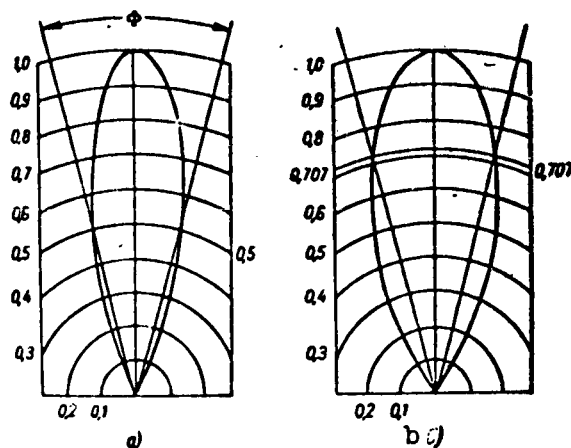


Fig. 6. Aperture angle of the directivity pattern plotted in terms of power (a) and field intensity (b).

the points corresponding to 0.707 of the maximum value (Fig. 6b).

The above-described directional action of transmitting antennas, resulting from focusing, is manifest in the fact that in some directions (one or two) the radiation intensity of the electromagnetic energy is predominant compared with others; by virtue of the reciprocity principle, which enables us to speak of the reversibility of transmitting and receiving antennas, it is from this direction that the most intense reception takes place, as compared with other directions.

For receiving antennas, the parameters described above have the following physical meaning.

The directivity coefficient of the receiving antenna is defined as the ratio

$$D = P/P_{sr},$$

where  $P$  is the power at the input of the receiver in the case of reception from the given direction and  $P_{sr}$  is the average value of the power for reception from all directions.

If we take into consideration the fact that the input power of the receiver is proportional to the square of the input voltage, the

foregoing expression for the directivity assumes the form

$$D = U^2 / U_{sr}^2,$$

where  $U$  is the voltage at the input of the terminal in the case of reception from the given direction and  $U_{sr}$  is the mean square value at the input of the receiver in the case of reception from all directions.

The efficiency of the receiving antenna is accordingly equal to the efficiency determined for the same antenna used as a transmitter.

The gain of a receiving antenna in a given direction is the ratio of the power received at the input of the receiver from the given direction to the power received at the receiver input using a standard antenna of one of the types referred to above.

Radar antennas for microwave frequencies are made predominantly in the form of parabolic reflectors. When such a reflector has a diameter  $D$  meters, its effective radiation area is equal to

$$A_e = \pi D^2 / 4$$

and forms a beam of round cross section. The calculated aperture angle of the directivity pattern (Fig. 6a) of the reflector is given by the expression

$$\Phi = \frac{\lambda}{D} = \frac{\lambda}{2 \sqrt{\frac{A_e}{\pi}}} \text{ radians.}$$

In practice this value of  $\Phi$  is approximately 25% higher.

If we take the ratio of the maximum density of the energy radiated by the reflector under consideration to the energy density of an isotropic radiator, then the gain will be

$$G = 8\pi A_e / 3\lambda^2. \quad (1)$$

In practice the radiation of a reflector is produced by a half-wave dipole placed at the focus of the reflector and making a right angle to the reflector axis. In such a position, the gain exceeds by one and a half times the gain of an isotropic radiator, i.e.,

$$G_0 = \frac{3}{2} \frac{8\pi A}{3\lambda^2} = 4\pi \frac{A}{\lambda^2}. \quad (1a)$$

The symbol  $A$  entering into this expression has the significance of an effective area in the case of a receiving antenna. It can be shown [27] that this concept and the concept of gain  $G_0$  introduced above are connected by the relations:

$$G_0 = 4\pi \frac{A}{\lambda^2},$$

$$A = \frac{G_0 \lambda^2}{4\pi}.$$

According to the reciprocity principle, these expressions hold true for any antenna possessing directional properties, whether used for transmission or reception.

In the general case the value of the gain  $G_0$ , determined in the direction of maximum radiation, is assumed to be as the nominal one for the given antenna, characterizing the gain produced by the antenna. It can also be used to construct relative diagrams (Fig. 5) of the absolute energy densities or fields. For this purpose the energy density  $W$  for a power  $P$  supplied to the antenna, at a distance  $R$  from the antenna, which density is equal to  $P/4\pi R^2$ , must be multiplied by the gain  $G_0$  in the direction of the maximum radiation in all other directions.

If the concept of the gain is defined as the ratio of the power  $P_2$  in the nondirectional antenna (standard) to  $P_1$  in the directional antenna, both antennas producing identical energy densities at a given distance, then the gain can be expressed in decibels using the following relation

$$G = 10 \lg \frac{P_2}{P_1} \text{ db.}$$

#### 4. RADAR SYSTEMS AND STATIONS

##### System with Continuous Radiation

This system operates in a mode in which the transmitting part (Figs. 7a and b) of the radar station generates continuously during the entire time. Because of this, the transmitting antenna radiates a

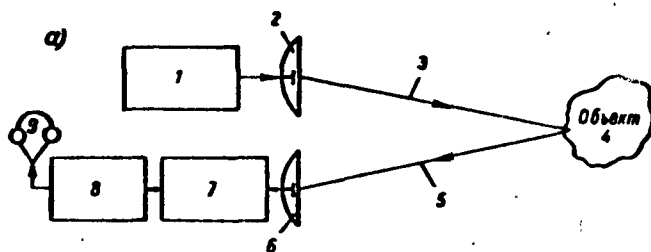


Fig. 7a. System with continuous radiation. 1) Transmitter; 2) transmitting antenna; 3) sounding beam; 4) object (target); 5) reflected signal in the receiving antenna; 6) receiving antenna; 7) receiver; 8) converter and amplifier; 9) indicator (head phone).

directional beam of radio waves with phase  $\exp(j\omega t)$ . An object located at a distance  $R$  reflects part of the energy, which returns to the antenna with a different phase, equal to  $\exp(j\omega t - 2kR)$ , where  $k = 2\pi/\lambda$ . The amplitude of the reflected signals at the antenna will always be considerably smaller than the amplitude of the radiated signal, and in practice can be  $10^{-9}$  times weaker. The latter circumstance raises considerable difficulties in the direct determination of the phase of the reflected signal.

A system with continuous radiation can be built using some type of modulation such as shown, for example, in Fig. 7b. Here the frequency of the radiated oscillations (the wavelength) changes monotonically and periodically from a certain mean value  $f_0$ , in both directions, by an amount  $\Delta f$ . Because of this, the frequency of the radiated oscillations has for each instant of time a value different from that it had directly before this instant. At the receiver input enter os-

cillations with frequencies  $f_1$  and  $f_2$ , as a result of which there is produced at the receiver output an oscillation with frequency  $f_3$ , as shown in Fig. 7b. At each instant of time the frequency is  $f_3 = f_1 - f_2$ ; it can be shown [23] that the frequency  $f_3$  is proportional to the determined distance  $d$ . This circumstance enables us to feed the voltage with variable frequency  $f_3$  from the output of the receiver to a measuring instrument such as a frequency meter, the scale of which is calibrated directly in units of distance to the observed object.

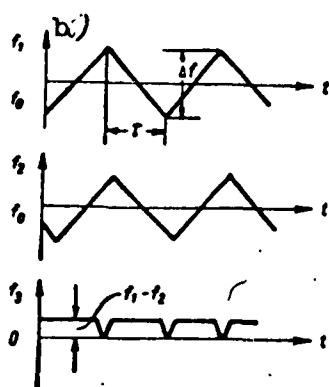


Fig. 7b. Formation of difference frequency  $f_3$  under the influence of frequency modulation of the radiated oscillations,  $f_1$  is the change in the radiated oscillations and  $f_2$  is the change in the reflected signal.

### Systems with Pulsed Radiation

The pulsed mode is characterized by generation and radiation into space of short-duration radio wave transmissions, called the main sounding pulses, of duration  $\tau_1$ . The main pulses alternate with longer pauses, of duration  $t_p$ ; during the time  $t_p$  the transmitter is disconnected from the antenna and the receiver connected. The latter receives during the pause the signals (reflected pulses) from the objects, which return to the antenna of the station.

A strict rhythm of the operating sequence of all the elements of the

radar station is maintained by a device called the timer.

A block diagram of a pulsed radar station is shown in Fig. 8. It includes the following:

an antenna intended to radiate electromagnetic energy in the form of radio pulses in the transmission mode, and to receive the energy of the radio waves reflected from the object in the reception mode;

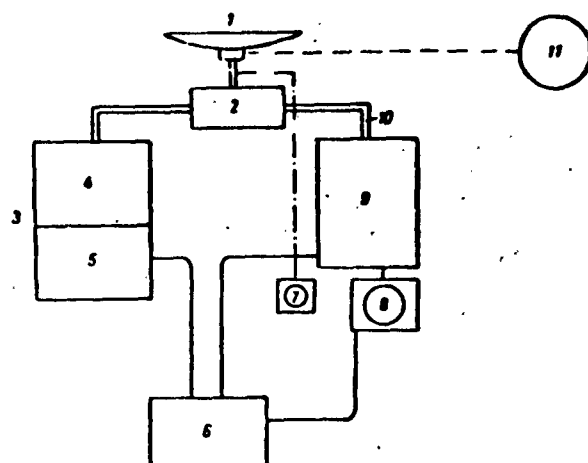


Fig. 8. Block diagram of pulsed system.  
 1) Antenna; 2) antenna switch; 3) trans-  
 mitter; 4) high-frequency generator; 5)  
 modulator; 6) timer; 7) antenna position  
 indicator; 8) indicator; 9) receiver;  
 10) transmission lines; 11) antenna motor.

a transmitter, which generates high-frequency oscillations in the form of radio pulses, the form and duration of which are set by means of the modulator in response to the triggering of the pulses of the timer;

a receiver, which receives and amplifies the reflected pulses and transforms them into a voltage which is fed to the indicators;

an antenna (TR) switch (usually not mechanical), used to connect the antenna alternately to the transmitter and to the receiver;

a timer, intended to generate triggering pulses in strictly determined time intervals; these pulses control, via the modulator, the repetition frequency and the duration of the high-frequency generator pulses. During the reception time  $t_p$  the timer unblocks the receiver circuits and in addition triggers the sweep circuits of the indicators.

The block diagram considered applies equally well to radar stations operating in the meter band and to stations in the centimeter band. The difference between these cases lies only in the construction



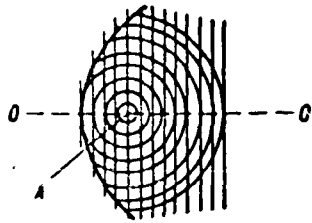


Fig. 9. Formation of a plane wave by a parabolic reflector. A) Radiator.

of the high-frequency elements, which include the antenna unit with the circuits feeding it and the receiver and transmitter circuits, including also the radio tubes.

Antennas for meter wavelengths are structurally arrays of elementary dipoles, and this ensures their increased directivity.

Antennas for centimeter and millimeter wavelengths comprise a combination of a waveguide, feeding the radio-frequency energy, and a radiating element located at the focus of a reflector. The latter ensures, as a result of its focusing action, the required form of the directivity pattern in transmission and reception. In the general case reflectors of this type are in the form of a paraboloid of revolution, but depending on the problem to be solved, the reflector may have a somewhat different form. The formation of a plane wave by such a structure during the course of the radiation of electromagnetic energy is illustrated in Fig. 9.

The gain of an antenna of this construction for a reflector of radius  $r$ , in the focus of which (Fig. 9) is situated a radiator 0 is given by the formula

$$G_0 = k \frac{\pi (nr)^2}{\lambda^2},$$

where  $k \approx 3.8$ .

The gain given here for the parabolic reflector characterizes the radiation in the principal direction, which coincides with the reflector axis. Simultaneously with radiation in the principal lobe (i.e., within the limits of the angle  $\phi$  on Fig. 6), however, there is also formed harmful radiation in the form of the so-called side lobes, which are symmetrically situated on both sides of the diagram of Fig. 6.



Fig. 10. Portion of sweep on a type-A indicator with visible noise (interference background).

Elimination of the undesirable radiation in the form of side lobes of the diagram is effected by choosing the optimum irradiation of the paraboloid, something done during the adjustment of the station in the plant.

As indicated above, the directional action of an antenna depends on the ratio of the reflector diameter to the wavelength at which the system operates. Therefore in practical conditions an increase in the directivity is attained in two ways. The first is to decrease the operating wavelength, this being one of the reasons for the evolution of radar units toward the use of shorter and shorter wavelengths. The second means is to increase the dimension of the radiator or reflector, something effected in the work described in the next chapter.

The receiver of a radar station performs the following tasks: together with the antenna it detects signals (even those of very low intensity) reflected from objects located at a certain distance; these signals are amplified to an amplitude sufficient for optical display on the indicator. The decisive factor in the operation of the receiver is the presence of interference, called noise, in analogy with acoustic noise produced by interference during the reception of sound signals in a loudspeaker or in earphones. The appearance of noise is manifest in the present case in the fact that the screen of the radar indicator is cluttered with visible images of the "background," in addition to the useful image, as shown in Fig. 10. It is unavoidable for the useful-signal image of low amplitude to remain undetected in the presence of such a background, and "drown" as it were in the image of the background. Because of this, naturally, the question arises of increasing the amplitude of the signal relative to the noise amplitude,

which leads to specific requirements imposed on the gain of a radar receiver.

In this connection, when determining the sensitivity of a radar receiver one starts from the signal/noise ratio. The nature of the noise is explained by the random motion of charges in the substance (so-called thermal motion), fluctuations of the current in vacuum tubes, and also electromagnetic processes of galactic and cosmic origin, i.e., noise entering the antenna from the outside.

The physical process of amplification in the radio receiver circuits excludes the possibility of first separating the noise from the useful signal so as to amplify the latter separately. In practice, a real receiver always possesses internal noise; consequently, for a quantitative estimate and comparison of receivers one starts from the signal/noise ratio at the output of the receiver and the concept of the noise figure, expressed in decibels, is used. For example, for the type SCR-584 radar, which operates in the centimeter band, this parameter amounts to 15 db [82].

The indicators of radar stations can be made in the form of a cathode ray tube, an instrument with a pointer type meter, in the form of an electroacoustical unit, etc. In meteorological radar stations one uses essentially indicators in the form of a cathode ray tube.

Such an indicator is similar in appearance to the screen of a cathode ray oscillograph (oscilloscope).

Among the large variety of cathode ray indicators, the ones used most frequently in meteorological radar are the circular-scan indicators (IKO) and type-A indicators.

The screen of a circular-scan indicator is shown in Fig. 11a. The center of the image coincides with the location of the radar station. The distances are determined along the radii; for convenience in read-

ing, the indicator is fed with voltage from a special unit called the calibrator, so as to form scale rings (range circles) on the screen.

The azimuth is determined on a scale surrounding the screen. A (weakly) strobing beam moves around the center, over the screen, with uniform velocity; its azimuthal position at each instant of time coincides with the direction in which the antenna radiates the main pulse. If an object reflecting the energy of the main pulse is situated in a given direction at a certain distance from the radar station, the strobing beam forms on the screen a bright spot, the position of which makes it possible to determine the azimuth and the distance of the object relative to the location of the station. The screen of such an indicator should have considerable persistence, i.e., it should be able to retain the image visible on it for a certain time.

The intensity of the reflected signal influences the brightness of the light spot it produces on the screen; this pertains to indicators with brightness marker (for more details see Section 4 of Chapter 6). This makes it possible, in particular, to judge to a certain degree the character (intensity) of the meteorological objects. The white spots on the indicator screen (Fig. 11a) represent the radar image of clouds; the same figure shows the radially located strobing beam, the position of which corresponds at this instant to an azimuth of about  $160^{\circ}$ .

With the aid of this indicator it is possible to observe the formation, location, and displacement of heavy clouds and thunderstorm fronts, under suitably chosen scale, within an area of several tens of thousands of square kilometers.

The type-A indicator does not give any data on the angular coordinates, and permits direct measurements of the range only. The use of this indicator necessitates the application of a separate indicator

a)



b)



Fig. 11. Exterior view of indicator screens: a) circular scan (IKO), b) with type-A sweep.

for the azimuth of the antenna.

The electron beam traces along the diameter of the screen, in a horizontal direction (usually from left to right), a bright line which forms a uniform time scale, comprising by the same token a uniform distance scale. The reflected signal received by the receiver causes a vertical displacement of the beam (usually upward), and as a result the image on the screen of such an indicator has the form shown in Fig. 11b. From the amount of vertical deflection one can estimate the intensity of the given reflection.

A type-A indicator is equipped with an external range scale, on which the distances are measured, or else a calibrating voltage is introduced into its circuits, such as to produce light calibration markers on the screen.

## 5. QUANTITATIVE RELATIONS

Even in the early (1945) work on the theory of radar it was shown [44] that the maximum range of radar observation depends on the parameters of the transmitting and receiving parts of the radar, and also on the properties of the target, and is given by the equation

$$R_{\max} = \sqrt[4]{\frac{P_t A_0 G_0 \sigma}{P_r (4\pi)^3}}.$$

where  $P_t$  is the (pulsed) transmitter power,  $P_r$  the (minimal) power at the input of the receiver,  $G_0$  the gain of the transmitting antenna,  $A_0$  the equivalent reflecting (scattering) area of the receiving antenna in square meters, and  $\sigma$  the reflecting surface area of the target in square meters. The value of  $\sigma$  takes account also of the directivity  $g$  of the target (anisotropic).

From the foregoing expression it is easy to obtain the value of the power  $P_r$ , fed under given conditions to the input of the receiver

$$P_r = \frac{P_t G_0 A_0 \sigma}{(4\pi)^3 R^4}. \quad (2)$$

Expression (2) contains the range  $R$  in the fourth power because the range  $R$  is regarded as the radius of a sphere twice: once during the propagation of the radio waves from the radar to the target and then upon reflection of the radio waves from the target to the receiving antenna of the radar.

The data presented in the preceding section enable us to stop and discuss some quantitative relations illustrating the nature of the expressions given above.

Let us consider a radar station located at point O in Fig. 12,

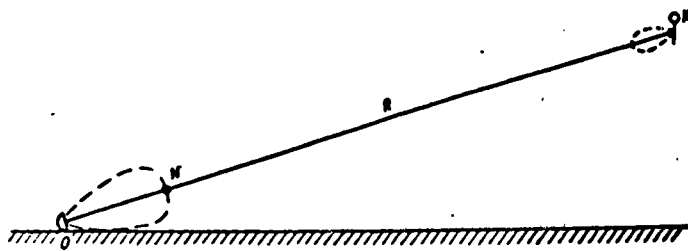


Fig. 12. Relative location of the radar and a target in air.

which has a common antenna for transmission and reception, with directivity coefficient  $G_0$ ; the directivity pattern of the antenna is also shown in the figure.

Denoting the transmitter power by  $P_t$ , we obtain for the general case of radiation over a sphere a power flux

$$S' = P_t / 4\pi R^2 \text{ w/m}^2,$$

or, taking into account the directivity coefficient, we write for the flux

$$S = PG_0 / 4\pi R^2 \text{ w/m}^2.$$

Assume that at a distance  $R$  there is located a reflecting object  $M$ , which has a certain equivalent scattering area  $A_e$ , and has a scattering directivity  $g$ , which is unavoidable for any real case (although it may be insignificant). Arguing in the same manner as in the determination of the flux  $S'$ , we obtain for the point  $O$  the following value of the flux of the reflected energy

$$S_{\text{otr}} = \frac{PA_e G_0 g}{(4\pi R^2)^2} \text{ watts/m}^2.$$

If we consider real values of the quantities prevailing in radar stations, for example  $P = 100 \text{ kw}$ ,  $G_0 = 1200$ , and  $R = 100 \text{ km}$ , then the power of the reflected signal at the output of the receiver will be

$$P_{\text{otr}} \approx 10^{-11} \text{ w.}$$

Naturally, reflected signals of such small amplitude call for appreciable gain. However, we are considering not only the quantitative

aspect of the problem. The gain effected by the receiving circuit must also be of high quality, in other words, the distortion of the amplified signals should be a minimum.

The signals (radio pulses) employed in radar have in most cases envelopes of rectangular form. When such signals are resolved into components, i.e., when their frequency spectrum is investigated, it is easy to verify that the bandwidth occupied by such signals is broad. In practice this means that the circuits of radar receivers and amplifiers should be broadband, i.e., capable of transmitting during the course of amplification voltages in a broad frequency spectrum, which in practice reaches several megacycles.

The factors that determine the employed bandwidth of a radar receiver are governed by the following two contradictory requirements. The first is a reduction in noise, as was already mentioned above, and is attained by narrowing the bandwidth. The second is to maintain the form of the pulse undistorted, and is attained by using a large bandwidth.

The optimum bandwidth  $\Delta f$  in the receiving and amplifying portion of the radar stations is chosen in accordance with the pulse duration  $\tau_1$ , using the equation

$$\Delta f = \frac{4-5}{\tau_1}.$$

This amounts to a bandwidth of about 0.5 megacycles for a pulse duration  $\tau_1 = 10 \mu\text{sec.}$

Manu-  
script  
Page  
No.

[Footnote]

28

Possessing an electric dipole moment (after P. Debye and J. Thomson).



Manu-  
script  
Page  
No.

[List of Transliterated Symbols]

13	пр = pr = provodimost' = conduction
13	см = sm = smeshcheniye = displacement
16	п = p = poterya = loss
22	а = a = antenna = antenna
33	гр = gr = granichnyy = boundary
33	пад = pad = padayushchiy = incident
33	отр = otr = otrazhennyy = reflected
33	пр = pr = prokhozhdeniye = transmission
38	ср = sr = sredniye = average
42	э = e = effektivnyy = effective
45	п = p = pauza = pause
53	э = e = ekvivalentnyy = equivalent

### Chapter 3

#### THEORY OF RADAR DETECTION OF METEOROLOGICAL TARGETS

##### 1. RADAR FORMULA FOR METEOROLOGICAL TARGETS

Radar objects (targets) of meteorological origin (zones of clouds, precipitation, etc.), unlike the objects mentioned earlier (airplanes, ships, etc.) are isotropic radiators: they are usually regarded as three-dimensional (distributed) targets [23].

In Chapter 2 above, we touched upon problems of spherical propagation of radio waves, and in particular we presented Expression (2) for the power  $P_r$  fed under these conditions to the input of the radar receiver. For the case of a radar antenna consisting of a half-wave dipole and a reflector we also gave Expressions (1) and (1a) for the values of the gain  $G$  and  $G_0$ , connected with the values of  $A_0$  of the effective area of the radar antenna.

Using Formula (1a), we write the expression for the gain  $G_t$  of the transmitting antenna in the following form:

$$G_t = \frac{8\pi A_p}{3\lambda^2}.$$

where  $A_p$  is the aperture, i.e., effective, area which determines the quantitative aspect of the radiation.

After substituting  $G_t$  in Eq. (2) we obtain

$$P_r = \frac{A_p P_s}{9\pi R^2 \lambda^2}. \quad (2a)$$

In this equation it is necessary to take into account the multiple character of the meteorological objects and the fact that under real

conditions the radio waves propagate in an absorbing medium.

The clouds and the precipitation consist of suspended and precipitated drops and ice crystals. The entire aggregate of the drops and the crystals contained in a certain volume is perceived as a single target. In the general case the scattering area of such a target varies depending on the distance between the particles of the clouds and the precipitation. Under real conditions one observes a random distribution of these particles in space, and this gives rise to a random distribution of the phases of the electromagnetic waves reflected from them.

The foregoing circumstance, with account of the distances between the particles, make it possible to assume in first approximation that this reflection is noncoherent, i.e., that the average power of the wave reflected from the particles at a given distance is the sum of the powers of the waves reflected from all particles.

Thus, the signal received at the input of the radar receiver from the meteorological target comes from a rather large number of elementary targets and constitutes one resultant signal. On the basis of the foregoing it can be stated that the scattering area per unit volume of a meteorological target consisting of identical particles is equal to the product of the number of these particles by the scattering area of each particle.

For clouds and precipitation, the actual scattering area is given by the relation

$$A_e = v\eta,$$

where  $v$  is the volume of the cloud or the rain, the reflected signals from whose particles enter the input of the receiver simultaneously, and  $\eta$  is the overall scattering area of all the drops per unit volume of the cloud or rain. The value of  $\eta$ , taking into account the particle

distribution by dimensions, can be determined as

$$\gamma = \sum_D N(D) \sigma(D, \lambda),$$

where  $\sigma(D, \lambda)$  is the scattering area of a particle with dimension  $D$  for the wavelength  $\lambda$  and  $N(D)$  is the number of particles having dimensions  $D$  per unit volume.

Let us determine from what volume the reflected signals come simultaneously to the input of the receiver.

From a point target, the reflected electromagnetic waves arrive at different instants of time during the time of the pulse. On the other hand, if the target is a three-dimensional cluster of cloud particles and precipitation, then the receiving antenna of the radar station receives simultaneously signals from all the particles located in a volume bounded in width and in height by the directivity pattern of the antenna (the dimensions of the radio beam) and limited in range to  $c\tau_1/2$ , where  $\tau_1$  is the duration of the radiated pulse and  $c$  is the velocity of propagation of electromagnetic waves in the atmosphere, equal to the velocity of light.

Indeed, assume that at some initial instant of time the main pulse in the zone of cloud and precipitation occupies the volume ABCD (Fig. 13). During the time  $\tau_1/2$ , the trailing front of the pulse AD reaches the particles on the surface MN, located at a distance equal to half the length of the pulse  $h/2$  from its initial position. During the same time, the leading front BC, becoming reflected from the particles which lie on its surface, will also reach the surface MN. Subsequently the trailing front AD, on reaching the particles lying on the surface MN and becoming reflected from them, will reach the receiving antenna of the radar simultaneously with the secondary radiation from the leading front of the particles lying on the surface BC. It

follows therefore that the depth of the region from which a secondary (reflected) radiation arrives at a given instant at the radar is

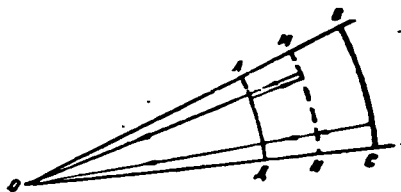
$$R + h - \left(R + \frac{h}{2}\right) = \frac{h}{2} = \frac{c\tau}{2}.$$

Since usually  $R \gg h$ , the volume filled with cloud or precipitation particles, from which the reflected energy reaches the receiving antenna simultaneously, amounts to\*

$$v = \frac{1}{2} \pi \left(\frac{R\theta}{2}\right)^2 h. \quad (3)$$

Consequently, this reflecting volume is half as large as the irradiated volume.

This relation holds true for any filling of the pulse with cloud



and precipitation particles, other than zero. The value of the reflecting volume itself lies usually within the limits

$$\frac{1}{2} \pi \left(\frac{R\theta}{2}\right)^2 h \geq v > 0$$

Fig. 13. Beaming and reflection volumes.

depending on the degree of filling of

the pulse with the cloud and precipitation particles. To take this circumstance into account in calculating the reflecting volume by Formula (3), it is necessary to multiply the obtained value of the volume by the filling coefficient  $k_z$ , which is equal to the ratio of the volume of the pulse filled with the cloud and precipitation particles to the entire volume of the pulse.

To take into account the attenuation during the propagation of the electromagnetic wave in an absorbing medium, it is necessary to introduce a coefficient  $k_a$ , which is connected with the attenuation coefficient  $\alpha(R, \lambda)$  by the relation

$$k_a = 10^{-0.2 \int_0^R \alpha(R, \lambda) dR} \quad (4)$$

where  $\alpha(R, \lambda)$  is the attenuation in decibels per unit length of path

at a distance R from the transmitter to the point of the cloud or precipitation zone under consideration.

Taking (2a), (3), and (4) into account we can write down the fundamental radar equation of atmospheric formations in the general form

$$P_r = \frac{P_t A_p^2 h^2}{72 \lambda^2 R^2} \sum_D N(D) \sigma(D, \lambda) k, k. \quad (5)$$

If  $P_r$  is the minimum observable signal, then the distance R is the maximum distance of detection of the atmospheric formation.

## 2. ANALYSIS OF THE RADAR FORMULA FOR METEOROLOGICAL TARGETS

Of great importance in the detection of clouds and precipitation are the physical characteristics of the latter. Clouds and precipitation consist of drops of water, hailstones, ice crystals, and snowflakes.

Let us consider a case when the clouds or precipitation consist of spherical water droplets only.

Figure 14a shows the distribution of the drop dimensions in certain forms of clouds, while Fig. 14b shows the relative distributions of the drop dimensions in rain.\* From the analysis and comparison of the curves on both figures we can see that cloud drops as a rule are limited to a radius of about 50  $\mu$ . Rain drops are much larger than cloud drops. The radius of the largest rain drops reaches 3-4 mm. The number of cloud drops per cubic meter is quite large and may reach  $10^8$ , whereas the number of rain drops in the same volume does not exceed 500-600. As was indicated above, the theory of radar detection of atmospheric formations, such as clouds and precipitation, is based on the assumption that the reflection is coherent, i.e., that there is no interference between the fields radiated by the individual particles. This assumption, however, may not be justified for certain wavelengths at which modern radar systems operate, since the distance between cloud

particles is on the order of 1 mm, i.e., it is as a rule noticeably smaller than the encountered wavelengths. In such cases, when the wavelength is much larger than the distance between particles, the scattering volume can be regarded as continuous. Then an important role in the determination of the power of the reflected signal will be played by the interference between the waves scattered by individual particles, and in solving the reflection problem one can regard the atmospheric formation as a continuous body. An account of the influence of the interference signifies that it is necessary to add not intensities but fields, taking into account the corresponding phases. The intensities always add up, whereas fields may also cancel each other if their phases are opposite.

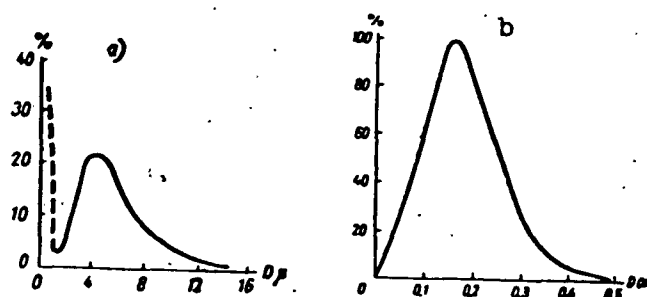


Fig. 14. Distribution of drops in stratus clouds (a) and in rain (b) with intensity 12.5 mm/hr.

K.S. Shifrin [30], who made a thorough study of this problem, has shown that the magnitude of the reflected signal is described in general with sufficient accuracy by the following relation:

$$S = NS_0 \left[ 1 + 0,752 \cdot 10^{-3} \frac{\lambda}{B} \left( \frac{\lambda}{l} \right)^2 \right], \quad (6)$$

where  $N$  is the number of particles per unit volume,  $S_0$  the intensity of the secondary radiation of each individual particle,  $\lambda$  is the wavelength,  $l$  the distance between cloud or precipitation particles, and  $B$  is the radius of the spherical volume equal in magnitude to the re-

flecting volume of the pulse,

$$B = \sqrt[3]{\frac{3}{4} (0R)^2 \frac{\lambda}{2}}. \quad (7)$$

The product  $NS_0$  describes a noncoherent radiation, while the terms in the square brackets represent a correction for coherence.

If we denote the ratio of the coherent part of the reflected intensity to the noncoherent part by  $\varphi$ , then we get from (6)

$$\varphi = 0,752 \cdot 10^{-3} \frac{\lambda}{B} \left( \frac{\lambda}{l} \right)^2. \quad (8)$$

When  $\varphi \ll 1$  the scattering is noncoherent; when  $\varphi \gg 1$  the scattering is coherent. When  $\varphi$  is close to unity we have an intermediate case and both terms in Formula (6) must be taken into account.

Using Relations (7) and (8) we can calculate the ratio of the coherent scattering to the noncoherent one,  $\varphi$ , for different ranges for clouds and precipitation separately. In this case the distance between cloud particles,  $l$ , is usually assumed to be 0.1 cm, while for rain one assumes it to be 10 cm.

### 3. EFFECTIVE RADAR SCATTERING AREA OF CLOUDS AND PRECIPITATION

From Mie's research on the diffraction of electromagnetic waves by a sphere it becomes possible to determine the radar scattering area of droplets, in the form of definite series of spherical Bessel functions of the parameter  $\pi m D / \lambda$ , where  $m$  is the complex refractive index of water for the wavelength  $\lambda$  and  $D$  is the drop diameter.

In the case when the drop diameter is  $D \leq 0.05\lambda$ , i.e., considerably shorter than the wavelength, its effective radar scattering area is expressed sufficiently accurately by the well-known Rayleigh relation

$$\sigma = \pi^3 \frac{\epsilon - 1}{\epsilon + 2} \left| \frac{D^3}{\lambda^3} \right|^2. \quad (9)$$

Here  $\epsilon$  is the complex dielectric constant of water, equal to the



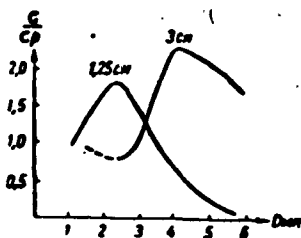


Fig. 15. Ratio of actual effective scattering area to the Rayleigh area.

square of the refractive index.

When  $D = 0.08\lambda$  the value of  $\sigma$  amounts to 0.8 of the value indicated in (9). The effective radar scattering area then doubles as compared with (9) at  $D/\lambda = 0.2$ , and with further increase in the drop dimensions it fluctuates about a constant value close to its transverse cross section area.

Figure 15 shows the ratio of the actual radar scattering area, calculated from the exact formulas, to the Rayleigh area for two wavelengths,  $\lambda = 1.25$  and  $\lambda = 3$  cm [31]. It is seen from the figure that Formula (9) is quite suitable for the calculation of  $\sigma$  of small drops, which make up clouds and fog. As regards rain drops, particularly large ones, the use of this formula can lead to undesirable errors, principally when  $\lambda = 1$  cm and shorter.

Table 3 lists the average values of  $ND^6$  for cloud and rain drops [69].

TABLE 3

Average Values of the Reflecting Characteristic  $ND^6$  of Clouds and Rain (in  $\text{cm}^3$ )

1 Форма облака	$ND^6$	2 Интенсивность дождя	$ND^6$
3 Слоистые . . . . .	$8.57 \cdot 10^{-17}$	8 Слабый (1,25 мм/час.)	$0.07 \cdot 10^{-10}$
4 Высоко-слоистые . . . .	$2.70 \cdot 10^{-17}$	9 Умеренный (5 мм/час.)	$0.7 \cdot 10^{-10}$
5 Слоисто-дождевые . . . .	$14.79 \cdot 10^{-17}$	10 Сильный (12,5 мм/час.)	$2.2 \cdot 10^{-10}$
6 Слоисто-кучевые . . . .	$9.9 \cdot 10^{-17}$		
7 Кучевые . . . . .	$6.13 \cdot 10^{-17}$		

1) Form of cloud; 2) intensity of rain; 3) stratus; 4) altostratus; 5) nimbostratus; 6) stratocumulus; 7) cumulus; 8) weak; 9) moderate; 10) strong; 11) mm/hr.

The principal radar equation for atmospheric formations in the case of detection of liquid-drop clouds and precipitation, when  $D \ll \lambda$ ,

can be written after making the substitution of (9) in (5) and carrying out simple transformations in the form

$$P_r = \frac{\pi^5 P_t A_p h}{48 R^2 \lambda^4} \left| \frac{z-1}{z+2} \right|^2 \sum_i N_i D_i^6 k k_i \quad (10)$$

From Table 3 and from Formula (10) we see clearly that the effective radar area of the drops, and consequently also the power of the received signal, depend very strongly on the diameter of the drops (as the sixth power). For example, doubling of the drop diameter leads to a 64-fold increase in the power of the received signal. Because of this the number of drops per unit volume exerts a much smaller influence on the magnitude of the signal. However, one must not always neglect small drops, since their number per unit volume may be  $10^6$ - $10^8$  times larger than that of large ones.

The effective radar area, as follows from (9), is inversely proportional to the fourth power of the wavelength at which the radar operates. This means that when the wavelength is decreased the probability of detection of small drops and the maximum range of detection of the precipitation zone increase. However, one must bear in mind here always the increase in the attenuation with decreasing wavelength, which may appreciably limit the maximum range of detection of the precipitation zones.

At the present time to detect clouds one uses radars operating most frequently at wavelengths 0.86-1.25 cm, while for precipitation zones the wavelength used is 3-10 cm [79]. The use of a 3-cm radar is advantageous in modern latitudes, where the intensity of the precipitation is on the average smaller than in tropical regions. Here, however, it is advantageous to use a 10-cm radar, since the attenuation at this wavelength is much smaller [31].

Strictly speaking, the power of the received signal depends on

the wavelength not only because of the factor  $1/\lambda^4$  contained in Eq. (10), but also because of the frequency dependence of the dielectric constant  $\epsilon$ . In practice, however, the influence of the last factor is small. Thus, at a temperature of  $18^\circ$ , the value of  $\epsilon$  changes from 78.5 - 112.3 for  $\lambda = 10$  cm to 34.2 - 135.9 for  $\lambda = 1.25$  cm. The corresponding change in the factor  $|\epsilon - 1/\epsilon + 2|^2$  in (10) lies in the limits 0.9286-0.9206.

Condensed water exists in the atmosphere not only in the form of liquid drops, but also in the form of ice crystals, hail, snow, etc., which in moderate latitudes are encountered no less frequently than liquid water particles. In calculating their effective scattering area the main difficulty consists of the fact that ice particles do not have such a simple geometrical form as the spherical water drops. Furthermore, in spite of the fact that the imaginary part of the refractive index, i.e., the absorption, can be neglected for ice and the dielectric constant can be regarded as a real number, the problem of reflection from ice particles has not been solved completely to this very date.

Ice crystals, which are found in cirrus clouds at temperatures below  $-40^\circ$ , represent for the most part platelets with transverse area of several microns and thickness of a fraction of a micron. In altostratus clouds at a temperature near  $-15^\circ$  one encounters most frequently small prisms with transverse dimension of a fraction of a micron and a height of several microns. In nimbostratus clouds crystals with hexagonal structure predominate.

However, as a result of the fact that the dimensions of all the ice crystals indicated above are much smaller than the wavelengths at which the modern radar receivers operate, only the electric dipole excitation is of importance. In first approximation we can regard this

to be a volume phenomenon only, not dependent on the form of the particles. It is therefore possible to extend Formula (9) to this case, too. Then the effective area per unit volume of the cloud, consisting of ice crystals, will be determined by the following relation:

$$\eta = 0.11 \frac{Wm}{\rho \lambda^4} \left| \frac{\epsilon - 1}{\epsilon + 2} \right|^2 k, \quad (11)$$

where  $W$  is the amount of ice in  $\text{g/m}^3$ ,  $m$  is the average mass of each crystal in grams,  $\rho$  is the density of ice, and  $k$  is a dimensionless coefficient close to unity, introduced because the shape of the crystal deviates from a sphere.

Inasmuch as the dielectric constant of ice is appreciably smaller than that of liquid water, the factor  $|\epsilon - 1/\epsilon + 2|^2 = 0.16$  and not 0.92. Consequently, the intensity of reflection from cirrus, altostratus, and nimbostratus clouds, which consist of ice crystals, is approximately one fifth that from clouds consisting of water drops of the same dimensions and the same concentration. In the icy clouds indicated above, the water content is very small and amounts to 0.01-0.1  $\text{g/m}^3$  at a particle dimension not exceeding several microns. Because of this, the intensity of reflection from such clouds is appreciably smaller compared with reflection from water clouds, let alone clouds which produce liquid precipitation.

In those cases when snow crystals are observed, the dimensions of which may reach 2-3 cm and which have a complicated form, the calculation of their effective radar scattering area becomes exceedingly difficult and insufficiently accurate. Some authors have made comparisons of reflections from snow and rain of identical intensity. The intensity was expressed in mm/hr. As a result it turned out that snow consisting of flakes weighing from 1 to 2 mg yields on the average the same reflection as rain of the same intensity.

Snow crystals frequently assume a complicated form, since individual snow flakes are produced as they are precipitated, with dimensions that can reach 2-3 cm. In this case their dimensions are comparable with the wavelength, and their complicated form makes rigorous calculations of the reflection from them very difficult. Furthermore, we must bear in mind the fact that the crystals forming the snow flakes are located at such short distances from one another as compared with the wavelength, that their radiation is coherent and the reflection is proportional to the number of such crystals squared. Thus, the snow precipitated in the form of flakes gives a reflection which is many times larger than snow falling in the form of individual small flakes. In the case when the snow crystals melt and are further transformed into rain drops, the reflection increases even more, principally because of the increase in the dielectric constant. During the time of melting, the small snow flakes have a falling speed which is close to that prior to the start of melting. Later on, however, they acquire rapidly the same speed as falling rain drops and their concentration decreases. This in turn leads to an increase in the magnitude of the reflection.

In the summertime the precipitation sometimes is in the form of hail. In the calculation of the effective radar area of an individual hail stone, some deviation in its form from spherical can be disregarded. However, the dimensions of hail stones frequently are comparable with the wavelength. Therefore to calculate the reflection from hail it is necessary to employ the exact formulas.

In those cases when the hail consists of hail stones of equal dimensions, its effective area per unit volume is given by the formula

$$\eta = \frac{q}{mv} I,$$

where  $I$  is the intensity of precipitation in  $\text{g/m}^2$  per sec,  $v$  is the

velocity of the falling hail stones at the earth's surface, in m/sec,  $m$  is the mass of one hail stone in grams, and  $\sigma$  the effective area of one hail stone in  $m^2$ .

Finally, it must be noted that other solid particles which are in suspended state in the atmosphere can produce a radar reflection. Sand storms, dust, smoke should also scatter electromagnetic waves. Inasmuch as in these cases the dimensions of the individual particles are considerably smaller than the wavelength, their effective radar area can be determined with sufficient accuracy with the aid of the Rayleigh relation.

The dimensions of sand particles are close to dimensions of rain drops, so that one can expect noticeable reflections from sand storms. On the other hand, dust particles usually have much smaller dimensions, not exceeding several microns. Consequently, and also because of their concentration, the reflection is proportional to the cube of the linear dimensions of the individual scattering particles. Therefore reflection from dust clouds and smoke is exceedingly small.

Electromagnetic waves may be reflected also from atmospheric formations on the boundaries subject to radical change in the dielectric constant  $\epsilon$ . This change may occur because of a radical change in the temperature or humidity of the air in the direction of radio-wave propagation. Such jumps can be observed on the boundaries of inversions and of convective and turbulent formations of the atmosphere.

If the inhomogeneity of the atmosphere represents an inversion layer characterized not only by the increase in temperature but also disclosing a drop in the air humidity with increasing height, one can assume that starting with a range  $R$  equal to the height of the inversion the refractive index  $n$  within the limits  $\Delta R$  of this layer will vary with a constant gradient. Further, denoting by  $Q$  the area of the

inhomogeneity, we can determine the effective area with the aid of the following relation:

$$\sigma = \frac{Q^2}{4\pi} \left[ \frac{d(n-1)}{dR} \right]^2 \sin^2 \left( \frac{2\pi \Delta R}{\lambda} \right). \quad (12)$$

where

$$n = 1 + \frac{79}{T} \left( p + \frac{4800e}{T} \right). \quad (13)$$

In Formula (13)  $p$  is the pressure of the humid air in millibars,  $T$  is the absolute temperature, and  $e$  is the partial pressure of water vapor in millibars.

Using the method of K.S. Shifrin, we can show that in the case of an abrupt change in the humidity by 10-15% the effective area of the inhomogeneous layer will be of the same order of magnitude as many types of clouds.

We can assume that the inhomogeneities consist of unevenly placed clusters of molecules and that the distribution of the refractive index within each such cluster is expressed by the relation

$$(n - n_0) = n_1 e^{-\frac{r}{a}(x^2 + y^2 + z^2)},$$

where  $a$  is the dimension of the cluster and the origin is located at its center.

Then the effective reflecting area of the cluster can be calculated on the basis of the formula

$$\sigma = \frac{1}{\pi} \left( \frac{2\pi}{\lambda} \right)^4 n_1^2 a^6 e^{-\frac{3\pi^2 a^2}{\lambda^2}}. \quad (14)$$

Formula (14) can apparently be used for an approximate calculation of reflections from convective and turbulent formations of the atmosphere. Individual portions of these formations represent the above-mentioned "clouds" of molecules, which scatter the radio waves noncoherently, and consequently the magnitude of the total reflecting area is the sum of individual effective areas of the "clouds."

In conclusion it must be noted that questions pertaining to the theory and practice of detection of dielectric inhomogeneities of the atmosphere still need further development.

#### 4. ATTENUATION OF ELECTROMAGNETIC WAVES

In the general case the magnitude of the received signal from the clouds and from the precipitation decreases in proportion to the square of the distance. For a single target, such as an airplane, this decrease is proportional to the fourth power of the distance. The indicated distance, as can be readily seen, is due to the fact that the reflecting volume of the cloud and precipitation zones increases with increasing range in proportion to the square of the distance.

In addition to the attenuation of the electromagnetic energy with increasing distance to the clouds and the precipitation, one must also bear in mind the attenuation due to the following factors: absorption by the water vapor and oxygen, molecular scattering by atmospheric gases, and finally scattering and absorption by the particles of the clouds and precipitation.

From among the gases contained in the atmosphere, electromagnetic energy is attenuated by oxygen and by water vapor, and this attenuation is almost exclusively by means of absorption. The molecules of oxygen interact magnetically with the field of the radio waves, while the molecules of the water vapor interact electrically with this field. Both in the case of absorption in oxygen and in the case of absorption in water vapor, there are frequency ranges where the absorption is large because of resonant phenomena. In the case of oxygen this region lies near wavelengths 0.5 and 0.25 cm, and at this resonant frequency the attenuation may exceed 15 db/km. In water vapor resonance takes place at a wavelength of 1.3 cm and the absorption is much smaller.

Figure 3 has shown the overall molecular absorption in moist air



(at a specific humidity  $7.5 \text{ g/m}^3$  and a temperature  $20^\circ$ ).

In those cases when the propagation of electromagnetic waves occurs in cloudy and precipitation zones, the molecular absorption in the gases is supplemented by attenuation due to scattering and absorption of energy by the particles of the cloud and the precipitation.

The attenuation of the flux of electromagnetic energy on passage through the atmospheric formations indicated above is described by the following relation:

$$S = S_0 e^{-\int \gamma dx},$$

where  $S_0$  is the Umov-Poynting vector to the zone of clouds and precipitation,  $dx$  is the width of the zone of clouds and precipitation, and

$$\gamma = \int_0^\infty N(D) Q(D, \lambda) dD.$$

Here  $N(D)dD$  is the number of particles per unit volume having diameters ranging from  $D$  to  $D + dD$ , and  $Q(D, \lambda)$  is the overall effective area of the particles, equal to the sum of the effective scattering and absorption areas  $Q = Q_s + Q_t$ .

In practice it is more convenient to express attenuation in terms of the parameter  $\alpha$ , which has the dimensionality of decibels per kilometer, and which is connected with  $\gamma$  by the relation  $\alpha = 4.43\gamma \text{ db/km}$ . In the general case  $N(D)$  and consequently  $\alpha$  and  $\gamma$ , are functions of the distance  $x$  along the propagation path of the electromagnetic waves. It is known from experimental data that the number and dimensions of particles making up the clouds and the precipitation exhibit great variation in space. Therefore an exact calculation of the attenuation is difficult and can be carried out only when the phase state of the particles and their distribution by dimensions are known. Yet the presently existing methods for measuring microphysical characteristics of

clouds and precipitation are not sufficiently accurate and furthermore such measurements are carried out only sporadically.

As was indicated above, for drops of small dimensions the effective scattering area is proportional to  $D^6/\lambda^4$ . On the other hand, the effective absorption area is proportional to  $D^3/\lambda$ . It is clear therefore that the effective absorption area is much larger than the effective scattering area. As a result of this, in the presence of drops of sufficiently small dimensions, the attenuation is determined almost completely by the absorption and is proportional to the diameter of the drops raised to the third power, i.e., to the water content. This condition is well satisfied for clouds and fog at all wavelengths, used in modern radars. For cloud drops it is applicable for decimeter wavelengths and within certain limits even for wavelengths of several centimeters.

It was found empirically that in the wavelength range from 0.5 to 10 cm [31] the attenuation can be expressed, accurate to 5%, by the following formula

$$\alpha = 0.438w/\lambda^2 \text{ db/km}, \quad (15)$$

where  $w$  is the water content in  $\text{g/m}^3$  and  $\lambda$  is the wavelength in cm.

By way of an example, Table 4 shows the values of the attenuation in clouds and fog at a water content of  $1 \text{ g/m}^3$  and a temperature of  $18^\circ$ .

TABLE 4

$\lambda$ , cm	0.2	0.7	1.0	1.25	2.0	3.0	5.0	10.0
$\alpha$ , db/km	7.14	0.88	0.438	0.280	0.112	0.05	0.0178	0.0045

1) cm; 2) db/km.

Both Formula (15) and the data on the attenuation listed in Table 2 are based on the assumption that the temperature of the drop is equal to  $18^\circ$ . To take into account the influence of the temperature, the right half of (15) must be multiplied by a coefficient whose values

at different wavelengths and different temperatures are listed in Table 5.

TABLE 5

$t^{\circ}$	$\lambda$ cm			
	0,5	1,25	3,2	10,0
0	1,59	1,93	1,98	2,0
10	1,20	1,29	1,30	1,25
20	0,95	0,95	0,95	0,95

It is seen from the table that when the temperature varies from 0 to 20°, the attenuation may decrease by 1.5-2 times.

For rain drops Formula (15) is no longer valid and it is necessary to solve the attenuation problem by using Mie's formulas.

Inasmuch as for meteorological practice it is necessary to know not the distribution of the raindrops by dimensions but the intensity of the precipitation expressed usually in millimeters per hour, the attenuation for various wavelengths is presented as a function of the precipitation intensity in Table 6.

TABLE 6

$I$ мм/час 1	$\lambda$ cm			
	0,3	1,0	3,2	10,0
0,25	0,305	0,037	0,00224	0,0000
1,25	1,15	0,228	0,0117	0,00041
2,5	1,98	0,492	0,0317	0,00072
12,5	6,72	2,73	0,298	0,00369
25,0	11,3	5,47	0,555	0,00724
100,0	33,3	20,0	2,80	0,0311

1) mm/hr.

The table lists the values of the attenuation at a temperature of  $18^{\circ}$  [31].

The data of Table 6 enable us to draw certain qualitative but important conclusions. The attenuation in rain of waves shorter than 10 cm is insignificant and can be neglected in practice. The attenuation of waves from 10 to 3 cm can be appreciable quite rarely, namely in the case of very intense rain.

When considering attenuation in rain, it must be borne in mind that although the intensity of the rain may be large at a given point during a short period of time, in order to produce noticeable attenuation the rain must be of large extent. For this reason, short-duration strong showers may be less significant than continuous rain covering a large region.

The attenuation of waves shorter than 3 cm in rain increases rapidly with decreasing wavelength, and waves 1.25 cm and shorter attenuate even in moderate rains much more strongly than in water vapor and in oxygen.

Table 6 lists the values of the attenuation coefficients  $\alpha$ , calculated at a temperature  $18^{\circ}$ . At other temperatures  $\alpha$  will generally speaking have other values. However, in the range of wavelengths for which the attenuation coefficient in rain must be taken into account in practice ( $\lambda$  less than 3 cm) the influence of the temperature does not exceed 20 or 30%, so that it can be neglected in many cases.

Attenuation in hail, dry snow, and ice crystals is many times smaller than in liquid-drop clouds and precipitation, and is therefore usually disregarded. An exception is wet snow, the attenuation in which, according to the investigations of N.V. Rogova, may be commensurate with attenuation in rain, and in some cases may even exceed it.

We have indicated above the values of the attenuation separately

for clouds, rain, and solid water particles. Under real conditions, when nimbostratus and cumulonimbus clouds and the associated precipitation are present, the propagation of radio waves will occur in different parts of these clouds, characterized by different phase state of the water particles and different dimensions of these particles. As a result, the accuracy with which the attenuation is determined under such conditions is appreciably lower.

The filling coefficient. In estimating the power of the reflected signals from meteorological targets or for an estimate of the limiting range of detection, it is essential to take into account the value of the so-called filling coefficient, which, as was indicated above, is the ratio of the volume of the pulse in space, filled with cloud and precipitation, to the entire volume of the pulse. The value of the filling coefficient depends in general on the geometrical dimensions of the irradiated zones of clouds and precipitation, the width of the directivity pattern, and the distance to these zones.

With increasing distance between the radar and the zones of the clouds and precipitation, the height of the electromagnetic beam above the surface of the earth, even at angles  $0^\circ$  and less, increases as a result of the earth's curvature. Since the zones of the clouds and the precipitation have limited vertical dimensions, starting with a certain distance the electromagnetic beam turns out to be above the upper limit of the zones indicated above.

The dependence of the height of the cross section of the beam on the distance, with account of UHF refraction, is expressed by the following simple relation:

$$H = R^2/16.9 + a,$$

where  $H$  is the height of the beam above the earth's surface, in meters,  $R$  is the distance to the zone of the cloudiness and precipitation in

kilometers, and  $a$  is the height of the radar above the earth's surface in meters.

For small ranges to the cloud and precipitation zones, the height of the beam above the earth's surface, even in the case of a large beam width, is smaller than the height of the upper limit of the indicated zones, and the filling coefficient is equal to unity. This is followed by a range interval in which the beam gradually turns out to be less and less filled with cloud and precipitation particles. Here the filling coefficient becomes less than unity and at a certain distance it vanishes. It is obvious that this distance is equal to the maximum possible range of detection and is independent of either the technical characteristics of the radar or of the intensity of the cloudiness and precipitation zones.

In observing nimbostratus clouds and continuous precipitation, and also frontal cumulonimbus clouds and the associated shower precipitation, which have large horizontal dimensions, the filling coefficient will depend on the range, the width of the directivity pattern, and the vertical thickness of these zones. Its value can be determined with the aid of the following expression

$$k_z = \frac{E - \left( \frac{R^2}{16.9} + a \right)}{R\theta_2},$$

where  $E$  is the height of the upper limit of the reflecting part of the clouds and the precipitation in meters and  $\theta_2$  is the width of the directivity pattern in the vertical plane in radians.

In those cases when intramass showers and thunderstorms are observed, whose horizontal dimensions as a rule do not exceed 10-15 km in width, the filling coefficient decreases much more rapidly with increasing distance to the shower. With this, its value can be calculated from the following formula:

$$k_3 = \frac{(R\theta_1 - L) \left[ \varepsilon - \left( \frac{R^2}{16.9} + a \right) \right]}{R\theta_1 L_2},$$

where  $\theta_1$  is the width of the directivity pattern in the horizontal plane and  $L$  is the dimension of the precipitation zone in a direction perpendicular to the radio beam.

#### 5. CHOICE OF WAVELENGTH FOR RADARS FOR METEOROLOGICAL PURPOSES

In the design of radar stations intended for the detection of clouds and precipitation, principal attention must be paid to the choice of the wavelength. Radar stations used for meteorological purposes operate in the 10, 5, 3, 1.25, and 0.8-cm bands [79, 62].

It frequently turns out that the meteorologist must use some particular radar station not because the wavelengths are the most suitable, but because it is necessary to use existing radars constructed for other purposes.

The effective reflecting surface of cloud and precipitation particles whose linear dimensions are insignificant compared with the wavelength, is proportional to  $1/\lambda^4$ . However, the increase in the attenuation of the incident and reflected electromagnetic energy at very short wavelengths can be larger than the compensation due to the higher reflecting ability, which in final analysis leads to a decrease in the detection range.

Recently questions concerning the choice of wavelengths for radar used in storm warning were dealt with by Ye.M. Salman and W. Hitchfield [37]. In connection with the fact that at the present time radar stations are coming into use not only for the detection of showers and thunderstorms but also for measurement of cloud altitudes [9], V.D. Stepanenko made a detailed analysis of the choice of optimal wavelengths for radars for meteorological purposes, with account of climatic characteristics of the clouds and precipitation, which are typ-

ical for medium latitudes.

### Detection of Regions of Shower Precipitation

To determine the most suitable wavelength it is necessary to carry out a thorough analysis of the backward scattering and attenuation, with account of those meteorological propagation conditions, which are characteristic from the climatic point of view for a given geographic region. The maximum range of detection  $R_{\max}$  of clouds and precipitation is proportional to the square root of the product of their scattering area by the attenuation coefficient, i.e.,

$$R_{\max} = \sqrt{V \sigma k}. \quad (16)$$

As was already indicated, the effective backward-scattering area per unit volume of clouds and precipitation can be expressed by the well-known relation, corrected for the deviation from the Rayleigh law,

$$\sigma = \frac{\pi^2 \Sigma N D^6}{\lambda^4} \left| \frac{\epsilon - 1}{\epsilon + 2} \right|^2 \cdot 10^{-30} c, \quad (17)$$

where  $D$  is the diameter of the drops in microns,  $N$  the number of drops per  $\text{m}^3$ ,  $c$  a correction coefficient which takes into account the deviation of the Rayleigh scattering from the real one ( $c = 1$  when  $D \ll \lambda$ );  $\sigma$  is expressed in  $\text{cm}^{-1}$  and  $\lambda$  in cm.

Inasmuch as the reflecting characteristic  $\Sigma N D^6$  correlates with the physical characteristics of the clouds used in meteorology, namely water contents  $w$  in  $\text{g}/\text{cm}^3$  and the precipitation intensity  $I$  in  $\text{mm}/\text{hr}$ , we shall express  $\sigma$  henceforth in terms of  $w$  and  $I$ . Indeed, for the backward scattering area per unit volume of rain we obtain

$$\sigma = 6 \cdot 10^{-3} \frac{I^{1.8}}{\lambda^4} c, \quad (18)$$

where  $\sigma$  is in  $\text{cm}^{-1}$ ,  $\lambda$  in cm, and  $I$  in  $\text{mm}/\text{hr}$ .

For clouds  $c = 1$  and

$$\sigma = 13.2 \cdot 10^{-12} \frac{w^2}{\lambda^4}. \quad (19)$$



where  $\underline{w}$  is in  $\text{g/m}^3$ .

The expression for the coefficient which takes into account the attenuation of radio waves in the troposphere can be written in the form

$$k = 10^{-0.2 [ \alpha_1 R_{\text{maks}} + \alpha_2 w R_2 + \alpha_3 R_3 ]} \quad (20)$$

The first term in the exponent takes into account the attenuation in the gases of the atmosphere ( $R_{\text{maks}}$  is the maximum detection range in km,  $\alpha_1$  is the attenuation coefficient in oxygen and in water vapor in db/km), the second takes into account the attenuation in the clouds ( $R_2$  is the extent of the clouds in the direction of radio-wave propagation, in km,  $\underline{w}$  their water content in  $\text{g/m}^3$ , and  $\alpha_2$  the attenuation coefficient in clouds in db/km/ $\text{g/m}^3$ ), while the third term takes into account the attenuation in rain ( $R_3$  is the extent of the rain in the direction of radio-wave propagation in km,  $I$  its intensity in mm/hr, and  $\alpha_3$  is the unit attenuation coefficient in rain in db/km/mm/hr).  $\alpha_1$ ,  $\alpha_2$ , and  $\alpha_3$  depend not only on the wavelength but also on the temperature. At one and the same temperature but at different values of  $\alpha$ , the change in these coefficients does not exceed 3 db in the range  $\lambda = 0.5-10$  cm [31].

On the basis of (18), (19), and (20) we obtain for rain

$$R_{\text{max}} = \sqrt{6 \cdot 10^{-8} \frac{I^{1.6}}{\lambda^4} c \cdot 10^{-0.2 [ \alpha_1 R_{\text{maks}} + \alpha_2 w R_2 + \alpha_3 R_3 ]}} \quad (21)$$

and for clouds

$$R_{\text{max}} = \sqrt{13.2 \cdot 10^{-12} \frac{w^2}{\lambda^4} 10^{-0.2 [ \alpha_1 R_{\text{maks}} + \alpha_2 w R_2 + \alpha_3 R_3 ]}} \quad (22)$$

In order to solve the question of the optimum wavelength for a meteorological radar station, it is necessary to find the right halves of the indicated relations for different wavelengths and to compare them with one another. The quantities necessary for the calculation are listed in Table 7, which is based on the data of several authors

[30, 42, 72].

TABLE 7

1 Длина волны, см	2 $\sigma_{\text{дождя}} \text{ см}^{-1}$	3 $\sigma_{\text{облаков}} \text{ см}^{-1}$	4 $\sigma_1 \text{ дБ/км}$	5 $\text{дБ/км/г/м}^3$	6 $\text{дБ/км/мм/час}$
	4	5		2	3
0,8	$13,6 \cdot 10^{-8}$	$33,3 \cdot 10^{-12}$	0,06	0,66	0,25
1,25	$2,45 \cdot 10^{-8}$	$5,35 \cdot 10^{-12}$	0,16	0,28	0,1
2	$4,0 \cdot 10^{-9}$	$8,2 \cdot 10^{-13}$	0,015	0,11	0,03
3	$7,4 \cdot 10^{-10}$	$1,6 \cdot 10^{-13}$	0,011	0,044	0,02
4	$2,3 \cdot 10^{-10}$	$5,7 \cdot 10^{-14}$	0,008	0,027	0,006
5	$10^{-10}$	$2,1 \cdot 10^{-14}$	0,007	0,018	0,003
6	$4,4 \cdot 10^{-11}$	$10^{-14}$	0,007	0,012	0,0015
7	$2,5 \cdot 10^{-11}$	$5,4 \cdot 10^{-15}$	0,0065	0,009	0,001
8	$1,5 \cdot 10^{-11}$	$3,2 \cdot 10^{-15}$	0,0065	0,007	0,0006
9	$9,0 \cdot 10^{-12}$	$2,0 \cdot 10^{-15}$	0,006	0,0054	0,0004
10	$6,0 \cdot 10^{-12}$	$1,3 \cdot 10^{-15}$	0,006	0,004	0,0003

1) Wavelength, cm; 2)  $\text{дБ/км/г/м}^3$ ; 3)  $\text{дБ/км/мм/час}$ ;  
4) of rain; 5) of clouds.

With the aid of Table 7 and Relations (21) and (22) it is possible to plot curves whose horizontal axes represent the wavelengths in cm and the vertical axes the right half of Relations (21) and (22). The plots of Figs. 16-19 are constructed for  $\lambda = 0.8, 1.25, 2, 3$  cm, etc., in steps of 1 cm up to 10 cm inclusive.

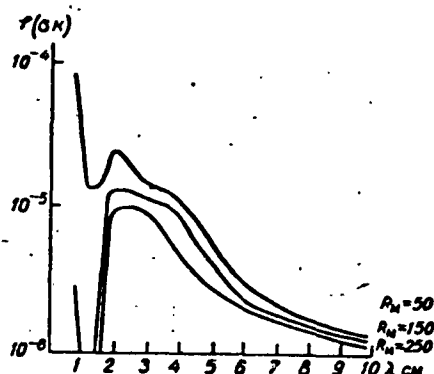


Fig. 16. Detection of the nearest boundary of the region of precipitation through a cloud;  
 $w = 0.3 \text{ г/м}^3$ .

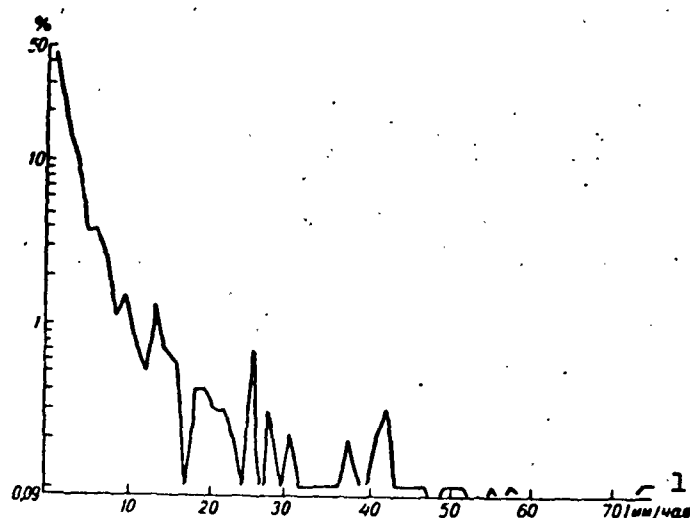


Fig. 17. Probability of precipitation of rain of different intensity. 1)  $I$ , mm/hr.

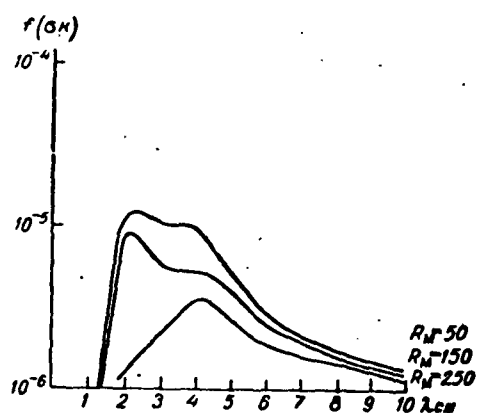


Fig. 18. Detection of the far boundary of the precipitation region;  $I = 10$  mm/hr,  $w = 1$  g/m<sup>3</sup>.

The plot of Fig. 16 pertained to the case of detection of a precipitation-region boundary closest to the radar station, located at distances 50, 150, and 250 km, in the presence of screening clouds and in the absence of screening precipitation. The horizontal extent of these clouds is taken to be one third the distance from the precipitation zone to the radar station, and their water content is assumed to be 0.3 g/m<sup>3</sup>. These conditions are apparently characteristic for the

warm time of the year under meteorological conditions that give rise to showers and thunderstorms.

An analysis of the plot shows that at small distances (up to 50 km) even the 8-mm band is effective. However, at large distances the optimal wavelengths are 2 or 3 cm. Most unsuitable is 1.25 cm, since the electromagnetic waves at this wavelength experience very strong attenuation in the gases of the atmosphere (0.16 db/km).

Cases can be observed when the radar station is separated from the precipitation region not only by clouds but also by precipitation zones. In the summertime of the year, as a rule, showers fall, a characteristic feature of which is relatively short horizontal extents, which rarely exceed 10 km\* [19].

The probability of a second region of shower precipitation being located between the radar station and a region of shower precipitation within 250 km is not large and amounts to approximately 10 or 15% (Fig. 17). Thus, for the shower precipitation region boundary closest to the radar station the best band, with probability 85-90% are the 2 and 3 cm bands, as can be readily seen on Fig. 16.

An analysis was also made of the detection of the far boundary of regions of precipitation of varying intensity, from weak rain (1 mm/hr) to showers (150 mm/hr) with a width of 10 km. The analysis has shown that in the case of weak and moderate shower rains up to 250 km, and at strong rains up to 150-200 km, the optimum wavelengths, with probability 85-90%, are also 2 and 3 cm. Only for the detection of far boundaries of strong rains, at a distance of 250 km, and of showers whose frequency amounts to only several percent (Fig. 18), wavelengths 4-5 cm become optimal.

During the cold time of the year in the shore regions of the Baltic, the north, and the east of the USSR, one frequently observes the

so-called snow showers, which move from the sea to the dry land. The intensity of the precipitation in these snow showers rarely exceed 2 or 3 mm per hour. Consequently, again the optimum wavelength for their detection is 2-3 cm.

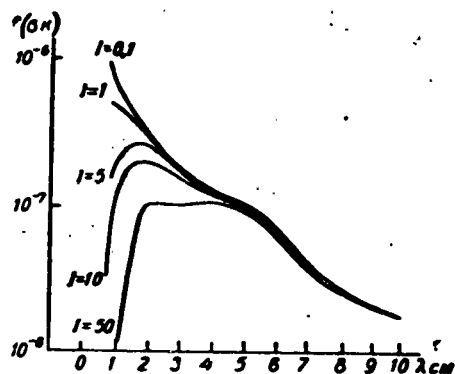


Fig. 19. Detection of the upper limit of nimbus clouds;  
 $w = 0.5 \text{ g/m}^3$ ,  $R_2 = 10 \text{ km}$ ,  
 $R_3 = 5 \text{ km}$ .

#### Determination of Heights of Clouds

The optimum wavelength for the determination of the heights of the lower boundaries of nonrainy clouds, located at a distance up to 10 km, in the absence of screening cloud layers, is 0.8 cm.

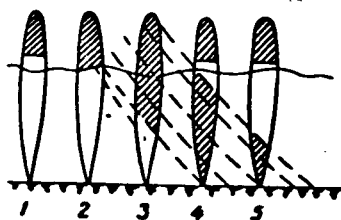


Fig. 20. Space-time pattern of nimbus clouds passing over a radar station.

For equal potentials of the radar station, the maximum range of detection at  $\lambda = 0.8 \text{ cm}$  is approximately 10 times larger than at  $\lambda = 10 \text{ cm}$ .  $\lambda = 0.8 \text{ cm}$  is also the best wavelength both for the detection of the upper limits of the clouds, including very dense ones ( $w = 1 \text{ g/m}^3$ ) within the limits of

the indicated distance (Fig. 19), and for the detection of the upper limits of clouds which produce drizzle and weak rain for any water content of the clouds, up to  $1 \text{ g/m}^3$ , when the vertical extent of the

rain zone does not exceed 5 km.\* Only when the rain intensity is not less than 5 mm/hr does the optimum wavelength rise to 2 or 3 cm.

The frequency of rains with intensity larger than 5 mm/hr amounts to about 25% for moderate latitudes. Thus, the 8-mm wavelength is optimal in 100% of the cases when determining the heights of all the non-rainy clouds and in 75% of the cases when determining clouds that give liquid precipitation. If we bear in mind the determination of the height of the upper limit of the clouds during the wintertime, when the precipitation has the form of snow, hail, etc., in which the attenuation of the radio waves is quite small, then the 8-mm band will have even a greater percentage of optimality.

In those cases when falling large water or ice particles are situated under the clouds, in the form of drops of drizzle, rain, hail, or snow, the use of radar stations operating at wavelengths much larger than the dimensions of the foregoing particles ( $\lambda \gg d$ ) for the measurement of the height of the lower limit of the clouds is either completely impossible, or accompanied by large random errors. Indeed, in the case when a rain, hail, or snow covers a large space, the radio beam is filled with the falling particles and the height of the lower limit of the clouds cannot be measured, since it starts at the start of the sweep ( $H_n = 0$ ). If drizzle falls in the form of individual inclined strips, the height of the lower limit of the clouds, measured with a radar station, is actually the height of the lower limit of the precipitation zone and consequently  $H_n < H_c$ .\*\*

To explain the foregoing let us turn to Fig. 20, which shows schematically the space-time pattern of the passage of rain clouds. This figure shows the position of the directivity pattern of the radar station relative to the passing clouds and precipitation, so that we can see the change and the difference in the radar height of the lower

limit of the clouds as compared with their actual height. In position 1 the radar is most likely to give too high a value for the lower limit of the clouds. Position 2 characterizes the time during which the lower radar limit coincides with the actual one. In position 3 the height of the lower limit of the clouds will be underestimated by the radar. In position 4 the lower limit merges with the image of the local objects. Finally, in position 5 we see well the upper limit of the precipitation and a somewhat too high limit of the clouds. In examining Fig. 20 we must bear in mind that in positions 1 and 5 the radar height of the lower limit of the cloudiness may coincide with the actual height if the water content of the clouds in the lower part is sufficient for detection.

The indicated peculiarities and errors in the measurement of the height of the lower limits of the clouds are inherent in the radar method at a wavelength considerably higher than the dimensions of the particles. In those cases when light waves are used ( $\lambda < d$ ), operating experience has shown that the actual height of the lower boundary of the clouds coincides with the measured one. This fact is attributed to the different laws governing the backward scattering at  $\lambda \gg d$  and  $\lambda < d$ . Indeed, why does a radar for which  $\lambda \gg d$  not measure the height of the lower boundary of nimbus clouds? The reason for it is that the increment in the signal due to the accumulation of small cloud drops on their lower boundary comprises a negligibly small quantity, which cannot be detected by modern means. In fact, when  $\lambda > d$  the scattering area of the drop is given by the Rayleigh relation (17).

Let us imagine precipitation from clouds consisting of clusters of drops with diameter  $d_1 = 2 \cdot 10^{-3}$  cm, in the form of rain drops with diameter  $d_2 = 0.2$  cm. For a cloud drop, according to (17), when  $\lambda = 3$  cm we have  $\sigma_1 = 3 \cdot 10^{-18}$  cm<sup>2</sup> =  $3 \cdot 10^{-22}$  m<sup>2</sup>. On the other hand, the scat-

tering area of a volume of  $1 \text{ m}^3$  containing  $10^9$  drops is equal to  $\sigma_1 = 1.9 \cdot 10^{-11} \text{ m}^2/\text{m}^3$ .

For  $1 \text{ m}^3$  of rain containing 300 rain drops, we have accordingly  $\sigma_2 = 2 \cdot 10^{-6} \text{ m}^2/\text{m}^3$ .

Comparing the scattering areas of the rain and the clouds we see that the former scattering area is five orders of magnitude larger than the latter. Since the rain drops are located not only in the space between the lower boundary of the clouds and the earth's surface, but also inside the clouds, the echo signal from the rain drops under the clouds is practically equal to the echo signal from the lower boundary of the clouds, where there exist not only rain drops but also cloud drops.

On the other hand, if the radar operates on a wavelength smaller than the dimension of the particles of the indicated atmospheric formations ( $\lambda < d$ ), the pattern of backward scattering will be entirely different. In this case the scattering area will in accordance with [7] be expressed by

$$\sigma = \pi d^2 F(\beta \rho), \quad (23)$$

where  $F(\beta \rho)$  is a function that depends on the scattering angle  $\beta$  and  $\rho = 2\pi d/\lambda$ .

With the aid of (2.43) and (2.44) from the paper of K.S. Shifrin [30] we obtain for  $F(\beta \rho)$

$$F(\beta \rho) = \frac{I(\beta \rho)}{\pi \rho^2}.$$

In turn

$$I(\beta \rho) = \frac{\rho^2}{4} \left[ \frac{\tau(\beta)}{2} + (a')^2(\beta) \right],$$

where

$$a' = \rho(1 + \cos \beta) \frac{J_1(\rho \sin \beta)}{\rho \sin \beta}.$$



Since we are interested in the back scattering,  $\beta = 180^\circ$ . At this value of  $\beta$  we have  $\tau(\beta) = 0.1918$  [30] and  $a' = 0$ .

The net result is

$$F(\beta) = \frac{\tau}{8\pi} = 7.7 \cdot 10^{-3}. \quad (24)$$

Thus, the scattering area of the rain drops and clouds, for which  $\lambda < d$ , is determined from the following formula, which is derived with account of (24):

$$\sigma(\pi) = \pi d^2 \cdot 7.7 \cdot 10^{-3}. \quad (25)$$

With the aid of Formula (25) we can find the scattering area of one cubic meter of rain and clouds:

for rain

$$\sigma_1 = 4.7 \cdot 10^{-5} \text{ m}^2/\text{m}^3, \quad (26)$$

for clouds

$$\sigma_2 = 2.5 \cdot 10^{-4} \text{ m}^2/\text{m}^3. \quad (27)$$

From a comparison of (26) and (27) it follows that the echo signal from the lower boundary of the clouds, where small cloud drops are located, exceeds by more than five times the echo signal of rain. This is fully satisfactory for suitable measurement of the height of the lower boundary of the clouds which produce precipitation.

It is also useful to compare the scattering areas for  $\lambda = 3 \text{ cm}$  and for the optical range. A comparison shows that the scattering area of clouds, calculated for the optical range, is approximately seven orders of magnitude larger than for the radio range, while that of rains is larger by approximately two orders of magnitude.

All the facts noted above indicate that it is preferable to use wavelengths  $\lambda < d$  for the measurement of the heights of the lower limits of clouds. However, in order to measure the heights of the upper limits of the clouds, and also to warn against showers and thunder-

storms, it remains advantageous to use wavelengths  $\lambda > d$ , for they are incomparably less subject to attenuation during the course of propagation than optical waves. Practical experience of operation of optical detection and radar detection confirms the foregoing conclusion. In this connection, it is recommended that multiband radar stations be used for meteorological purposes, and that one band be in the optical range.

Manu-  
script  
Page  
No.

[Footnotes]

- 58 For simplicity the volume is assumed to be cylindrical. In this case, as shown by G.M. Burlov, the errors for most radars used in meteorology, starting with a distance 1.5-2 km, do not exceed 1 or 2%.
- 59 The number of drops 0.15 cm in diameter is assumed here to be 100%.
- 81 We have in mind intramass showers and thunderstorms.
- 83 In our latitudes this vertical extent of the rain is close to maximal.
- 83 Here  $H_n$  is the height as determined by the radar and  $H_c$  the actual height.

Manu-  
script  
Page  
No.

[List of Transliterated Symbols]

- 48  $\varepsilon = e = \text{effektivnyy} = \text{effective}$
- 57  $\text{и} = i = \text{impul's} = \text{impulse}$
- 75  $\varepsilon = z = \text{zapol'neniye} = \text{filling}$
- 78  $\text{макс} = \text{maks} = \text{max} = \text{maximum}$

## Chapter 4

### PRACTICE OF RADAR DETECTION OF ATMOSPHERIC FORMATIONS

#### 1. USE OF RADAR FOR THE DETECTION AND INVESTIGATION OF CLOUDINESS AND PRECIPITATION

To ensure high grades of observations of cloudiness and precipitation, the correct choice of the location of the radar is of great significance. The principal requirement that must be satisfied by the place where the station is located is that the space can be readily surveyed in all directions.

To this end, the radar should be mounted on an open and high space (the roof of a building, a hill, etc.) so that local objects located around it do not rise above the horizon by  $2^{\circ}$ , or better still so that these objects are below the level of the radar installation.

When the station is installed it must be leveled and also oriented with respect to the compass directions. These operations must be repeated periodically in order to exclude the possibility of errors in the determination of the azimuth and the elevation angle during measurements of cloudiness and precipitation zones. After the radar is installed, it is necessary to study the images of the local objects on the receiver screens. For this purpose observations are made during clear weather or weather with little cloudiness, and the images of the local objects on the receiver screens are photographed. The photographs obtained make it possible to distinguish the images of the meteorological targets from the images of the local objects.

During the course of radiometeorological observations, the re-

ceiver screens must be photographed without fail in order to maintain complete documentation.

At the present time there is a clear-cut distinction made between radars intended for the detection of a precipitation zone, particularly for warning in advance against storms and showers which are of great danger to aviation, and radars used to detect and investigate clouds and other dielectric inhomogeneities of the troposphere.

Radar stations used to detect precipitation zones operate in the wavelength range from 3 to 10 cm and use a main pulse of large power [72]. During the operation of such stations, the search for the precipitation zones must begin with a distance equal to the maximum operating radius of the employed radar. This is necessitated primarily by consideration of timely warning of the interested institutions of the approach of such dangerous phenomena as showers, thunderstorms, and hail.

For a better observation of showers and thunderstorms it is necessary to carry out observations with antenna elevation angles  $0-2^{\circ}$ , varying this angle smoothly after each rotation of the antenna in azimuth.

Observation of continuous precipitation is best carried out at large antenna elevation angles, namely  $5-10^{\circ}$ .

If the operating radius of the radar is 150-200 km, then timely warning of individual regions can be provided 5-8 hours in advance, taking account of the encountered speeds of displacement of the continuous and shower precipitation.

An image of the precipitation zone traced or photographed from the circular-scanning indicator (IKO) makes it possible to determine its distance from the radar station and its azimuth, and also to estimate approximately the form and dimensions of the horizontal area, if

the sweep scale is known. In addition, from the results of two or more observations carried out within not less than 10 or 15 minutes, it is possible to determine the direction and velocity of displacement of the precipitation zone.

We shall show below circular-scan images at different instants of time obtained from one and the same precipitation zone, located in a direction  $290-330^{\circ}$  and at distances 12-20 km (see Figs. 27 and 28). It is easy to see that during the 10-minute time interval the center of gravity of the precipitation region shifted 6 km in a west-northwest direction. This shift corresponds to a speed of 36 km/hr.

In addition, it is possible to estimate approximately the area of the reflecting precipitation zone, the intensity of the precipitation (from the brightness of the glow on the circular-scan screen), and its evolution.

Along with obtaining images of continuous and shower precipitation using a circular scan, which gives the radio echo picture in a horizontal plane, it is also important to have vertical sections.

Such sections are obtained either by using special receivers or with the aid of a circular-scan indicator in which the sweep can rotate in synchronism with the rotation of antenna both in azimuth and in elevation from  $0$  to  $90^{\circ}$ .



Fig. 21. Vertical time section through precipitation zone. Sounding height 4200 meters.

In this case, knowing the sweep scale, it is possible to determine the width and height of the reflecting precipitation zone from the

given azimuth.

Inasmuch as the time of antenna rotation in elevation from 0 to  $90^\circ$  usually does not exceed 10-20 seconds, it can be assumed that this method gives an instantaneous image of the reflecting zone in the vertical plane. Along with such sections it is possible to obtain vertical time sections in the height-time coordinates. In the latter case the antenna is set at an elevation angle of  $90^\circ$ , i.e., vertically upward, and the image of the stationary sweep line is projected with the aid of a special photographic attachment on film which is wrapped around a drum rotating at a rate such as to make one revolution in 20-30 minutes. During the time that the precipitation passes over the station, the glow brightness of the individual portions of the sweep line on the circular-scan indicator will depend on the distribution of the reflecting properties of the precipitation in a vertical direction. As a result, a picture similar to that shown in Fig. 21 is obtained on the photographic film.

The procedure for detection of clouds and other atmospheric formations, which produce weak reflected signals, consists primarily of using radar equipment operating in the wavelength region from 3 cm downward [9, 66].

Under the guidance of V.V. Kostarev, a radar installation (Fig. 22) with large reflector was developed and built at the TsAO. The radio beam produced by the antenna unit of the radar station is stationary and directed vertically upward.

By photographing on a moving film the stationary sweep line on an indicator with target brightness indication (IKO), vertical time sections of the clouds and other inhomogeneities are produced in their transport direction. The rate of motion of the film is usually between 1 and 5 mm/min.

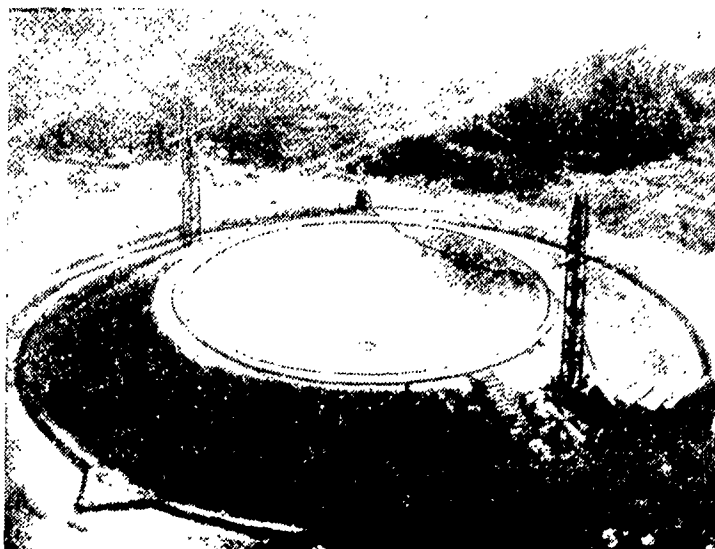


Fig. 22. Over-all view of modernized radio installation of the TsAO.

Recently, in connection with progress in radar technology, equipment operating in the millimeter band came into use for these purposes [62, 79]. Within this range, the radars are capable of detecting not only precipitation zones and all forms of clouds, but also certain dielectric inhomogeneities of the atmosphere.

## 2. RADAR IMAGES AND THEIR PHYSICAL INTERPRETATION

By now much factual material has been accumulated on radar images of precipitation zones. There are much fewer data on the results of radar images behind clouds and other atmospheric formations.

Engaging in the analysis and physical interpretations of radar reflections (which we shall call briefly radio echos) were N.F. Kotov, P.N. Nikolayev, R. Wexler, M. Ligda, and others [10, 67, 69].

### Image of Precipitation Zone

In the analysis and systematization of the images of precipitation zones on radar indicator streams, it is necessary to take into account the fact that the character of these images depends on the procedure used in the radar sounding.

We consider below the classification of radar images of precipitation zones on a radar for the 3 cm band, type H2X [82] and CPS-9 [62]. This classification can be extended without much error to include other radar equipment, too.

The first type of radio echo - a bright strip or layer - is usually observed in the fall or in the spring upon passage above the radar of a nimbostratus cloud which produces weak continuous rains or wet snow, the intensity of which does not exceed 2 mm/hr. Most frequently this precipitation is due to the passage of warm fronts, occlusion fronts, or cold fronts of the first kind.

On the basis of the results of simultaneous radar, airplane, and radio sounding it was established that the bright strip is the image of the layer in which the snow flakes that fall from the nimbostratus clouds melt. The upper boundary of this layer almost coincides with the zero isotherm. Its thickness is on the average 300 m. There are no images above and below the bright strip.

The occurrence of the bright strip can be explained in the following manner. The small snow flakes falling above the zero isotherm have a small effective scattering area, and the weak signal from them is not registered by the radar. On falling lower and reaching the height of the zero isotherm, the snow flakes begin to melt and are covered with a film of liquid water. Because the dielectric constant of water is several times larger than that of ice, the reflected signal from the melting snow flakes will also be larger. Also contributing to the increase in the signal will be the fact that at below-zero temperatures that are close to zero, i.e., as the snow crystals approach the level of the zero isotherms, the crystals can easily stick to one another and form larger snow flakes than those situated above.

With further drop of the snow flakes, after crossing the zero-



isotherm level, their melting becomes more and more intense and at a certain height they turn into rain drops. The dimensions of these drops and their concentration is smaller, owing to the rapid rate of fall, than that of the falling snow flakes. Because of this the signal reflected from the rain drops is also smaller and if the rain has a low intensity it may not be registered at all by the radar.

The bright strip on different types of indicators and under different methods of radar sounding has different forms. When vertical sections are obtained, its appearance is usually as shown in Fig. 23. In the case when the antenna rotates around a vertical axis at a definite elevation angle, the bright strip on a circular-scan indicator has the form of a concentric white ring. It is obvious that the radius of the ring depends on the elevation angle of the antenna and on the height of the bright strip. To determine the actual height and width of the bright strip it is necessary to multiply the radius of the ring by the sine of the elevation angle.

On an indicator with amplitude marker (range), it is best to view the bright strip at antenna elevation angles  $10-20^{\circ}$ . The amplitude of the signal received from the melting layer is small, and the form of the signal is symmetrical.

The second type of radio echo is observed also in continuous precipitation, the average intensity of which amounts to 2-4 mm/hr. This continuous precipitation can be classified as moderate to strong. Usually it is connected with the passage of clearly pronounced warm fronts and occlusions.

The second type of radio echo is a bright strip with an image of the zones situated above or below the strip. In the vertical section, the zone situated above the bright strip can have the form either of layers inclined to the bright strip, or horizontal layers, or finally



Fig. 23. First type of reflection from precipitation. Image of bright strip in a vertical cut through continuous precipitation. Distance between scale markers is 2 km.

formations that have no definite form.

The zones located under the bright strip consist of minute suspended cloud drops and falling rain drops which are larger than in the first type of radio echo. As regards the images above the bright strip, it was at first assumed that they are the image of only sufficiently large snow flakes that fall inside the cloud. It turned out later, however, that the images above the bright strip can be attributed equally well to either the falling snow drops or to suspended or falling supercooled drops of water. This is confirmed by practice gained in radio-meteorological observations, for it is very rarely possible to obtain the image of a snowfall in "pure form," i.e., in the layer from the lower boundary of the cloud to the earth. At the same time, the images located above the bright strip are encountered quite frequently, in spite even of the fact that as a rule they are located farther away from the radar than the images of the snow that falls directly above

it. This circumstance brings to mind the idea that the contribution of the supercooled drops to the formation of the image above the bright layer is appreciable if not commensurate.

This contribution can also be direct when there is added to the scattering of the radio waves by the snow flakes also scattering by the supercooled drops of water, or may be the result of continuous settling of relatively large drops on the surface of the snow flakes. During the time that the latter fall, something like a supercooled film of liquid water is formed. The fact that a cloud is seeded with supercooled drops is well known. In this case, under particularly favorable conditions, it can lead to a sharp increase in the dielectric constant of the snow flakes, and consequently to an increase in the scattering of the radio waves in the granulated layer. As the snow flakes pass through the granulated layer and enter into layers with smaller drops, which do not coagulate with the snow flakes, they can again have only one ice phase. Their dielectric constant again decreases and this leads to a decrease in the scattering of radio waves and to a vanishing of the image on the radar indicator.

The second type of radio echo has its own modifications, in which one observes either a bright band with the image of the supercooled zone only, or else with a zone of rain under it.

A typical view seen in vertical sections is the one shown in Fig. 24.

On indicators with amplitude markers, the second type of radio echo is characterized by a few splashes, the height and width of which is somewhat larger than in the first type.

The third type of radio echo is observed usually in the case of intensive rain at the surface, averaging 10 mm/hr. Participating in its formation are principally cumulonimbus clouds and shower



Fig. 24. Second type of reflections in vertical section of moderate continuous precipitation. Distance between scale markers is 2 km.

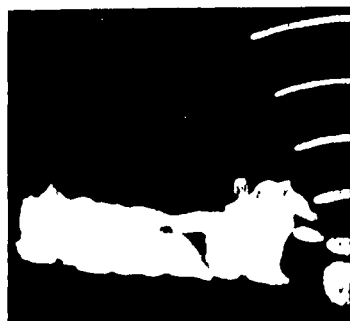


Fig. 25. Third type of reflections in vertical section through moderate shower precipitation. Distance between range scale markers is 2 km.

precipitation, connected with the passage of secondary cold fronts or cold occlusion fronts. One obtains on the radar indicators a quite distinct region of rain and a less noticeable region of melting. Figure 25 shows the third type of radio echo in a vertical plane. The figure shows clearly other characteristic features of this type, connected with singularities in the structure of cumulonimbus clouds, with their microphysical structure, and with their geometrical shape. The images represent white bright spots, on the upper or middle parts of which one can notice the melting layer. The latter, which is usually intermittent, is thicker than in the first and second types of reflections. Frequently the main image merges with the image of the melting layer. The

considered (third) type is apparently connected with the following state of the cumulonimbus cloud. In the upper part of the cloud, in the zone above the zero isotherm, the precipitated water particles represent predominantly soft or hard hail. If they pass through the supercooled layer, they produce an image above the melting layer. In the opposite case there will be no image observed of the supercooled zone. If the hail enters the region of above-zero temperatures, it begins to melt without appreciably changing its rate of fall and the dimensions. As a result they turn into rain drops. The dielectric constant and the



Fig. 26. Third type of reflection in circular scan. Distance between scale markers 2 km.

number of particles remain practically unchanged from the height of the zero isotherm to the earth. Consequently, the bright band merges with the image of the rain. In those parts of the cumulonimbus cloud where the precipitating particles predominate in the form of snow, the bright band becomes noticeable.

A typical image of the third type of radio echo in the case of circular scan is shown in Fig. 26.

The last and fourth type of radio echo comprises reflections from powerful frontal and intramass cumulonimbus clouds, which produce strong shower rains with intensity on the order of 40-50 mm/hr, or else hail. The characteristic feature of the fourth type of radio echo is the complete lack of visible images of the melting layer, i.e., of bright strips. This is the only type of radio echo in which one can observe images of supercooled parts of a cumulonimbus cloud in the absence of a bright strip. Another feature of this type of radio echo is the large vertical extent, which reaches heights of 10-12 km.

Figures 27, 28, and 29 show characteristic patterns of this type of radio echo in the horizontal plane on a circular-scan indicator and on an indicator with amplitude marking, respectively. A striking feature of the last figure is the exceedingly large amplitude of the received signal.

The formation of images from thick cumulonimbus clouds can be explained in the following manner. First, the absence of a bright strip indicates that the hail stones predominate absolutely over the snow flakes in the zone of below-zero temperatures. Second, the large ver-

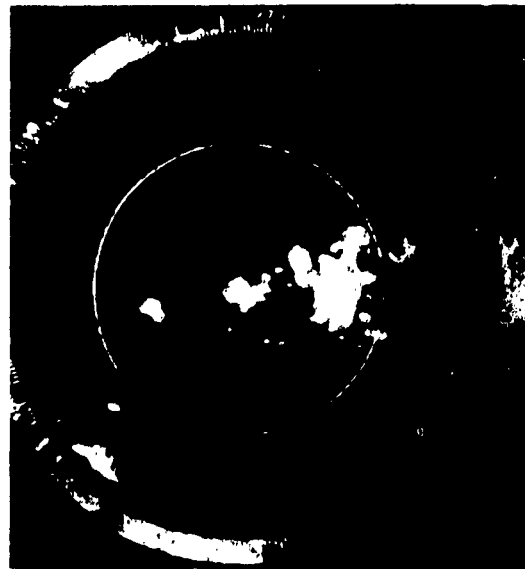


Fig. 27. Fourth type of reflections in a horizontal section through strong shower precipitation. The scale marker is at a distance of 10 km.



Fig. 28. Fourth type of reflections in circular scan. Scale marker every 10 km.

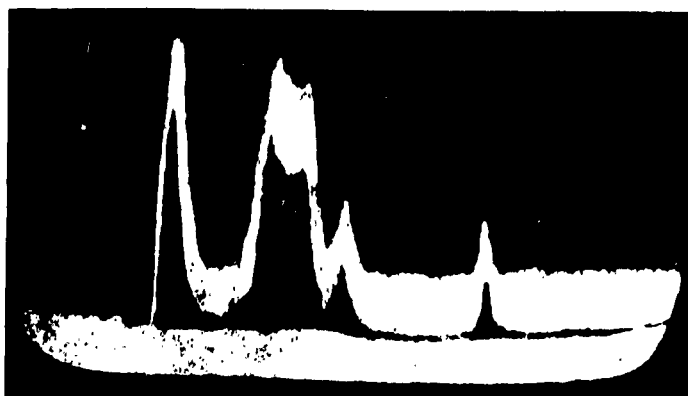


Fig. 29. Fourth type of reflections on an indicator with amplitude marking.

tical extent suggests that there is possibly a considerable difference in the distribution of the temperature inside the cumulonimbus cloud as compared with its distribution outside the cloud (the temperature is higher inside the cloud). In addition, an important role is also played by the factor of wetting and seeding of the hail drops. Because of this, a considerable part of the supercooled zone can have almost the same dielectric constant as the melting and rain zone.

#### Images of Clouds

Radar as used for the detection of clouds uses antennas which are directed vertically upward. Because of this one obtains on the indicator screens an altitude-time section through the clouds passing over the station.

We shall consider below the characteristics of vertical images of the fundamental forms of clouds which produce no precipitation, obtained by observation with two radar stations: the modernized radar of the TsAO and the 1.25-cm foreign APS-34 equipment [9, 66].

Cumulus clouds. In the detection of vertical-development clouds, one of the principal factors in the production of the radio echo is the degree of development of these clouds. As a rule, only thick cumulus clouds begin to give images (Fig. 30). Cumulus clouds in good

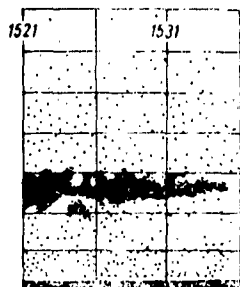


Fig. 30. Reflections from thick cumulus clouds. Sounding height 7800 meters.



Fig. 31. Reflections from stratocumulus clouds. Sounding height 4800 meters.

weather and broken cumulus clouds do not produce images, with rare exceptions. In the initial state the radio echo of thick cumulus clouds is weak, and has an uncertain outline. When the thick cumulus cloud is in the developed state, the peak of the radio echo becomes sharp and the radio echo then assumes the shape of a column. One observes images of the falling bands, the curvature of which in a vertical direction corresponds to the vertical wind photograph.

Stratocumulus clouds (Fig. 31). The images of translucent and opaque stratocumulus clouds are rather weak and differ little from each other. They have a shaggy upper boundary, made up of short tightly packed strips. The dense portions of the radio echo have the same appearance as the horizontally converging air streams. The density of the radio echo decreases in the lower and middle parts toward its upper part. Observations show that stratocumulus clouds are best observed at below-zero temperatures.

Stratus clouds (Fig. 32). In spite of the closeness to the radar, stratus clouds are observed well only when drizzle is observed. The radio echo has the form of fluffy strips with a rather even upper boundary. The base of stratocumulus clouds is rarely observed, since it is usually masked by images of local objects and by the drizzle. The density of the radio echo changes little in time and in altitude, owing to the homogeneous structure of the stratus clouds.

Alto cumulus clouds. The images of alto cumulus translucent clouds





Fig. 32. Reflection from dense stratus and altostratus clouds. Sounding height 8000 meters.

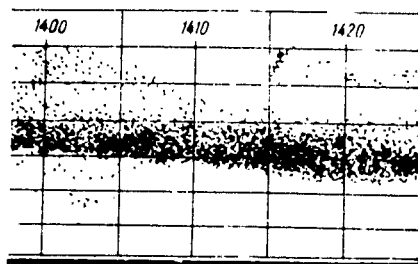


Fig. 33. Reflection from transparent altostratus clouds. Sounding height 7800 meters.

have the form of closely arranged strips, the bases of which are bent backward at an average angle of  $45^\circ$  to the horizon. An increase in the density in the upward direction is most frequently observed.

Altostratus clouds. Translucent altostratus clouds produce images (Fig. 33) a characteristic feature of which is the even outline of the base and top. The lower part of the cloud is homogeneous, and has a medium density. Toward the upper part the density of the radio echo decreases until the image completely disappears.

Weather-flight results have shown that the majority of altostratus clouds are encountered at temperatures between  $5$  and  $-35^\circ$  and the radar images were frequently due to crystals of ice or snow.

Cirrus clouds. The clouds of the upper layer give very weak radio echos and are detected relatively rarely. The easiest to detect among the cirrus clouds are the cirrostratus clouds, the radio echos of which are very similar to the radio echos of altostratus clouds and differ only in having a lower density.

Image of turbulent and convective formations. The radio echos of turbulent and convective formations, obtained under the guidance of V.V. Kostarev, were observed only during the bright time of the day at

the start of cloudiness and in cloudless weather. Their appearance on the screen of the radar indicator is apparently due to reflection of electromagnetic waves from the eddy formations, which are regions in space where the dielectric homogeneity is disturbed, and on whose boundaries one observes a considerable change in the temperature and humidity.

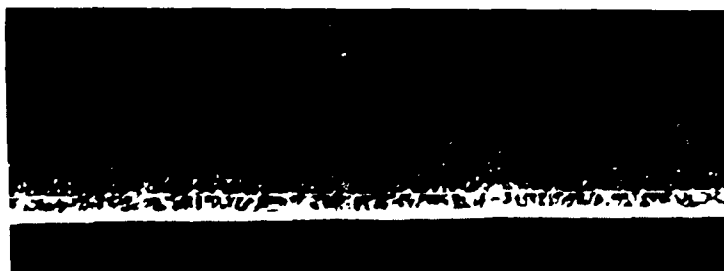


Fig. 34. Reflection from convective and turbulent formations. Sounding height 8000 meters.

In the given case the radar reflection has the form of short strokes or bars (Fig. 34). The width and length of these strokes corresponds to the dimensions of the eddies. The limiting height of detection of such reflections amounts to about 5 km.

### 3. ERRORS IN RADAR OBSERVATIONS OF CLOUDS AND PRECIPITATIONS

Only recently has the accumulated experience made it possible to investigate the errors in radar observations of clouds and precipitations. Yet an estimate of the errors in meteorological observations is very useful.

At the same time, a preliminary evaluation of the errors is in practice exceedingly difficult, so that as a rule the errors are classified as random. Studies of radar observation errors were made by V.V. Kostarev, K.S. Shifrin, V.D. Stepanenko, and D. Atlas [8, 9, 61].

Errors due to the dimensions of the sounding pulse. As is well known, the length of a radio pulse in space and its angular width are due to the directivity pattern of the antenna and the mode of the

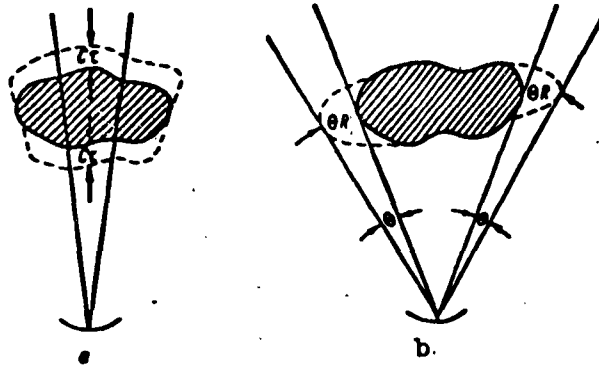


Fig. 35. Explaining the distorted form of the precipitation zone due to the finite duration of the pulse (a) and the finite width of the directivity pattern (b).

radar transmitter.

The length of the pulse does not depend on the distance to the target, and the width varies as  $R^2$ . Indeed, the sounding pulse has a spatial extent  $c\tau_1 = h$ . When the pulse passes through the precipitation zone, the reflected signal arises at the instant when the leading front of the pulse touches the reflecting particles (the forward boundary of the cloud or precipitation zone), then increases and reaches a maximum value upon complete entry of the radio pulse into the reflecting medium. When the pulse leaves this region, the reflected signal vanishes only after the trailing front of the pulse is situated in a space free of cloud and precipitation particles.

Assuming that even very small reflected signals can be discerned on the indicator, we reach the conclusion that the radial dimension of the precipitation zone will be increased by a factor  $2c\tau_1 = 2h$ . If we assume that only the maximum signal corresponding to total penetration of the radio pulse into the precipitation is observed, then the radial dimension will be decreased by the same amount  $2c\tau_1 = 2h$ . Obviously, the error will be eliminated if the signal appears on the indicator at the instant when half the extent of the pulse has entered the precipi-

tation zone.

Figure 35a shows the distortion of the actual form of the precipitation zone caused by the duration of the pulse.

Inasmuch as for existing radars  $\tau_1$  may have values 0.1, 0.3, 0.5, 1.0, and 2.0  $\mu\text{sec}$ ,  $h$  will, respectively, equal 30, 100, 150, 300, and 600 meters.

In the case of warnings against storms and showers, owing to the appreciable distances the radars usually operate in a mode with long pulse duration ( $h = 300\text{-}600\text{ m}$ ), so that this compensates to a certain degree for the attenuation of the reflected signal due to the distance. Consequently, the most frequent error occurs in the determination of the distance to the shower and its geometrical parameters in a radial direction, amounting to 600 - 1200 meters.

However, taking into account the features of thunderstorms and showers, their variability in time and in space, this error can be neglected in practice. Indeed, what practical value can be attached to the fact that the distance to a thunderstorm located 100 km away has been determined with an error of  $\pm 600$  or 1200 meters?

The situation is different if one determines the height of the reflecting layers of clouds and precipitation situated above the station. It is quite clear that a determination of height with the errors indicated above (600-1200 m) is very crude. Consequently, the radar operates in the mode where the values of  $\tau_1$  are the smallest, i.e., 0.1, 0.3, and 0.5  $\mu\text{sec}$  ( $h = 30, 100, \text{ and } 150\text{ m}$ ). Consequently, the heights of the clouds will be determined with absolute errors on the order of 30-150 meters. It is therefore easy to see that layers of clouds and precipitation which are spaced in height by less than  $h$  may appear to be merged.

Further, as a result of the increase in the width of the beam

with increasing distance from the target to the station, the error in the direction perpendicular to the beam axis increases. The linear dimension of the false broadening is  $2\theta R$ , where  $\theta$  is in radians.

Figure 35b shows the distortion of the image of the precipitation zone resulting from the finite angular width of the electromagnetic beam, while Table 8 shows its values at different distances for a radar in which  $\theta = 3^\circ$ .

TABLE 8

R, km	1	10	100
$\theta R$ , km	0.052	0.52	5.2

It is seen from Table 8 how important the error can be in a direction perpendicular to the beam axis. It must be particularly taken into account when determining the vertical thickness of showers which are located at large distances. Indeed, at a distance of 100 km this error may reach 5 km.

Errors due to "secondary sweep." The phenomenon of secondary sweep usually takes place in radars characterized by a short operating radius (on the order of 30-60 km). This phenomenon is observed on the circular-scan indicator screen in the form of false images of the precipitation zones.

The secondary sweep is due to signals from showers located beyond the limits of the theoretical range of the station. The reflected signals produced by them are much larger in intensity than the ordinary signals and are therefore observed at anomalously large distances. The time of travel of the radio waves from the transmitter to the reflecting shower and back to the receiver is longer at such large distances than the time interval between pulses. Since the cycle of motion of the sweep spot begins every time during the instants that a pulse is emitted and terminates before the transmission of the next pulse, the

signal received from a shower situated beyond the range of the station is "delayed" and is received by the receiving unit after the radiation of the next pulse. As a result, this image will appear among the images of the signals from the close-lying targets, arriving during the next operating cycle of the station. In this case the range will appear to be much shorter than the true one, and the form of the image will not correspond to the real outlines of the precipitation zone.

To determine the true range one uses the relation

$$R_1 = R' + c/2F,$$

where  $R'$  is the range to the image in the case of secondary sweep,  $c$  the velocity of propagation of light, and  $F$  the pulse repetition frequency.

One can visualize a case in which the time elapsed from the instant of radiation to the instant of reception of the reflected signal exceeds twice the time interval between pulses. However, in practice this case is little likely, since the reflected signals arriving from the precipitation zones will be too weak to be detected and in addition the height of the electromagnetic beam above the earth's surface will at such large distances undoubtedly be much larger than the height of the precipitation zone.

The dimension of the reflecting region of the precipitation zone, which produces the secondary-sweep image, can be determined from the following formula (if the filling coefficient is  $K_z = 1$ )

$$L_1 = L'R_1/R',$$

where  $L_1$  is the tangential dimension of the image, corresponding to the actual size of the precipitation zone, and  $L'$  is the width of the zone as read on the circular-scan indicator in the case of secondary sweep.

It can be shown that there exists a region which has the form of

a ring with a center at the location of the radar station, inside of which precipitation zones are not observed in either the form of ordinary bright images or in the form of secondary-sweep images. The width of this "blind" ring B can be represented by the formula

$$B = c/2F - R_{\max},$$

where  $R_{\max}$  is the maximum range which can be obtained on the circular-scan indicator.

Images obtained as a result of secondary sweep have characteristic attributes which make it possible to distinguish them with sufficient accuracy from ordinary images of precipitation zones. These attributes are as follows:

the height of the peak of the reflecting zone is abnormally small and usually cannot be measured at all,

the image is stretched out in a radial direction.

From the secondary-sweep image, using the formulas given above, we can readily determine the true range and the dimensions of the source of reflection, and also the velocity and direction of the displacement. The azimuth of the displacement is determined directly, while the velocity must be multiplied by the quantity  $R_1/R'$ .

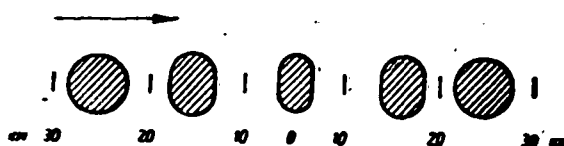


Fig. 36. Visible (apparent) variations of the area of the shower due to variation of the scale along the sweep.

Errors occurring when the scale changes along the sweep. In addition to the errors in radar detection of clouds and precipitation as considered above, it is necessary to bear in mind the errors due to the change of the scale along the sweep on a circular-scan indicator.

In the existing types of radar stations it is encountered quite frequently and is connected with the nonlinearity of the charging of the sweep-generator capacitor with time.

The variation of the scale can be readily detected by measuring the distance between neighboring scale rings (range markers). What is striking is the constant increase in distance between range markers in a direction away from the center of the screen (of the circular-scan indicator) to its periphery.

The change in scale along the sweep causes the image of the melting layer, on taking a vertical section through nimbostratus clouds from 0 to 90°, to have the appearance of not a horizontal bright strip but of a curve.

It is important to note how significant the increase of the scale along the sweep is. Indeed, at a distance of 2-3 km this increase amounts to 30-40%, while at 8 km its value is 50%.

Let us consider now the detection of an individual precipitation zone, which moves in a direction toward the radar, without changing its area or configuration (Fig. 36). Further, for simplicity, we shall assume that the radio waves do not attenuate and the images of the shower zone are not subject to distortion due to the change in the distance to the shower. Finally, we assume that the dimensions of the zone allow us to neglect the variations of the scale within the width of the zone itself.

As this zone approaches the radar, its image on the circular-scan indicator will become compressed, as it were, something particularly noticeable in the direct vicinity of the radar.

On the other hand, if the precipitation zone moves away, the converse will be observed, i.e., the image of the zone will increase as it were with increasing distance from the radar.



Finally, when the precipitation zone moves along a circle, no change of area will occur at all, in view of the constancy of the scale.

It was indicated above under what assumptions Fig. 36 was drawn. Under actual conditions, when the area of the precipitation zone and its intensity vary in time and in space, and also as a consequence of the attenuation of the electromagnetic waves, it will be exceedingly difficult to separate from the entire set of factors which cause the area of the radar images to change the particular factor connected with the change in scale along the sweep.

This problem is much easier to solve in the case of spatial vertical sounding of cumulonimbus clouds and continuous precipitation, when a bright strip is observed on the circular-scan indicator screen.

From the practical point of view, within the limits of 10-20 km it is perfectly permissible to assume the bright strip (the melting layer) horizontal. However, experience in obtaining spatial vertical sections shows that the bright strip is frequently a bent strip of the type shown in Fig. 23. Such an unusual form of the bright strip is precisely the consequence of the change in the scale along the sweep. A curved bright strip whose height decreases above the station can be obtained also theoretically, by using the variation of the scale along the sweep and its height.

It becomes clear from the foregoing that in determining the vertical and horizontal dimensions of the atmospheric formations it is necessary without fail to take into account the variation of the scale along the sweep. The account consists of using the scale which is observed at the range corresponding to the atmospheric formation.

Errors due to technical parameters of the radar and to the range and structure of the clouds and precipitation. We have considered

above errors in the radar detection of cloud and precipitation zones, when the operator observes the image of such zones on the radar indicator screens. These errors influence in one form or another the accuracy with which the range and the geometrical parameters of these zones are determined, and can be taken into account. Yet there are more significant errors, which depend on the technical parameters of the radar, on the range and structure of the clouds and precipitation, and which frequently cannot be evaluated at all.

The reasons and consequences of these errors become more easily understood after the following reasoning. If we denote the factor  $\pi^5 P_t A_p h / 48 \lambda^4 |\epsilon - 1/\epsilon + 2|^2$  in Formula (10) for the radar detection of clouds and precipitation consisting of liquid particles by  $C$ , the formula can be rewritten as

$$P_r = C \frac{\sum_i N_i D_i^6}{R^2} k k_r.$$

Let us illustrate, using the detection of precipitation as an example, the errors connected with the different values of the radar constant  $C$ .

A connection between  $\sum_i N_i D_i^6$  and the precipitation intensity  $I$  was obtained experimentally. For moderate latitude the most suitable connection is

$$z = 220 I^{1.6}, \quad (28)$$

where

$$z = \sum_i N_i D_i^6 \text{ mm}^6/\text{m}^3,$$

and  $I$  has the dimensions of mm/hr.

Then

$$P_r = C_1 \frac{I^{1.6}}{R^2} k k_r. \quad (29)$$

For what follows it is convenient to introduce the quantity  $\mu =$

$= P_r/P_{rmin}$ , where  $P_{rmin}$  is the minimum value of the power of the received signal, which can still be detected by the radar. The quantity  $\mu$  characterizes the brightness of the image on the circular-scan indicator screen or the height of the pulse on the range indicator. When  $\mu > 1$ , the image appears on the screen, and when  $\mu \leq 1$  the image disappears. Consequently, the geometrical locus of the points for which  $\mu = 1$  will be the boundary of the area of the images of clouds, precipitation, and other atmospheric formations.

Dividing both halves of (28) by  $P_{rmin}$ , substituting  $k$  in expanded form, and assuming the filling coefficient to be  $k_z = 1$ , we obtain

$$\mu = C_2 I_{(x)}^{1.6} (R+x)^{-2} \cdot 10^{-0.2\alpha \int_0^x I(x) dx}, \quad (30)$$

where  $I(x)$  is the distribution function of the precipitation intensity along the path of propagation of the sounding pulse,  $x$  the path covered by the pulse in the precipitation, and  $R$  the distance from the station to the forward boundary of the precipitation.

After taking logarithms of Eq. (30) we obtain

$$\lg \mu = \lg C_2 + 1.6 \lg I(x) - 2 \lg (R+x) - 0.2\alpha \int_0^x I(x) dx. \quad (31)$$

Equation (31) can be used to calculate the contour of the precipitation-zone image, if we set  $\mu$  equal to unity. In the calculations it is necessary to bear in mind that for  $\lambda \geq 5$  cm the coefficient is  $\alpha = 0$ , while for  $\lambda < 5$  cm it rapidly increases with decreasing wavelength. When  $\lambda = 3$  cm, the value of  $\alpha$  can be assumed to be 0.031 db/km/mm/hr [31].

It must be noted that different radars detect in different fashions the same atmospheric formations.

Along with the distortion considered above, an important role is played by distortion due to the distribution function of the precipi-

tation along the direction of propagation of the electromagnetic waves and due to the range to the precipitation.

It must be noted that a change in the range greatly influences the character of the image of one and the same shower. Its rear parts are particularly strongly distorted. The distortion occurs both because of the increase in the range and because of the attenuation of the radio waves in the shower. The influence of the last factor becomes particularly noticeable, if screening precipitation is found between the observed shower and the radar.

An interesting fact is that for  $\lambda = 5$  cm the increase in the intensity of the precipitation zone leads directly to an increase in the power of the received signal from all parts of the zone and, consequently, to a decrease in the distortion, and vice versa. In the latter case there occurs an instant when the entire precipitation zone produces a signal smaller than  $P_{\text{rmin}}$  and no image of the precipitation or other atmospheric formation is observed by the radar.

For  $\lambda < 5$  cm the increase in the intensity of the precipitation leads first to an increase in the power of the received signal, and thus to a decrease in the distortion. However, starting with certain values of the intensity and the width of the precipitation, the attenuation of the electromagnetic wave begins to predominate. This leads to a decrease in the power of the received signal and to an increase in the distortion, particularly in the rear parts of the precipitation zone.

Distortions in the geometrical dimensions of atmospheric formations are confirmed by the results of simultaneous radar and airplane observations of cumulonimbus and nimbostratus clouds and the associated precipitation. The results of these observations are shown in Fig. 37, from which it is seen that the vertical power of the radio echo on

a circular-scan indicator of a radar for storm warning is always appreciably smaller than the vertical extent of the cumulonimbus and nimbostratus clouds.

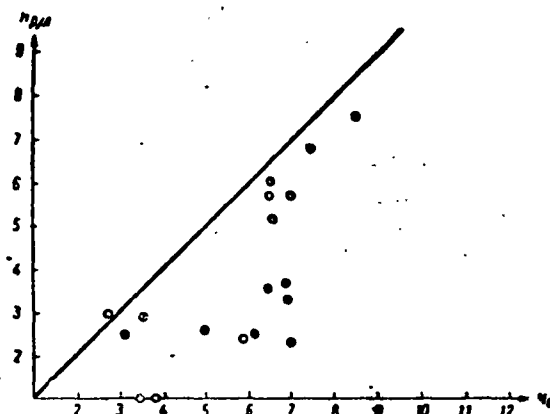


Fig. 37. Correlation between the real height of cumulus clouds and their radar height.

This radar detects the indicated cumulus clouds if their vertical extent is not less than 1 or 2 km. In 55% of the cases of their detection the upper boundary is located at heights larger than 6 km.

As regards the distortion of the horizontal dimensions, the most distorted are the nimbostratus clouds and the associated precipitation, inasmuch as their image on the circular-scan indicator of the aforementioned radar does not exceed as a rule 40 km in diameter. At the same time the actual horizontal dimensions of these clouds amount to hundreds of kilometers. The least to be distorted are cumulonimbus clouds, owing to their smaller dimensions and larger intensity of the precipitation falling from them.

#### 4. MEASUREMENT OF INTENSITY OF PRECIPITATION AND WATER CONTENT OF CLOUDS BY RADAR METHODS

Radar stations are used not only to observe the clouds and the precipitation, but also for quantitative measurements of the intensity of the precipitation and the liquid-water content of the clouds. The

results of these measurements make it possible, in addition, to formulate and solve such important practical problems as the quantitative estimate of the intensity of icing of airplanes, bumpiness, visibility in clouds, etc.

The theoretical basis for these measurements is the fact that the characteristic of the reflection of clouds and precipitation

$$z = \sum_i N_i D_i^4,$$

to which the power of the received signal is proportional, and the intensity of the rain, are connected for the case of moderate latitudes, as indicated above, by the expression

$$z = 220I^{1.6}.$$

For the liquid-water content of clouds  $w$ , when  $0 \leq w \leq 1.3 \text{ g/m}^3$ , we obtain

$$z = 0.048w^2.$$

Consequently, if we can determine quantitatively the power of the received signal relative to the sensitivity of the receiver  $\mu$  and use the relation

$$\mu = C_2 \frac{I_{(z)}^{1.6}}{(R+z)^2} k k_3, \quad (32)$$

we can determine the intensity of the rain.

For a reliable determination of the intensity of the precipitation one first determines by experiment the radar constants  $C_2$  which are contained in Relation (32). The radar measurements of the power of the reflected signal are made simultaneously with the meteorological measurements of the intensity of the rain. The meteorological measurements are usually carried out at short distances from the radar so as to reduce the influence of the attenuation coefficient. From the results of these measurements one obtains the constants  $C_2$  of the radars. Subsequently these constants are used for quantitative measurements of

atmospheric formations and for estimates of the effectiveness of their detection.

It must be noted, however, that in the constructions of surface, marine, and aircraft radars used in meteorology, the overwhelming majority of the equipment is equipped only for the detection of targets and not for the measurement of the power of the reflected signals. This circumstance raises certain difficulties when it comes to using radar stations for the aforementioned quantitative measurements of the meteorological elements and phenomena.

Recently, however, R. Langill, R. Donaldson, Ye.M. Sal'man, and A.B. Shupyatskiy [11, 18, 62] and others published data on methodological developments aimed at measuring the power of reflected signals from clouds and precipitation and their quantitative estimate.

Direct measurement of the power of the reflected signal is difficult in this case, since it is necessary to measure powers on the order of  $10^{-6}$ - $10^{-12}$  watt and less. When measuring such small values of power, the bolometric method cannot be employed. A convenient method is to compare the power of the measured field with the power produced at the same frequency by a signal generator.

To measure the power of reflected signals one uses the following control and measurement apparatus: radar tester 31 IM and oscilloscope EO-7. Information on the measuring instrument 31 IM is given in Chapter 7 below.

#### Measurement of the Power of the Reflected Signal

One distinguishes between different methods for measuring the power of a reflected signal, particularly between measurement of its amplitude on a type-A indicator and measurement with the aid of a calibrated attenuator at the input of the receiver.

Let us take some receiver used for the measurements. Let the power

of the reflected signal be regulated by the knob of an attenuator, the angle of rotation of which is read against the scale of a stationary dial with the aid of a pointer which is rigidly connected to the knob. Then the determination of the power of the received signal from the known value of its attenuation in decibels can be explained by means of the following arguments.

If we denote the power of the received signal by  $P_r$ , and its attenuation by  $\underline{n}$  (db), then after the attenuation we receive a signal  $P_{r,n}$ , which is smaller than the signal  $P_r$  by an amount  $10^{-0.1n}$ . We consequently get

$$P_{r,n} = 10^{-0.1n} P_r$$

If, for example,  $n = 20$  db, then  $P_{r,n}$  is smaller than  $P_r$  by 100 times.

Let us assume that we decrease the gain of the receiver by such a number of decibels,  $\underline{n}$ , which makes the signal  $P_{r,n}$  equal to  $P_{rmin}$ , i.e., equal to the sensitivity of the receiver, then

$$P_{r,n} = P_{rmin} = 10^{-0.1n} P_r \quad (33)$$

The latter relation enables us to determine the power of the received signal  $P_r$  from the known receiver sensitivity  $P_{rmin}$ , which is determined before each series of measurements, and from the attenuation  $\underline{n}$ .

The most accurate way of performing measurements of this type is by using a type-A indicator. However, in view of the relatively long measurement time, due to the fact that such measurements cannot be carried out with a continuously rotating antenna, it is advantageous in many cases to carry out the measurements with a circular-scan indicator. This makes it possible to obtain quite rapidly, after 10-15 seconds, a photograph of the power distribution of the reflected signal in a horizontal or vertical plane, and from this distribution deter-



mine the distribution of the intensity of the precipitation or the liquid-water content.

Photography of the circular-scan indicator with the antenna rotating is carried out in order to determine the values of  $\underline{n}$ , the attenuation of the received signal: in the case of weak and moderate precipitation the photographs are taken every 2 db, while in the case of showers they are taken every 5-10 db.

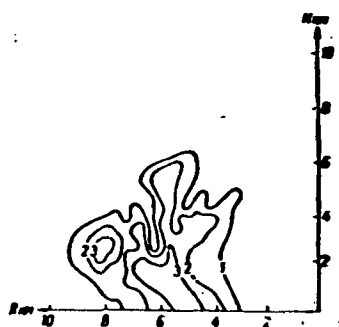


Fig. 38. Vertical distribution of rain intensity in a weak shower. The lines of equal rain intensity are drawn every millimeter per hour.

If the horizontal structure of the precipitation or of the liquid-water content is investigated, one records for each photographic frame the time, the scale, and the value of  $\underline{n}$  in decibels. In the case of vertical sections, the azimuth is also recorded.

The measurements are carried out from full gain down to the vanishing of the image on the screen. Each photograph gives the contour of the region corresponding to the minimum signal at a given receiver gain  $\underline{n}$  in a horizontal or vertical plane. The series of the photographs makes it possible to determine from the contours the distribution of the intensity of the precipitation or the water content of the clouds. For rain intensity one uses the relation

$$C_2 R_{(x)}^{1.5} (R+x)^{-2} 10^{-0.1n} k k_3 = P_{\text{min}} \quad (34)$$

By way of an example Fig. 38 shows the vertical distribution of rain intensity obtained by the radar method.

When working with a radar having  $\lambda > 5$  cm and  $k = 1$ , and also in the case of complete filling of the pulse, the last-mentioned relations make it possible to obtain in rather simple fashion reliable data. In those cases, however, when  $\lambda < 5$  cm, it becomes necessary to

take into account the attenuation of the rain [63].

Using the measurement of rain intensity as an example, let us illustrate the procedure whereby the attenuation of the electromagnetic wave is taken into account. After taking logarithms, we rewrite Eq. (34) in the following form, assuming that the rain fall begins at the radar station and fills the radio beam completely (under these assumptions  $R = 0$  and  $k_z = 1$ ):

$$0 = 10 \lg C_2 + 16 \lg l - 20 \lg x - n - 2 \int_0^x (k_1 + k_2 w + \alpha) dx, \quad (35)$$

where

$$k = 10^{-0.2 \int_0^x (k_1 + k_2 w + \alpha) dx}.$$

Here  $k_1$ ,  $k_2$ , and  $\alpha$  are the per-unit attenuation coefficients for the gases of the atmosphere, the clouds, and the rain, respectively.

Putting  $C_2 = (1/C_2^1)^{1.6}$  we rewrite (35) in the form

$$Y = 16 \lg l - 20 \lg x - 2 \int_0^x \alpha dx - 16 \lg C_2, \quad (36)$$

where

$$Y = n + 2 \int_0^x (k_1 + k_2 w) dx.$$

The quantity  $Y$  represents the reflected signal, corrected for the attenuation due to the atmospheric gases and the clouds. The attenuation of the electromagnetic waves by the gases of the atmosphere can be readily determined if the pressure and the humidity of the air are known. As regards the attenuation produced by the clouds, it can have practical significance only for wavelengths shorter than 3 cm, i.e., for those rare radar stations which detect clouds.

Relation (36), in the form in which it is written, does not make it possible to determine the intensity of the rain, since the value of

the attenuation in rain, i.e., the term  $2 \int_0^x \alpha dx$ , still remains unknown. To find this term we use experimental data which make it possible to express the per-unit attenuation coefficient  $\alpha$  as a function of the rain intensity  $I$  for different wavelengths. In general form, this dependence is expressed by the following relation:

$$\alpha = \alpha_1 I^{z-1}. \quad (37)$$

Then

$$\int_0^x \alpha dx = \int_0^x \alpha_1 I^z dx.$$

In those cases when  $\alpha$  is given in db/mile|mm/hr, we have for  $\lambda = 3$  cm the value  $\alpha_1 = 144 \cdot 10^{-4}$ , and  $z = 1.3$ ; for  $\lambda = 5-6$  cm we have  $\alpha_1 = 47 \cdot 10^{-4}$  and  $z = 1.1$ ; finally, when  $\lambda = 10$  cm we have  $\alpha_1 = 4.9 \times 10^{-4}$  and  $z = 1$ .

Taking (37) into account, Relation (36) is rewritten as

$$Y = 16 \lg I - 20 \lg x - 2 \int_0^x \alpha_1 I^z dx - 16 \lg C_2. \quad (38)$$

This equation can be represented in a form more convenient for the solution, namely:

$$Y = D \ln I - E \ln x - F \int_0^x I^z dx - D \ln C_2', \quad (39)$$

where

$$\begin{aligned} D &= 16 \cdot 0,4343 = 6,944, \\ E &= 20 \cdot 0,4343 = 8,680, \\ F &= 2\alpha_1. \end{aligned}$$

After differentiating (39) we get

$$\frac{dy}{dx} = \frac{D}{I} \frac{dI}{dx} - \frac{E}{x} - FI^z.$$

Making the substitution  $u = I^{-z}$  we obtain a linear differential equation, which can be solved with respect to  $I$ . The result of the solution is

$$I = \frac{x \frac{E}{D} \frac{Y}{D}}{\left[ \left( \frac{1}{C_2} \right)^2 - \frac{ZF}{D} \int_0^x \frac{E}{D} \frac{Y}{D} dx \right]^{\frac{1}{2}}}, \quad (40)$$

where  $(1/C_2)^2$  is the integration constant.

In principle  $C_2$  can be determined from (35) and (40). This is difficult to do algebraically, however. Consequently,  $C_2$  is frequently determined experimentally by simultaneously measuring the power of the reflected signals at the radar and the intensity of the rain with the aid of a pluviograph.

Another method of measuring the average values of the power of signals reflected from clouds and precipitation and their intensity is the method of standard target, used and developed in our country by A.B. Shupyatskiy [18]. If the echo signal from the precipitation is compared with the signal from the standard target sufficiently rapidly, it can be assumed that the instability of the radar parameters influences both signals to an equal degree.

The standard target employed is a corner reflector or sphere, whose effective surface should be commensurate with the effective area of the rains. For  $\lambda = 3$  cm it is sufficient to employ a trihedral corner reflector in which the length of each side is 130 cm. When the sides are perpendicular to one another, this guarantees an effective surface  $\sigma_{\Delta} = 1.17 \cdot 10^4 \text{ m}^2$  (see Table 14).

To install the standard target, it is best to use wooden masts, sufficiently far away from the radar. The height of the mast should guarantee direct visibility of the standard target from the location of the radar antenna.

The sequence of the measurements reduces to the following stages. First the investigated rain region is observed on the screen of the circular-scan indicator. Then, aiming the radar antenna onto this re-

gion, the amplitude of the reflected signal is measured on a type-A indicator and photographed. For this purpose one can recommend the use of the SI-1 oscillograph. The antenna is then rotated in the direction of the corner and the measurement and photography repeated. As a result of the measurements one can determine the magnitude of the reflecting characteristic of the rain  $z$ , and consequently also its intensity.

Indeed, the ratio of the squares of the amplitudes of the signals reflected from the rain and from the corner  $A^2$  will, in accordance with Formulas (2a), (10), and (3'), be

$$A^2 = \frac{P_r}{P_{rA}} = \frac{3\pi^5 h R_A^4 \sum_1 N D^6 k k_3}{16 \lambda^2 \epsilon_A k_A R^2} \quad (41)$$

Combining all the constants in (41) and putting  $\sum_1 N D^6 = z$  we get

$$z = B A^2 R^2 \frac{k_A}{k k_3} \quad (42)$$

If  $k_\Delta = k = k_z = 1$  this method makes it possible to determine rather simply the value of  $z$ , and consequently also the intensity of the rain from the ratio of the amplitudes of the echo signals from the rain and from the standard target, using the practically linear part of the amplitude characteristic of the radar receiver.

It must be borne in mind that it is advantageous to use this method if the radar of the TsAO is used only if no rain falls between the radar and the standard target. For radars operating at wavelengths that are insignificantly attenuated by rain, the use of this method is more universal.

#### Errors in Radar Measurements

An estimate of the errors of the radar measurements of reflected signals is a difficult problem, since it becomes necessary to take into account a large number of errors in the radar and in the measure-

ment apparatus; in addition, the accuracy of the initial formulas with the aid of which the intensity of the precipitation and the microphysical characteristics of the clouds are determined from the magnitude of these signals, is low.

In radar measurements it is necessary first of all to be assured of the stability of the technical characteristics of the radar, characteristics which determine the constant  $C_2$  in Formula (34).

For most radars it can be assumed that, starting with a range of 1.5 km, the receiver has constant sensitivity. Up to 1.5 km the sensitivity can vary within  $\pm 3$  db [28].

As regards the changes in the wavelength and in the pulse duration, these do not exceed several hundredths of a percent during the course of operation of the radar. Thus, the over-all maximum error of the measurements of the reflected signals may amount to 40-50%. The probable error will undoubtedly be smaller.

To estimate the accuracy of the radar determination of the rain intensity it is necessary, in addition, to take into account the errors in the initial formula (34), since the latter has been obtained by experiment. As a result, the over-all error in the measurement of the rain intensity will be quite large. This circumstance, which restricts somewhat the application of radar in meteorology, is compensated to a considerable degree by other advantages of the radar method, namely the operation at a distance, the speed, and the possibility of carrying out measurements under all conditions and with a great degree of detail.

To confirm the foregoing we can cite the results of simultaneous radar and meteorological measurements of rain [38]. The radar installation employed operated on a wavelength of 3 cm. Provisions were made for changing abruptly the sensitivity of the receiver during each rota-

tion of the antenna. The meteorological rain-measuring network consisted of 33 rain meters, distributed over an area of about 162 km<sup>2</sup>. The distance between rain meters was on the average 2.7 km. The accuracy with which the amount of rain was measured was 0.1 mm. The results of four comparisons are shown in Table 9.

Case 1 is of interest because the rapidly moving region of shower rain with thunderstorm passed through the center of the observation region. The amount of rain as determined by radar measurements was 29% less than that registered by the rain meters. This error is equivalent to the error in a rain-measuring network with a density of one rain meter for every 104 km<sup>2</sup>.

TABLE 9

Случаи	2.Количество выпавшего дождя в районе наблюдений (мм)				8	9
	3	4	5			
			среднее по району			
			6	7		
минимальное	максимальное	дождемерная сеть	радиолокационные наблюдения	Погрешность радиолокационных наблюдений (%)	Плотность дождемерной сети, эквивалентной по ошибкам радиолокационным наблюдениям (км <sup>2</sup> на один дождемер)	
1	0,00	8,0	1,75	1,25	—29	104
2	2,2	6,0	3,0	4,8	+58	400
3	4,2	19,8	11,0	4,5	—59	650
4	6,5	19,8	11,0	10,0	—9	72

1) Cases; 2) amount of falling rain in the observation region (mm); 3) minimum; 4) maximum; 5) average over the region; 6) rain-measuring network; 7) radar observations; 8) error of the radar observations (%); 9) density of rain-measuring network, producing an error equivalent to that of the radar observations (square kilometers per rain meter).

In case 2 the rain was weak and fell over a large area. Measurements with the aid of the radar are equivalent with respect to their errors in this case to measurements using one rain meter every 400 km<sup>2</sup>.

Case 3 pertains to the measurement of rain associated with a rap-

idly moving front. The rain intensity reached 135 mm/hr. As shown by the comparison, the radar measurements gave for the amount of falling rain a value which was 59% too low compared with the data of the rain-measuring network. So large an error can be attributed to the fact that no account was taken of the attenuation of the electromagnetic waves in the 3-cm band in the rain.

Statistical reduction of all the cases has shown that on the average, with a probability of about 95%, radar measurements are equivalent from the point of view of error to measurements with a rain-measuring network having a density of one rain meter every 163 km<sup>2</sup>.

#### 5. QUANTITATIVE ESTIMATE OF THE WATER CONTENT OF CLOUDS AND OF ICING OF AIRPLANES BY RADAR METHODS

At the present time certain types of radar stations operating in the centimeter and millimeter bands are used to detect not only rain clouds, but also clouds without precipitation [9, 66]. This has given rise to a real possibility of using radar methods for a quantitative estimate of the liquid-water content of clouds and the icing of airplanes within the operating radius of the radar station [17].

As is well known, light, moderate, and heavy icing occurs when the supercooled drops of the clouds and precipitation collide with parts of the airplane.

The degree, or strength of the airplane icing depends on the microphysical characteristics of the clouds and the precipitation, on the type of the airplane, and also on the duration and the flying conditions in the icing zone. The degree of icing is usually characterized by the overall thickness of deposited ice, with simultaneous estimate of the influence of the icing on the flying conditions and on the piloting technique.

In addition, in order to obtain an objective estimate of icing



initiated in flight, and also to calculate the power rating of the de-icing system, it is necessary to know the intensity (speed) of ice growth.

The main factors which determine the amount of growing ice is the liquid-water content, the dimensions of the drops of the supercooled clouds, the extent of the cloudiness, the air speed of the airplane, and also the aerodynamic characteristics of those parts of the airplane, on the surface of which the ice is produced.

The amount of ice and the rate of its growth are influenced not by the total water content of the cloud (drops plus crystals), but the amount of liquid water per unit volume.

In general form, the rate of growth of ice on any portion of the airplane is given by the following formula [21]

$$Q = \beta E(D) \frac{\rho_v}{\rho_i} v_\infty w \text{ cm/sec}, \quad (43)$$

where  $\beta$  is the freezing coefficient, equal to the ratio of the mass of the growing ice to the mass of the settling water during the same time and on the same surface,  $E(D)$  is the capture coefficient, equal to the ratio of the number of settling drops to their total number,  $w$  is the water content in  $\text{g/cm}^3$ ,  $\rho_v$  is the density of the water in  $\text{g/cm}^3$ ,  $\rho_i$  is the density of the ice in  $\text{g/cm}^3$ , and  $v_\infty$  is the air speed of the airplane in  $\text{cm/sec}$ .

It follows from Formula (43) that the growth intensity and consequently also the thickness of the ice are proportional to the water content of the clouds. This dependence was confirmed experimentally in specially organized flights, by simultaneous measurements of the water content and the rate of ice growth.

The foregoing dependence can be fairly well approximated (with a probable error of 0.2 mm/min) by the following formula for  $v = 250$

km/hr and  $0.2 \leq W \leq 2 \text{ g/m}^3$ :

$$Q = 0.83w - 0.2. \quad (44)$$

A diagnosis of the danger of airplane icing calls for solution of two basic problems. First, it is necessary to determine the horizontal and vertical extent of the icing zone with account of the temperature stratification of the atmosphere and the flying speed, and second, it is necessary to determine the thickness of the growing ice with account of the flight trajectory in the indicated zone.

#### Determination of the Horizontal and Vertical Dimensions of the Icing Zone

When applied to this problem, the radar makes it possible to obtain almost instantaneously a spatial horizontal or vertical section

through the cloudiness and the precipitation within its operating radius.

Using radio and airplane sounding data, and in the case of continuous precipitation using the position of the melting layer as obtained by radar observations, it is possible to determine the height of the zero isotherm, and consequently the vertical extent of the supercooled zones of the clouds. However,

in order to determine the vertical extent of the icing zone it is necessary to take into account the influence of the air speed of the airplane.

Indeed, when flying in the atmosphere at speeds greater than 200 or 300 km/hr, it is necessary to take into account the kinetic heating of the airplane parts, due to the compression and friction of the air stream. Consequently, the lower icing limit will be located above the zero isotherm, which leads to a reduction in the vertical dimension of the icing zone. Consequently, the vertical dimension of the icing zone

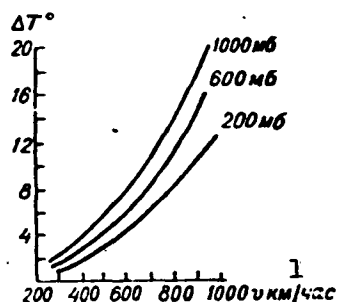


Fig. 39. Kinetic heating during icing at different heights.  
1) km/hr.

depends not only on the vertical dimension of the clouds and the height of the zero isotherm, but also on the airplane flying speed.

To determine the magnitude of the kinetic heating one can use the results of specially organized flights under icing conditions (Fig. 39).

From the plot of Fig. 39 it is possible to determine the temperature of the unperturbed air stream, at which icing of the airplane begins for a given flying speed and altitude (pressure).

From the determined temperature one can readily find, using aerological data, the height of the lower limit of the icing zone, and knowing the position of the upper limit of the supercooled clouds from radar observations, it is possible to determine the vertical and also the horizontal dimensions of this zone.

#### Determination of the Water Content of Clouds and the Thickness of the Growing Ice

It was indicated above that at a constant flying speed the thickness of the ice formed on the frontal parts of the airplane is determined principally by the water content of the clouds. On the other hand, the water content of the clouds is connected by the following empirical relations with the reflecting characteristic of the clouds, which determines the power of the reflected signal [80]:

$$z = 0.048w^2, \quad (45)$$

where  $z$  is in  $\text{mm}^6/\text{m}^3$  and  $w$  is in  $\text{g}/\text{m}^3$ .

Let us write out the fundamental radar equation for clouds and precipitation in the following form, and let us solve it by the method developed in [62],

$$P_r = C \frac{w^2}{R^2} e^{-2 \int_0^R \alpha_w dR} e^{-2 \int_0^R \alpha_d dR}, \quad (46)$$

where

$$C = 2.9 \cdot 10^{-25} P_r G^2 \theta_1 \theta_2 h \left| \frac{m^2 - 1}{m^2 + 2} \right|^2.$$

Here  $P_t$  is in watts,  $\theta_1$  and  $\theta_2$  in degrees,  $h$  in meters, and  $\lambda$  in centimeters.

Let us divide the left half of (46) by  $P_t$  and let us take logarithms. Then

$$\ln \frac{P_r}{P_t} = 2 \ln C_1 + 2 \ln w - 2 \ln R - 2 \int_{R_0}^R \alpha_1 w dR - 2 \int_0^R \alpha dR, \quad (46')$$

where  $C_1^2 = C$ .

Grouping the terms that characterize the attenuation of the received power as a result of the range and the gases of the atmosphere, we obtain

$$y^2 = \left( \frac{P_r}{P_t} \right) R^2 e^{2 \int_0^R \alpha dR}. \quad (47)$$

Then

$$2 \ln y = \ln \frac{P_r}{P_t} + 2 \ln R + 2 \int_0^R \alpha dR.$$

Substituting (47) and (46') we obtain

$$\ln y = \ln C_1 + \ln w - \int_{R_0}^R \alpha_1 w dR. \quad (48)$$

Differentiation of this equation with respect to the range leads to the following expression:

$$\frac{d \ln y}{dR} = \frac{1}{w} \frac{dw}{dR} - \alpha_1 w.$$

If we put

$$u = 1/w, \quad (49)$$

then

$$\frac{1}{y} \frac{dy}{dR} = u \frac{dw}{dR} - \frac{\alpha_1}{u},$$

and since

$$\frac{dw}{dR} = \frac{1}{u^2} \frac{du}{dR},$$

then

$$\frac{1}{y} \frac{dy}{dR} = -\frac{1}{u} \frac{du}{dR} - \frac{\alpha_1}{u}.$$

Furthermore,

$$u \frac{dy}{dR} = -y \frac{du}{dR} - \frac{\alpha_1}{u}.$$

then

$$\frac{d}{dR}(uy) = -\alpha_1 y.$$

Inasmuch as

$$\int u y dR = - \int \alpha_1 y dR,$$

we get

$$uy = - \int_{R_0}^R \alpha_1 y dR + \text{const}$$

or, with allowance for (49),

$$\frac{y}{w} = - \int_{R_0}^R \alpha_1 y dR + \text{const.} \quad (50)$$

The integration constant can be readily calculated by making the substitution  $w = 0$  ( $\alpha_1 = 0$ ). Taking (46) into consideration, we obtain  $\text{const} = C$ .

From (50) we obtain at last the final expression for the determination of the water content of clouds at any range  $R = R_1$ , where the power of the reflected signal is  $y = y_1$

$$w = \frac{y_1}{R_1} \cdot C_1 - \int_{R_0}^R \alpha_1 y dR$$

In many cases it is advantageous to employ a somewhat different method of determining the water content, based on the measurement of the power of the reflected signals with the aid of a two-band radar station [80]. In this case the wave bands are chosen such as to produce

a noticeable difference in the attenuation coefficients.

Using (46') and expressing the attenuation in decibels, we can write

$$10 \lg P_r = 10 \lg \left( \frac{z}{R^2} \right) - 2 \int_{R_1}^{R_2} \alpha_1 w dR - 2 \int_0^{R_1} \alpha dR. \quad (51)$$

Let the measurement of the power of the reflected signals be carried out at two ranges  $R_1$  and  $R_2$ , within the limits of which the average water content is  $w = \text{const}$ . Then the difference in the power of the indicated signals, expressed in decibels, will be

$$A = 10 \lg \frac{P'_{r,a}}{P''_{r,a}} = 10 \lg \frac{z_1 R_2^2}{z_2 R_1^2} - 2\alpha_{1,a} \bar{w} (R_2 - R_1) - 2\alpha_a (R_2 - R_1). \quad (52)$$

For the other band of the radar we have accordingly

$$B = 10 \lg \frac{P'_{r,b}}{P''_{r,b}} = 10 \lg \frac{z_1 R_2^2}{z_2 R_1^2} - 2\alpha_{1,b} \bar{w} (R_2 - R_1) - 2\alpha_b (R_2 - R_1). \quad (53)$$

Subtracting (53) from (52) we obtain

$$A - B = 2(R_2 - R_1) (\alpha_{1,b} - \alpha_{1,a}) \bar{w} + 2(R_2 - R_1) (\alpha_b - \alpha_a). \quad (54)$$

Equation (54) enables us to find the average water content  $\bar{w}$  from the known values of the powers of the reflected signals A and B, the per-unit attenuation coefficients in the clouds  $\alpha_{1,b}$  and  $\alpha_{1,a}$ , and also from the per-unit coefficients of attenuation in the gases of the atmosphere,  $\alpha_b$  and  $\alpha_a$ , for the two wave bands.

Using wavelengths of 0.86 mm and 3 cm at a temperature of  $0^\circ$ , we obtain  $\alpha_{1,a} = 1.121 \text{ db/km/g/m}^3$  and  $\alpha_{1,b} = 0.076 \text{ db/km/g/m}^3$ .

In the gases of the atmosphere  $\alpha_a = 0.06 \text{ db/km}$  and  $\alpha_b = 0.01 \text{ db/km}$ .

Assuming the accuracy with which the difference in the powers of the reflected signal  $A - B$  is measured to be 0.5 db, we can find the minimum water content of the clouds, below which measurements are impossible for a given thickness  $R_2 - R_1$  of the layer (Table 10). The

data in the table are given for  $\lambda = 3$  cm and  $\lambda = 0.86$  cm.

TABLE 10

$R_2 - R_1$ , km	0.2	0.4	0.6	0.8	1.0
$w$ , g/m <sup>3</sup>	1.15	0.55	0.35	0.28	0.19

An analysis of Table 10 and Formula (54) shows the advantages and disadvantages of this method. On the one hand, the advantage of the method is the fact that the water content does not depend on the quantity  $z = \Sigma ND^6$ . This is particularly important, since the first method, which uses the correlation relation  $z = 0.048 w^2$ , is characterized by a large probable error when the drop diameter exceeds 30  $\mu$  and the water content exceeds 1.3 g/m<sup>3</sup>. According to the latest measurements of the spectrum of cloud elements, made at the TsAO, in nonrain clouds there are frequently contained drops 100-200  $\mu$  in diameter. In spite of the fact that their concentration is small and they make a negligible contribution to the water content of the cloud, their influence on the quantity  $z = \Sigma ND^6$  is quite appreciable. On the other hand, the accuracy of the measurement of the ratio of the signals reflected from the same volumes of clouds, which amounts to 0.5 db, imposes a lower limit on the water content, below which measurements are impossible. Consequently, the first method is conveniently used if the clouds are characterized by small values of the water contents with narrow spectra of the cloud drops, and the second is best used for clouds with broad spectra and relatively large values of the water content.

Knowing the water content of the liquid-drop phase of the clouds, it becomes possible to make a quantitative estimate of the intensity of ice growth or its thickness from the known power of the reflected signal and from the other parameters contained in Relations (50) and (54).

However, in order to solve the question of the degree of danger of icing it is necessary to have, for specific types of airplanes, the connection between the characteristics of the ice formation and its influence on the flying conditions of the airplane and on the piloting technique. Usually such connections are established experimentally by flying through clouds that give rise to different degrees of icing. The main characteristics of the ice are in this case its thickness and its shape. As regards the shape of the ice, it is very difficult to calculate, whereas the thickness of the ice can be measured relatively simply. As a result, one uses for the estimate of the icing danger the thickness of the ice formation on the parts of the airplane not equipped with deicers. Let us assume that the dependence of the strength of icing on the ice thickness is such as shown in Table 11.

TABLE 11

Light	Moderate	Heavy
Up to 10 mm	10-20 mm	>20 mm

To determine the thickness of the growing ice it is more convenient to use not the water content  $w$ , but the layer of the deposit of ice  $h$ . For a given flying velocity, the thickness of this layer, formed on some part of the airplane after a flight of one meter, is equal to

$$h = \beta \frac{p_2}{p_1} E(\sigma) \cdot 10^{-2} w, \quad (55)$$

where  $h$  is in mm and  $w$  in  $g/m^3$ .

According to experimental data [17], the product of the first three factors in the right half of the relation ranges between 0.2 and 0.5. From this it is easy to determine  $h$  if the flight trajectory and the distribution of the water content are known.



### Limitations and Errors of the Method

The method considered for a quantitative estimate of the icing danger is not universal at the present-day stage of development of radiometeorology, in the sense that apparently it is difficult to employ in an arbitrary meteorological installation. Theoretically, its field of application covers only liquid-drop clouds. However, at below-zero temperatures there can exist along with the supercooled drops also ice particles. In calculating their scattering area, the main difficulty lies in the fact that the ice particles do not have a simple geometrical form like the spherical water drops.

Let the clouds consist of ice crystals. Because of the fact that the dielectric constant of ice is smaller than the dielectric constant of water, the power of the reflected signal from cirrus, altostratus, and stratus clouds, which consist of ice crystals, is approximately one fifth as large as from clouds consisting of water drops of the same dimension and of the same concentration.

In the ice clouds indicated above, the water content of the solid phase is very small and amounts to  $0.01\text{--}0.12\text{ g/m}^3$  for particle dimensions not exceeding a few microns. This circumstance will also decrease the received power. Consequently, a symptom that distinguishes clouds consisting of ice crystals can be the small power of the signal reflected from them. Even if we assume that these clouds are made of water, the error in the estimate of the degree of icing will be small, for at such a signal and at the observed geometrical parameters of the clouds the icing will as a rule be light.

It is much more complicated to employ the given method in meteorological situations in which precipitation falls. In the main, the precipitation can fall in the form of dry and wet snow, hard and soft hail, rain, and drizzle. The falling of dry snow occurs only at

below-zero temperatures. The dimensions of the snow crystals can reach 2-3 cm, and the intensity of the snow fall converted into liquid quantities rarely exceeds 2-3 mm/hr. Most frequently the intensity of the snow fall is less than 0.1-0.2 mm/hr.

When estimating the danger of icing in clouds that produce precipitation, considerable difficulties arise in connection with the fact that it is necessary to separate from the over-all resultant power of the reflected signal, the component due to supercooled drops, collision with which causes formation of ice. If snow is observed to fall, it is necessary to separate the signal from the supercooled drops, considered against the background of the over-all signal (the signal from the drops plus the signal from the snow flakes). Under the assumption that the intensity of the snow fall during the process of the measurement does not vary with altitude, the separation of the signal from the supercooled drops can be made in the following fashion.

If we aim the antenna at small elevation angles, close to  $0^\circ$ , then the reflected signal will be the signal from the snow flakes falling in the space limited in altitude by the lower limit of the clouds and by the earth. Let us denote this signal by  $P'_r$ . If the antenna is aimed at large elevation angles, the signal received from the particles located above the lower limit of the clouds will represent the sum of the signals  $P'_r + P_r$ , where  $P_r$  is the signal from the supercooled drops. Under the assumption made above, the signal from the drops is determined as the difference between these two signals. However, for practical utilization of this method of separating the useful signal it is necessary that the ratio of the signal from the drops to the signal from the snow be larger than the distinguishability coefficient

$$m = (P_r/P'_r)_{\min}. \quad (56)$$

When observing useful signals against the background of signals from precipitation on a circular-scan indicator we have  $m = P_r/P'_r = 1.6$ .

Bearing in mind the aforementioned power ratio  $P_r/P'_r$ , we can determine with the aid of Relation (56) and the equation of the meteorological target (10) the values of water content at which clouds can be observed and the values at which they cannot. It was indicated above that  $P'_r \sim 200I^{1.6}$ , where  $I$  is the intensity of the snowfall in mm/hr. This ratio was established for  $0.1 \leq I \leq 2$  mm/hr [43]. It can apparently be extended to include also values of  $I$  somewhat smaller than 0.1 mm/hr. The power of the signal reflected from the liquid-drop phase of the clouds is  $P_r \sim 0.048 w^2$ .

Using Relations (28) and (45), we obtain

$$w = (520I^{1.6}/0.048)^{1/2}. \quad (57)$$

The solution of Eq. (57) with a snowfall intensity  $I = 0.1$  mm/hr gives a tremendous value of water content (on the order of  $20 \text{ g/m}^3$ ). At larger values of  $I$ , the value of the water content turns out to be even larger. These values of water content are not encountered even in the summertime in cumulonimbus clouds. Consequently, the increment in the signal due to the suspended cloud drops in the case of snowfall will not reach a value that is practically noticeable and measurable at the ordinary indication of the reflected signals. Actually, however, when snow flakes fall through liquid-drop or mixed clouds, the increment in the signal should be larger, because coagulation and seeding of the snow flakes by the supercooled drops takes place. This seeding is more appreciable during the warm half of the year than during the cold one, since during the warm half of the year the number and dimensions of the particles of the liquid-drop phase in supercooled clouds is larger than during the cold part of the year.

As is well known, layers with large drops, in which the seeding of the falling snow flakes takes place, are called the upper bright strips. The upper strips occur in moderate and weak rains observed on earth. The reflected signal from the upper strips can exceed the signal from the rain zone below the zero isotherm. Taking into account the mechanism of formation of the upper bright strips, one must expect that flight through them can be accompanied by an airplane icing which is of considerable strength. A quantitative estimate of the water content is a much more complicated matter in such cases, and is less definite as compared with the estimate given for clouds without precipitation. The difficulty lies in the fact that, first, there is as yet no connection established between the degree of seeding and the scattering area of the snow flakes, and second, there is added to the attenuation in the atmosphere and in the clouds also attenuation in the rain zone, in the melting layer, and in the supercooled zone.

In the summertime, shower precipitation and hail can fall from the intramass and frontal cumulonimbus clouds. The water content in such clouds may reach  $5-8 \text{ g/m}^3$ . In spite of the much smaller horizontal dimensions of cumulonimbus clouds as compared with the dimensions of the nimbostratus clouds, they can be much more dangerous from the icing point of view. Furthermore, when flying in the direct vicinity of such clouds, and particularly inside them, very strong bumping of the airplanes is observed. Consequently, it is natural to assume that intense icing takes place in the supercooled part of the cumulonimbus cloud. In such a case the radar is useful as a means which makes it possible to determine from a distance the cumulonimbus cloud from the form and power of the reflected signal.

The accuracy with which the thickness of ice on the airplane is detected also depends on the degree to which the linear relation be-

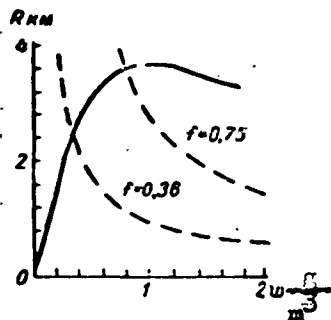


Fig. 40. Maximum ranges of cloud detection of millimeter-band radars.

tween the attenuation  $\alpha$  and the water content is satisfied. According to literature data [31, 62] the deviation of the attenuation calculated from the exact formulas from the Rayleigh approximation can differ by not more than a factor of two when  $\lambda = 1$  cm for drops 0.6 cm in diameter and when  $\lambda = 3$  cm for drops 1.3 cm in diameter. On the other hand, if the drop diameter is 0.3 mm, then when  $\lambda = 1$  cm

the attenuation calculated from the exact formulas is found to be only 20% too high. Accordingly, for  $\lambda = 3$  cm the drop diameter is equal to 0.5 mm.

Thus, the attenuation coefficient calculated after Rayleigh is applicable with small errors not only for clouds but also for drizzle.

As regards the relation connecting the reflecting ability  $z$  with the water content  $w$  ( $z = 0.048 w^2$ ), it was derived for cloud particles with average diameter not exceeding  $30 \mu$ . However, for small raindrops and for drizzle drops with an average diameter from 0.1 to 0.5 mm, it is also possible to derive the relation  $z = Pw^2$ , where  $P = 200$ . This is much larger than the value of  $P$  obtained for clouds.

In addition to the question of whether the radar signal expresses only the water content of the clouds, it is necessary to solve still another important problem. This problem, for the radar now available, is the efficiency of detecting various clouds, which depends, on the one hand, on the technical characteristics of the radar, and on the other on the water content of the clouds and on their distance.

Figure 40 shows the effectiveness of detecting clouds by means of a TPQ-6 radar [63]. The analysis of the curves on this figure shows that the TPQ-6 at a distance of 3 km detects only those clouds which

have a water content not less than  $0.7 \text{ g/m}^3$ . If the water content is smaller than this value, then the power of the reflected signal will be less than the sensitivity of the radar receiver, and such a signal can of course not be measured. However, in spite of this, the upper limit of the water content, and consequently also the upper limit of the degree of icing, can be established. Errors of a different kind are those due to the integral of the attenuation in the clouds and in the gases of the atmosphere. An error of  $2^\circ$  in the determination of the air temperature can change the attenuation in the clouds by 10%. Errors in the determination of the attenuation integral in the gases of the atmosphere are quite small for the wavelength band  $\lambda = 0.86 \text{ cm}$  even when standard atmosphere is used.

In measuring the power of the reflected signal, errors will also arise as a result of the errors in the calibration of the radar, in the measurement of the radiated power, and the sensitivity of the receiver [11].

#### Practical Use of the Method

To determine the water content of clouds and the intensity of growth of ice with the aid of Relations (50) and (55) it is necessary to measure the power of the signals reflected from the clouds.\*

In our experiments the power of the reflected signals was measured with the aid of an SI-1 oscillograph, the input of which was connected to the output of the second detector of a radar station modernized for meteorological purposes. The received power was measured relative to the sensitivity of the receiver, which was monitored during the course of the measurements with the aid of a signal from an echo-resonator. The measurement range amounted to about 60 db.

In practice the determination of the water content of clouds and of the rate of growth of the ice with the aid of Relations (50) and

(55) is best carried out in the following sequence.

1. The most important stage is the determination of the coefficient  $C_1$ , i.e., the calibration of the radar. The coefficient  $C_1$  must be calculated using Relation (29), by simultaneous measurements of the power of the reflected signals from clouds and from their water content, which is determined with the aid of corresponding instruments during the time of airplane or balloon sounding. Under our conditions, the radar and the airplane measurements were carried out simultaneously using radio communication. The radar operators used a small-size radio station operating both in transmission and reception.

The sounding airplane was equipped with the following instruments: an airborne SM-43 meteorograph, which was mounted in a special frame under the fuselage, a shielded airplane thermometer SET, a microphotography installation for the measurement of the spectrum of the drops, a meter for the transparency of the clouds, and water-content meters SIV-2 and SIV-3. To measure the rate of growth of the ice, its shape, and its thickness, a new version of ice meter was developed on the basis of the preceding instrument designs.

An exceedingly important condition for the calibration of the radar is that the airplane measurements of the microphysical characteristics of the clouds occur within the limits of the width of the upward-directed radio beam, or at least sufficiently close to it, not farther away than a distance corresponding to the time necessary to gather the samples of the drops or to measure the water content of the clouds. For the drop samples this time amounted to about one or two seconds, while for the water content measurements it was from 10 to 30 seconds in the case of not dense clouds. Thus, at a flying speed of 250-260 km/hr, averaged values of the drop spectra were obtained for distances not less than 72 m, while those for the water contents were

from 720 to 2100 m. On this basis, the location of the radar station at the airport was chosen. The radar was located at a distance of 200 meters from the landing strip. The measurements of the water content and of the drop spectra on the airplane, and also the simultaneous measurements of the power of the reflected signals, took place when the airplane, moving within the pattern of the homing radio stations, moved past the nearby homing station and flew over the strip at a specified altitude. It then made a standard turn and again passed over the homing stations, but at a different altitude, etc.

From the results of the ground and airplane measurements one could calibrate the radar station, i.e., find the average value of the coefficient  $C_1$ . For the radar station employed it was found as a result of the measurements that the experimental value of  $C_1$  is approximately three times larger than the theoretical value.

2. The curve characterizing the variation of the power of the reflected signals with altitude is broken up into  $n$  layers, inside each of which the variation of the power is practically linear. This is followed by a determination of the average temperature of the layer, and using the data of [31] by the determination of the value of the correction to the coefficient  $\alpha$  in Formula (50).

3. Taking logarithms of (45), each value of the power is corrected for the range and attenuation in the gases of the atmosphere, after which the power is divided by the radiated power (determination of  $y$ ). For each wavelength the attenuation coefficient in the atmosphere  $\alpha$  is a function of the temperature, the pressure, and humidity of the air [31]. By dividing each value of  $y$  by the calibration constant  $C_1$ , one determines the water content  $w$ . The determined water content and the range corresponding to it represent a point on a plot made for the specific radar station. An example of such a plot for the TPQ-6 radar



is shown in Fig. 39.

If the plotted point turns out to be to the left of the curve  $f = 0.35$ , then it is not advisable to correct the obtained value of the water content for the attenuation of the radio waves in the clouds, since this attenuation is very small. If the plotted point is situated between the curves  $f = 0.35$  and  $f = 0.75$ , it is necessary to account in the determination of the water content for the attenuation of the radio waves in the clouds, using the method indicated in item 4 [62]. On the other hand, if the plotted point turns out to be to the right of the curve  $f = 0.75$ , it is not advisable to determine the water content in view of the large error.

4. One evaluates the integral characterizing the attenuation in the clouds,

$$\int_{R_0}^R \alpha_1 y dR,$$

where  $R_0$  and  $R$  are, respectively, the near and far boundaries of the clouds detected by the radar. As is well known, a sufficiently satisfactory solution of the integral is obtained in the form

$$\int_{R_0}^R \alpha_1 y dR = \Delta R \left[ \frac{(a_1)_0 y_0}{2} + (a_1)_1 y_1 + \dots + \right. \\ \left. + (a_1)_{n-1} y_{n-1} \frac{(a_1)_n y_n}{2} \right].$$

5. Using (50), one determines the water content in  $\text{g/m}^3$ .

6. To estimate the danger of icing, it is necessary to know the geometrical parameters of the icing zone. Therefore one determines from the radar data and from the height of the  $0^\circ$  isotherm the height and the thickness of the icing zone, with allowance for the flying speed, and also the horizontal dimension of this zone.

7. To determine the overall thickness of the ice formed after the airplane crosses the icing zone, and also to determine the rate of

growth of the ice, it is necessary to find the distribution function of the layer of the deposited ice over the flight trajectory in the icing zone, i.e., it is necessary to solve the integral

$$H = \int_R h(R) dR, \quad (58)$$

where  $H$  is the overall thickness of the ice in mm, and  $h(R)$  is the distribution function of the layer of deposited ice in mm;  $h(R)$  can be readily determined with the aid of Formula (55) if  $w(R)$  is known.

8. After determining the thickness of the ice  $H$  and its rate of growth, it is possible to estimate with the aid of Table 11 the danger of airplane icing.

By way of examples illustrating the effectiveness of the radar method of estimating the danger of icing, let us consider the case of 4 November 1959 (Fig. 41). The cloudiness observed that day was strato-cumulus and altocumulus without precipitation. The ground temperature was  $6^{\circ}$ , the wind from the south at 5 m/sec, the pressure 765.5 mm, the relative humidity 83%, and the visibility 4 km.

The lower layer of the clouds was not fixed by the radar, since it was visible against the background of local objects, and its water content did not exceed on the average  $0.034 \text{ g/m}^3$ . The second layer of dense altocumulus clouds was located at altitudes from 1800 to 2700 m. The vertical distribution of the water content was almost typical of these clouds: near the lower limit, on the average  $w = 0.098 \text{ g/m}^3$ , at altitudes of 2.0 and 2.5 km, respectively, the water content was 0.26 and  $0.393 \text{ g/m}^3$ , and, finally, near the upper boundary of the opaque altocumulus, at an altitude of 2.65 km,  $w = 0.121 \text{ g/m}^3$  (Fig. 41).

The radar station fixed a layer of clouds having a water content from 0.26 to  $0.393 \text{ g/m}^3$ . The measured values of the reflected-signal power were, respectively,  $10^{-11.2}$  and  $1.81 \cdot 10^{-11.2}$  watt. In these

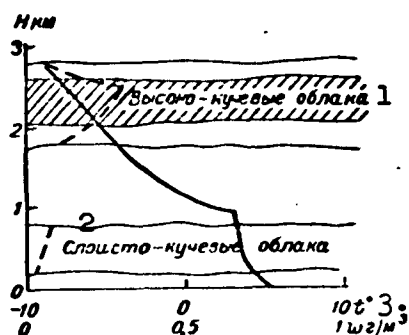


Fig. 41. Flight of 4 November 1959. The shading shows the part of the cloud fixed by the radar. 1) Altocumulus clouds; 2) stratocumulus clouds; 3)  $\text{g/m}^3$ .

parts of the clouds, the rate of ice growth was from 0.16 to 0.52 mm/min. As a result of a 35-minute flight in the altocumulus, three areas were plotted at altitudes 2.0, 2.5, and 2.65 km. The first two corresponded to a duration of about 10 minutes, and a third to 14 minutes. The increase in the thickness of the growing ice was 2.5, 3.6, and 0.4 mm at the first, second, and third altitudes, respectively.

As was already indicated, the radar fixed these clouds with water content not less than  $0.26 \text{ g/m}^3$  on the average. Consequently, the quantitative estimate of the icing could be obtained from the airplane flight only for the first two areas.

The theoretically calculated total thickness of the ice on the sensitive element of the meter should have equaled 10.2 mm after 24 minutes of flight and should have corresponded to moderate icing, since moderate icing is observed when the ice thickness is between 5 and 15 mm. Actually the thickness of the ice was 6.5 mm.

The difference between the theoretically calculated ice thickness and the actual ones was qualitatively attributed to many causes, including the change in the capture coefficient of the sensitive element due to the distortion of its shape by the growing ice, the errors in the empirical formulas connecting the reflecting ability of the clouds and the water contents, the error in the measurement of the power of the reflected signals, and the impossibility of carrying out in our experiments radar measurements of the water content along the flight trajectory.

However, in spite of all this, it was possible to make a much more reliable diagnosis of the danger of the airplane icing than by the synoptical method alone.

#### 6. ESTIMATE OF TURBULENCE BY THE RADAR METHOD

The frequency of the radio waves reflected from objects moving with velocities  $v_s$  along their line of propagation differs from the frequency of the incident radio waves. This change in frequency is determined by the well-known Doppler formula

$$\Delta\omega = \omega_0 \frac{2v_s}{c}, \quad (59)$$

where  $\omega_0$  is the frequency of the main pulse and  $c$  is the velocity of light.

In atmospheric formations consisting of a large number of reflecting particles, it is possible to observe both the average velocity of motion of the particles along the radio-wave propagation line, and the velocity of motion of the particles relative to one another. The average velocity causes a change in the frequency of the reflected signal, whereas the relative motion causes fluctuations in its amplitude. For those velocities of motion possessed by the cloud and precipitation particles, the determination of  $\Delta\omega$  with the aid of ordinary radar stations is impossible without the use of special equipment, since the transmitter frequency changes by 0.2-0.3 Mc, while  $\Delta\omega = 666$  cps at  $v = 10$  m/sec.

A study of the fluctuations of the amplitude of the reflected signal can be used for the determination of the value and the spectrum of the random velocities of the reflecting particles.

The radar signal reflected from some volume of clouds or precipitation can be written in the form

$$A = a_0 \cos \omega_0 t + \sum_1^N a_s \cos (\omega_s t - \varphi_s), \quad (60)$$

where  $a_0 \cos \omega_0 t$  is the overall signal from the particles which do not move along the propagation line,  $\omega_0 = 2\pi f_0$  is the frequency of the main pulse, while  $a_s$ ,  $\omega_s$ , and  $\varphi_s$  are the random amplitude, frequency, and phase of the signal reflected from the moving particles.

Assuming that the velocities of the random motion of the particles have a Gaussian distribution, we can write the following expression for their mean square velocity  $v_0$ :

$$v_0 = \frac{\lambda |\overline{A_n - A_{n+1}}|}{4\pi \Delta t \sqrt{a_0^2 \omega_0^2 + 2\omega_0^2}}, \quad (61)$$

where  $\Delta t$  is the period of the pulse repetition frequency and  $A_n$  and  $A_{n+1}$  are two successive values of the signal amplitude.

In the case when  $a_0 = 0$  and  $\omega_0 = 2\overline{A}^2/\pi$  Relation (61) assumes the form

$$v_0 = \frac{\lambda |\overline{A_n - A_{n+1}}|}{8\Delta t \overline{A} \sqrt{2}}. \quad (62)$$

If  $a_0 \neq 0$ , Eq. (60) must be used. In this case

$$a_0 = \sqrt{2\overline{A}^2 - (\overline{A})^2} \text{ and } \omega_0 = \overline{A}^2 - (\overline{A})^2.$$

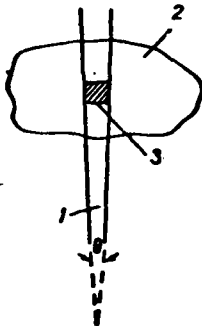


Fig. 42. Position of isolated volume in a cloud, in which one measures the turbulent motions.  
1) Radio beam;  
2) radio echo of the cloud;  
3) isolated volume of cloud.

We see that to determine  $v_0$  it is necessary to carry out a prolonged processing which calls for the use of computers as part of the operating procedure. To carry out an approximate estimate of the random velocity one can use a simplified method.

It follows from (59) that the envelope  $F_s$  and the velocity of motion  $v_s$  are connected by

$$v_s = F_s \lambda / 2.$$

The frequency  $F_s$  is determined by the number of maxima of the envelope of the pulses per second. The number of maxima  $n$  over a selected period of time  $\Delta T$  can be determined, in turn, from the relation  $n = F_s \Delta T$ . Hence

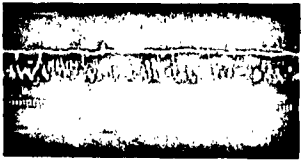


Fig. 43. Recording of instantaneous and average values of echo signals from rain.

$$v_s = n\lambda/2\Delta T. \quad (63)$$

According to experimental data, the difference between the velocities obtained from the accurate and the approximate methods does not exceed 50%.

The principle of radar measurement of turbulence in clouds, developed at the TsAO by A.G. Gorelik, V.V. Kostarev, and A.A. Chernikov [6] is explained with the aid of Fig. 42. Let the antenna of their radar station be directed upward. Part of the energy of the main pulse from the transmitter, passing through the cloud, is scattered in the opposite direction and reaches the receiver of the radar. At the output of the receiver is a special device, a radar-signal selector. The selector is turned on for a short time interval  $\tau_{sel}$  during the interval between the transmission of two neighboring main pulses. By varying the delay of the on instant, it is possible to measure the amplitude of the signal reflected from any part of the cloud, located within the limits of the radio beam. The volume isolated for observations is limited in this case by the width  $\theta$  of the beam and by the time  $\tau_{sel}$  that the receiver is on. The selector segregates from among the assembly of signals received by the radar receiver the particular signal reflected from the investigated volume of the cloud, which is located at the altitude of interest to us. Later on this signal is transformed without amplitude distortion to a form convenient for observation and recording. The instrument employs the method of time selection of the radar receiver video signal.

To observe and register the fluctuations of the signals from the investigated volume it is possible to use a long-persistence oscilloscope and small sweep rates, so that the sequence of pulses visible on

its screen can be photographed.

Recently special magnetoelectric automatic recorders MPO-2 and others have found use in the recording of sequences of pulses. To simplify the recording of a sequence of pulses, a tape recorder is used, the data of which are processed with a spectrum analyzer. Figure 43 shows one of the recordings of pulses reflected from a rain zone, obtained by P.A. Rublev and S.M. Gal'perin with the aid of the MPO-2 instrument.

#### 7. EFFECTIVENESS OF DETECTION OF CLOUDINESS AND PRECIPITATION ZONES BY RADAR STATIONS

At the present time the effectiveness of the radar detection of precipitation zones with the aid of storm-warning radars have been investigated with sufficient detail. On the other hand, data on the effectiveness of the detection of clouds are scanty and need additional verification.

The practical possibilities of radar detection of clouds and precipitation can be determined sufficiently completely after first finding the ranges for the detection of zones of precipitation of varying intensity or of water content of the clouds, and then knowing the probability of observing these zones at different distances. By probability of detection is meant the ratio of the number of precipitation or cloudiness zones fixed by the radar to the actual number of such zones.

The first characteristic of the effectiveness of radar detection depends on the type of the radar, on the intensity of the precipitation, or on the water content of the clouds and the distance to them\* and the second characteristic is determined in addition by the frequency of the indicated atmospheric formations in some particular geographic regions. Thus, the probability of radar detection is in a certain sense a climatic characteristic of the effectiveness of detection.

its screen can be photographed.

Recently special magnetoelectric automatic recorders MPO-2 and others have found use in the recording of sequences of pulses. To simplify the recording of a sequence of pulses, a tape recorder is used, the data of which are processed with a spectrum analyzer. Figure 43 shows one of the recordings of pulses reflected from a rain zone, obtained by P.A. Rublev and S.M. Gal'perin with the aid of the MPO-2 instrument.

#### 7. EFFECTIVENESS OF DETECTION OF CLOUDINESS AND PRECIPITATION ZONES BY RADAR STATIONS

At the present time the effectiveness of the radar detection of precipitation zones with the aid of storm-warning radars have been investigated with sufficient detail. On the other hand, data on the effectiveness of the detection of clouds are scanty and need additional verification.

The practical possibilities of radar detection of clouds and precipitation can be determined sufficiently completely after first finding the ranges for the detection of zones of precipitation of varying intensity or of water content of the clouds, and then knowing the probability of observing these zones at different distances. By probability of detection is meant the ratio of the number of precipitation or cloudiness zones fixed by the radar to the actual number of such zones.

The first characteristic of the effectiveness of radar detection depends on the type of the radar, on the intensity of the precipitation, or on the water content of the clouds and the distance to them\* and the second characteristic is determined in addition by the frequency of the indicated atmospheric formations in some particular geographic regions. Thus, the probability of radar detection is in a certain sense a climatic characteristic of the effectiveness of detection.



Let us examine each characteristic in detail.

To determine the limiting detection ranges for precipitation of varying intensity or for the water content of the clouds, it is first necessary to find by experiment the constants  $C$  of the radar, contained in Eqs. (34) and (50). Radar measurements of the power of the reflected signal are carried out in this case simultaneously with meteorological measurements of the intensity of the rain with the aid of a pluviograph and measurements of the water content of the clouds with the aid of an airplane. The meteorological measurements are usually made at short distances from the radar so as to reduce the influence of the attenuation coefficient. The radar constants are determined from the results of the measurement.

These constants are subsequently used to calculate the limiting detection ranges for the atmospheric formations indicated above, i.e., for the determination of the first characteristic of the detection effectiveness. The calculation is usually carried out under the following simplifying assumptions: the rain intensity and the water content of the clouds along the path of propagation of the electromagnetic waves are assumed constant; it is assumed that there are no screening rains; the vertical thickness of the reflecting region is assumed to be 3 km for rain with intensity not larger than 10 mm/hr, 5 km for intensity from 10 to 20 mm/hr, and 7 km for rain intensity larger than 20 mm/hr. The vertical thickness of the rain zone is necessary for the determination of the filling coefficient. Having now all the initial data for the solution of our problem, Eq. (34) can be written, after taking logarithms and considering all the assumptions made, in the form

$$2\lg(R+x) = \lg C_2 + 1.6\lg I + \lg k_z + \lg k. \quad (64)$$

Putting  $k_z = 1$  and assuming that  $x = 0$ , since the very fact of the detection of the front part of the rain zone is satisfactory, we

obtain

$$2\lg R = \lg C_2 + 1,6\lg l + \lg k. \quad (65)$$

Specifying now the values of the precipitation intensity in mm/hr, we can readily obtain the values of R in km from (65). Thus, rain zones with intensity 10 mm/hr will be detected at distances not exceeding 37 km for the 3-cm H2X radar [82]. At larger distances from the radar this precipitation will not be detected, since the signal received from them is smaller than the sensitivity of the receiver.

It is of undoubted practical interest to estimate the effectiveness for the detection of precipitation zones by other radar stations, including those in regular operation. However, in solving this problem one frequently encounters greater difficulties, connected principally with the lack of systematic observations. In addition, these radar observations are not accompanied as a rule by measurements of the precipitation intensity (or the water content of the clouds). The latter circumstance does not make it possible to determine the radar constants by the same method as was done for the H2X radar. Consequently, one resorts to a computational procedure of determining the constants contained in Eq. (34). The gist of this procedure is to calculate the distances from the tactical-technical data of the radar for which these constants are determined, and from analogous data on radars for which these constants are known. In our case such a quantity is the constant of the H2X radar, namely  $C_2 = 28$ .

Indeed, we can assume that

$$C_2/C'_2 = B/B',$$

where  $C_2$  is the constant of the H2X radar, which is equal to 28,  $C'_2$  is the constant of the unknown radar, B is a coefficient determined by the technical characteristics and by the attenuation and filling coefficients of the H2X radar, and B' is the same quantity for the unknown

radar:

$$B = \frac{\pi^2 P_t A_p h}{48 \lambda^4} \left( \frac{\epsilon - 1}{\epsilon + 2} \right)^2 k k_s,$$

$$B' = \frac{\pi^2 P_t' A_p' h'}{48 \lambda'^4} \left( \frac{\epsilon' - 1}{\epsilon' + 2} \right)^2 k' k_s'. \quad (66)$$

Using the technical characteristics of some ground radars [36, 79], we can calculate their constants  $C'_2$ . The average values of these constants are listed in Table 12.

In compiling the table, the values of the filling coefficients are calculated for precipitation zones of varying vertical dimensions, with allowance for the different attenuation of waves of different length.

With the aid of the constants listed in Table 12, it is possible to obtain, by solving (34), also the limiting values of the range for the detection of precipitation of varying intensity using different types of radars. From the analysis of these data it can be concluded that the most effective for the detection of precipitation zones is the 10-cm WSR-57 radar, and the worst is the weapons sighting radar SCR-584.

In those cases when it is impossible to measure the power of the reflected signals, the curves of Fig. 44 can be useful for an approximate estimate of the lower limit of the intensity of the precipitation zone or the water content of the clouds.

The estimate made of the limiting ranges for the detection of precipitation of varying intensity is very useful in the organization of a radar network for storm and shower warning, since it helps decide the distances at which the radars must be located in order that the radar field produced by them be dense enough for all the dangerous showers, let alone the thunderstorms.

In this connection, there is undoubted interest in ascertaining

TABLE 12

1 Тип радаростанции	2 Вертикаль- ная мощ- ность линии (км)	3 Дальномер (км)				
		20	40	60	80	100
4 Наземная РЛС обнаружения WSR-57	3	260	280	350	390	400
	5	260	280	280	320	400
	7	260	280	280	280	280
5 Орудийной наводки SCR-584	3	8	8	8		
	5	8	8	8		
	7	8	8	8		
AN/TPS-10	3	69	69	87	105	
	5	69	69	69	71	
	7	69	69	69	69	

1) Type of radar; 2) vertical thickness of shower (km); 3) range (km); 4) ground detection radar; 5) weapons sighting.

which showers are dangerous and which are not. Obviously, an answer to this question can be obtained only for some specific meteorological servicing of a given branch of the national economy, transportation, or the military. If we have in mind meteorological service to aviation, showers with intensity starting at 5-10 mm/hr and above can be regarded as dangerous, for in moderate latitudes they can be accompanied by thunderstorms, by strongly developed bumpiness, poor visibility, etc. [20].

On this basis it is possible to determine with the aid of the plots of Fig. 46 the so-called meteorological radius of each radar station relative to the rain intensity indicated above. It is obvious that to create a continuous radar field for the detection of thunderstorms and showers it is necessary to locate the radar stations at distances which in any case do not exceed double their meteorological operating radius.

To determine the limiting ranges for the detection of clouds we use Relation (32), in which we replace the rain intensity  $I$  by the water content  $w$ . After taking logarithms we obtain

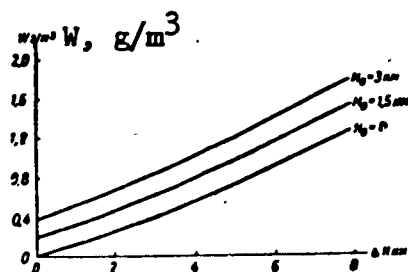


Fig. 44. Limiting heights for the detection of clouds with different water contents with the aid of the modernized TsAO installation.

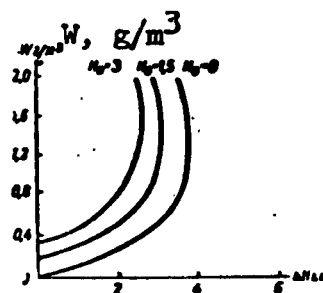


Fig. 45. Limiting height for the detection of clouds with different water contents by the TPQ-6 radar.

$$2 \lg(R+x) = \lg C_s + 2 \lg w(x) + \lg k. \quad (67)$$

Specifying now different values of the height and thickness of the cloud layers, and also assuming that the water content of the clouds is constant in height, we can readily obtain from Eq. (67) with allowance for the attenuation of the electromagnetic waves in clouds and gases of the atmosphere the values of the water content (Figs. 44 and 45).

The curves on Figs. 44 and 45 enable us to determine the limiting ranges for the detection of clouds with varying water content. Thus, for example, the radar installation modernized at the TsAO is capable, with a height of the lower boundary of the clouds at 1.5 km, of detecting these clouds up to 5 km, if their water content is not less than  $1 \text{ g/m}^3$ . The TPQ-6 radar station, owing to the stronger attenuation of the 8.6-mm waves, will detect these clouds only up to 3 km [62].

Another characteristic of the effectiveness of detection of atmospheric formations is the detection probability. The probability can be readily determined if a large series of radar observations is made. For example, G.M. Burlov has found on the basis of 1500 observations of showers with the aid of a type H2X radar that the probability of their detection decreases with increasing range (Fig. 46).

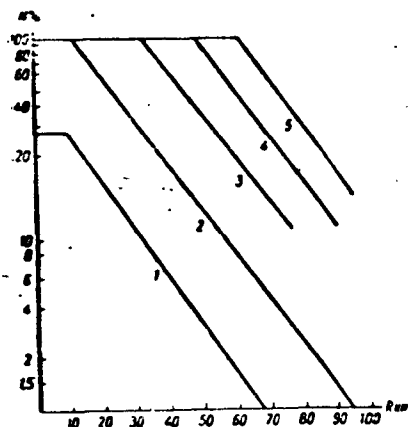


Fig. 46. Probability of detection of showers by means of various radar stations. 1) 10-cm weapons sighting radar SCR-584; 2) type H2X radar; 3) AN/TPS-10; 4) improved radar type H2X; 5) 10-cm detection radar WCR-57.

Indeed, within a radius of 10 km this radar detects all the showers, and at a distance of 50 km it detects on the average 15%, while at 100 km it detects about 1% of all the showers that are produced. It follows therefore that wherever the H2X radar shows a shower, the shower actually exists. However, where it does not show a shower, the shower may also exist. The probability of such an error increases with increasing distance to the shower or with decrease in the shower intensity. As regards the probability of detecting con-

tinuous precipitation, a radar of the type H2X detects all the continuous precipitation with intensity 0.3-0.5 mm/hr at a distance of 2-3 km, half of them at a distance 7-8 km, and 2 or 3% at a distance of 20 km.

For an approximate determination of the mean values of the probability of detecting precipitation by other radar, use can be made of the relation

$$\mu = \mu' \frac{C_2'}{C_2} \frac{P_{r, \text{min}}}{P_{r, \text{min}}'} \quad (68)$$

This relation remains valid for any number  $N$  of cases of detection of meteorological targets. Multiplying the left and right half of this equation by  $N$  and taking the limiting detection cases, when  $\mu = \mu' = 1$ , we verify that the probability of detection say with a radar type H2X, expressed by the left half of (68), is equal to the same detection probability multiplied by the dimensionless coefficient

$C'_{2P} \text{ min} / C_{2P} \text{ r min}$ . The latter can be smaller or larger than unity, depending on the parameters of the radar. In the plots (Fig. 46), the ordinates of the points of curve 2 represent the probability of detection of showers and continuous precipitation from data of the type H2X radar. If we take the values of these ordinates for different ranges and multiply them by the above coefficient, we can obtain the probability of detection for other radars.

Of all the radars considered, the highest probability is possessed by the detection-type (spotting) radar. The lowest probability for the detection of precipitation is that of the weapons-sighting radar. Even in the direct vicinity, only 1/3 of the precipitation is observed. In addition, this station has a rather limited operating radius, not exceeding 60 km.

Along with the detection of precipitation zones a very urgent problem of meteorological service for aviation is to differentiate showers from thunderstorms. Recently Ye.M. Sal'man and N.F. Kotov [10, 11] established the following main symptoms by which to distinguish reflections from thunderstorms and from showers: the top of the radio echo of thunderstorms is located as a rule above the  $-13^{\circ}$  isotherm; the reflecting characteristic of precipitation,  $z$ , decreases slowly with altitude in the case of thunderstorms; in thunderstorms the precipitation intensity exceeds as a rule 7-10 mm/hr.

Along with an estimate of the probability of detection of continuous precipitation, shower precipitation, and thunderstorms, great interest attaches to the determination of the probability that the radar will detect clouds which produce no precipitation.

In working with a type H2X radar it was established that this station does not detect clouds which produce no precipitation. From among the other radars indicated above, only a detection radar is capable of

fixing thick cumulus cloudiness within a radius of 50 km. The reason for it is the relatively small value of the constant  $C_2$ .

To detect clouds and dielectric inhomogeneities in the transparent atmosphere it is necessary to make use of radars whose constants  $C_2$  are large. Such radars are cloud-measuring radars, whose probability of cloud detection is listed in Table 13.

The data presented in Table 13 characterize the probability of radar detection of clouds in the case of vertical sounding, i.e., with the antenna directed vertically upward. The values of the probabilities themselves comprise the ratios (percentages) of the number of cases of radar detection of clouds of various forms to the number of cases of clouds actually seen passing over the radar.

In analyzing the tabular data, we are struck by the fact that the probability is as a rule less than 100%. On the average, approximately half the clouds which produce no precipitation can still not be detected by modern radars.

TABLE 13  
Probability of Radar Detection (%)

		1 Форма облаков													
		4	5	6	7	8	9	10	11	12	13	14	15		
2 Радиолокатор		кучево-дождевые	мошно-кучевые	слоисто-кучевые плотные	слоисто-кучевые просветляющие	слоистые	слоисто-дождевые	высоко-слоистые плотные	высоко-слоистые просветляющие	высоко-кучевые просветляющие	высоко-кучевые плотные	перисто-слоистые	кучевые		
3 Модернизированная РЛС ЦАО		100	100	80	50	—	100	60	—	50	—	30	5		

1) Form of clouds; 2) radar; 3) modernized radar of TsAO; 4) cumulonimbus; 5) thick cumulus; 6) opaque stratocumulus; 7) translucent stratocumulus; 8) stratus; 9) nimbostratus; 10) opaque altostratus; 11) translucent altostratus; 12) translucent altocumulus; 13) opaque altocumulus; 14) cirrostratus; 15) cumulus.

This leads to another important conclusion, namely that the thickness and the height of cloud layers, determined by cloud-measuring



radars, frequently differ from the actual values. It can be assumed that the upper boundary of the clouds will appear to be lower and the lower boundary appear to be higher; but the extent to which this is so is a subject for further research.

In order for the probability of detection of clouds of all forms to be 100% and for the thickness of the clouds to correspond more closely to the results of the measurements, it is necessary to increase the constants  $C_3$  of the cloud-measuring radars by a factor of several times ten.

#### 8. RADAR OBSERVATIONS OF PRECIPITATION ZONES FROM ARTIFICIAL SATELLITES\*

At the present time artificial earth satellites are used abroad to observe cloud zones using television and photographic cameras. It turns out that one of the principal shortcomings of such observations

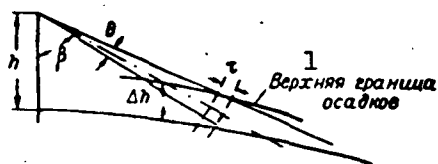


Fig. 47. Geometry of radar beam. 1) Upper boundary of precipitation.

is the lack of information on the distribution of the precipitation zones and the heights of the clouds. Yet the radar is at present the only means capable of eliminating this shortcoming.

A meteorological radar station mounted on a satellite should have [81] small weight, small power consumption, a sufficient view of the earth's surface, a suitable wavelength guaranteeing small attenuation in the atmosphere, and large values of effective precipitation scattering areas, and also take into account the influence of interfering reflected signals from the water and earth surfaces.

The visibility area on earth and the thickness of the atmosphere above the earth's surface, observed by the radar from the satellite, depend on the resolution in vertical direction, on the travel time of the pulse from the radar to the target and back, and on the information

storage and computing capacity. In order to guarantee the required swept area on earth, the radio beam must be scanned in a plane perpendicular to the satellite velocity vector.

The resolution  $\Delta h$  of the radar in the indicated vertical plane, causing the observation of precipitation zones with minimum vertical height, depends on the height of the satellite  $h$ , on the duration of the sounding pulse  $\tau$ , on the width of the radio beam  $\theta$ , and on the sighting angle  $\beta$  (Fig. 47). This dependence is given by the formula

$$\Delta h = \sqrt{\left[ \tau + \sqrt{R^2 - (R+h)^2 \sin^2 \left( \beta - \frac{\theta}{2} \right)} - \right.} \\ \left. - 2(R+h) \sin \beta \sin \frac{\theta}{2} \right]^2 + (R+h)^2 \sin^2 \left( \beta + \frac{\theta}{2} \right) - R}, \quad (69)$$

where  $R$  is the radius of the earth.

At definite sighting angles  $\beta$ , the lower part of the sound pulse may touch the earth's surface, and the middle and upper parts strike the precipitation zone. As a result, the signals reflected from the earth's surface arrive at the radar receiving antenna simultaneously with echo signals from the precipitation and make their observability worse. Solution of Eq. (69) shows that  $\Delta h$  depends more on the width of the radio beam than on the pulse duration  $\tau$ .

Another factor determining the visibility area is the time of travel of the pulse from the radar station to the precipitation and back. For a chosen type of scanning, the time during which the radar antenna makes a given sighting angle  $\beta$  is a function of the width of the radio beam, the total scanning angle, and the height of the satellite.

At a smaller radio-beam width, it is necessary to increase its oscillations per unit time so as to obtain a continuous visibility strip on the earth's surface. Large scanning angles call for large angular displacement velocities of the radio beam.

For the customarily used radar antenna, employed for both transmission and reception, the time during which the antenna turns through an angle equal to the width of the radio beam should be larger than the time required for the main pulse to travel to the target and back. Calculations have shown that for a satellite located at a height of 550 km, the scanning angle must not exceed  $35^\circ$ . At the same time, for complete visibility of the equator the required scanning angle is  $125^\circ$

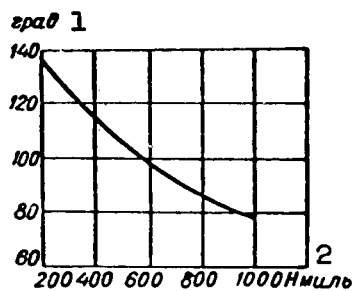


Fig. 48. Scanning angle for complete visibility of the equator. 1) Degrees; 2) miles.

(Fig. 48) [81].

Another important factor is the possibility of storing information on board the satellite and the carrying capacity of the transmission line from the satellite to the ground station, necessary for reading the obtained information.

The total number of chosen volume elements along the orbit is proportional to the scanning angle, to the maximum height of the precipitation zone, and is inversely proportional to the duration of the main pulse, to the height of the satellite, and to the square of the width of the beam.

If the given stored information is read directly on the orbit, it can be conveniently expressed in the form of a product of time by the bandwidth necessary for complete reading. Calculations have shown that this product reaches several megacycle minutes for a complete survey of the earth's surface.

At a satellite height of 1100 km, a radio beam width  $0.5^\circ$ ,  $\tau = 0.5 \mu\text{sec}$ , resolution along the earth 5 km, and height of precipitation zone 2 km, the information that must be read from the orbit for complete coverage at the equator is  $(0.18 \mu\text{min}) \cdot 10^6 \cdot 60 \cdot 2 = 21.6 \cdot 10^6$  bits [81].

A radar station installed on a satellite for the detection of precipitation zones can have optimum wavelengths less than 3 cm, since the precipitation zone will be observed as a rule from above and consequently the attenuation of the radio waves will play a lesser role than in the case of ordinary land-base observations. It can be assumed that it is advantageous to use radar wavelengths of 3 and 0.8 cm [81].

We have pointed out above the fact that in radar observation of precipitation zones from a satellite account must be taken of echo signals from the earth or water surfaces. In the case when the task is not only to detect the precipitation but also to determine their vertical dimensions, the signals reflected from the earth can be useful, since it is much more convenient to measure the indicated dimension of the precipitation from the earth than from the satellite. However, at relatively small sighting angles, the echo signals from the earth's surface turn into interfering signals, which can mask the useful echo signals from the precipitation zones. The effective reflecting area of the earth and water surfaces can change by more than a factor of 300, depending on the character of the soil, vegetation, or waviness of the water surface. It depends little on the wavelength and, in the case of dry land, on the sighting angle. For a water surface, the dependence on the sighting angle is more clearly pronounced.

There are various methods for recognizing the precipitation zones.

It is necessary to use above all the difference in the outlines of the echo signals from the precipitation and the displacement of these signals. In addition, one can use the Doppler frequency shifts due to the finite velocities of the falling rain drops. One can also use the differences in the amplitudes of the reflected signals from the precipitation and from the earth's surface, using a two-band radar. This is possible, inasmuch as the scattering area of the earth's sur-

face depends little on the wavelength, while that of the precipitation is proportional to  $1/\lambda^4$ .

Correlation methods based on differences in the statistical (fluctuation) characteristics of the echo signals from the precipitation and the echo signals from the earth's surface can also be useful for recognition purposes.

Manu-  
script  
Page  
No.

# [Footnotes]

- 139 We give below a measurement procedure described in [17].
- 148 Under the assumption that the filling coefficient is equal to unity.
- 157 This section is based on materials from the foreign press [81].

Manu-  
script  
Page  
No.

# [List of Transliterated Symbols]

- 89 ИКО = IKO = indikator krugovogo obzora = circular-scan indicator
- 91 ЦАО = TsAO = tsentral'naya astronomicheskaya observatoriya =  
central astronomical observatory
- 105 и = i impul's = pulse
- 107 з = z = zapolneniye = filling
- 107 и = i = izobrazheniye = image
- 114 р/л = r/l = radiolokatsionnyy = radar
- 126 в = v = voda = water
- 126 л = l = led = ice
- 127 мм = mb = millibars
- 147 цел = sel = selektsiya = selection

## Chapter 5

### USE OF RADIOTECHNICAL STATIONS FOR WIND AND TEMPERATURE SOUNDING OF THE ATMOSPHERE

A very important problem in the use of radiotechnical stations (radar) in meteorology is the measurement of the velocity and direction of the wind in the free atmosphere. These measurements, unlike those with the aid of pilot balloons using aerological theodolites, are called radiopilot measurements.

The main advantage of radiopilot measurements compared with pilot balloon measurements is that the former can be carried out under arbitrary meteorological conditions day and night, independently of the visibility of the balloon, and up to large altitudes. If properly organized, the accuracy of radiopilot measurements is found to be not lower than the accuracy of observations made at bases. As a rule, radiopilot measurements of wind are accompanied by radiosounding of the atmosphere. To measure wind at various altitudes, two radiometric methods are used, radio direction finding and radar.

#### 1. RADIO DIRECTION FINDING METHOD OF DETERMINING THE WIND

The gist of the radio direction method of determining the wind consists of determining with the aid of a special radio direction finder the angular coordinates of a radio transmitter (elevation angle and azimuth) which is launched in free flight. Inasmuch as usually a radiosonde is connected to the electric circuit of the radio transmitter, the third coordinate necessary for the determination of the wind, namely the altitude, is obtained from the pressure and temperature sig-

nals of the radiosonde.

An example of a radio direction finder constructed especially for meteorological purposes is the domestic radio direction finder – the "Malakhit" radio theodolite.

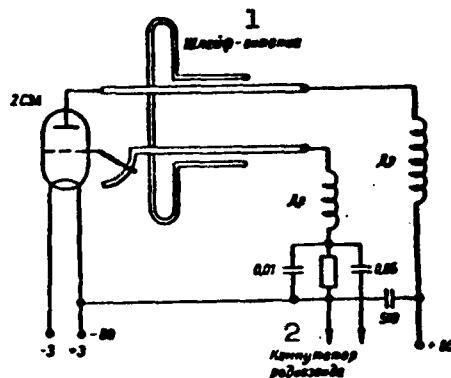


Fig. 49. Schematic diagram of direction finder transmitter type PRB-1.5. 1) Folded dipole; 2) radiosonde commutator.

Figure 49 shows the schematic diagram of the direction finding transmitter, while Fig. 50 shows the block diagram of the radio theodolite; an over-all view of the latter is shown in Fig. 51.

The transmitter employs a self-exciting UHF oscillator with self-modulation by means of a type 2S3A triode.

The tank circuit is made up of a long line connected between the grid and plate of the tube.

A slider moving over a wire arc serves to tune the tank circuit to the operating frequency between 5 and 6 Mc.

The transmitter has two operating modes, depending on whether the radiosonde is connected to its circuit or not. When the radiosonde is connected, the pulse repetition frequency is  $f_1 = 500$  pulses per second, and without the radiosonde  $f_1 = 3000$  pulses per second.

The pulses with low repetition frequency are used to transmit the temperature, pressure, and humidity signals, while the pulses with the

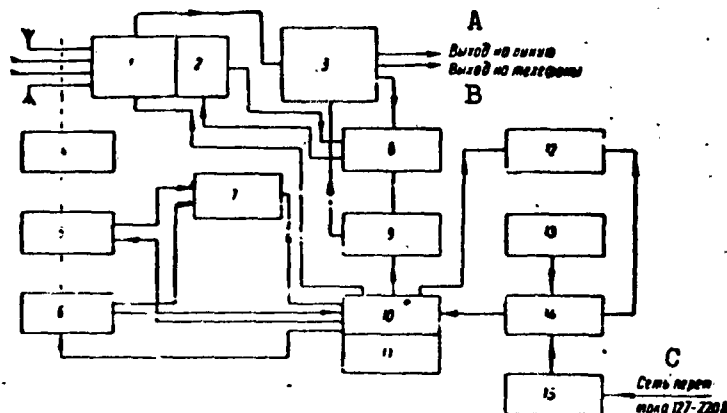


Fig. 50. Block diagram of "Malakhit" radio theodolite. 1) Antenna commutator; 2) voltage control generator; 3) receiver; 4) antenna drive; 5) angle coordinate (fine) transducer; 6) angle coordinate (coarse) transducer; 7) precision reading block; 8) angle coordinate indicator; 9) power supply; 10) distribution and protection block; 11) coarse reading sel-syns; 12) charging unit; 13) AB-2-0-230 power supply; 14) power panel; 15) pole panel. A) Output to line; B) output to telephones; C) 127-220 volt AC line.

high repetition frequency fill the pauses between the radiosonde signals.

The carrier frequency of the radio pulses is maintained constant all the time at 216 Mc; the bearing of the radiosonde is taken, in order to determine its angular coordinates, at both pulse repetition frequencies of the PRB-1.5 transmitter.

The high-frequency energy is fed to the antenna with the aid of an open-end segment of a long line, inductively coupled with the operating line of the transmitter. The antenna is a folded dipole made of aluminum wire 3 mm in diameter. The transmitter is fed from dry cells. To feed the plate circuit, a GB-70 battery is used, while a BON-3 battery is used for the filament.

When launching a radiosonde with a PRB-1.5 transmitter, the radio theodolite is used to receive both the working signals, the character



and duration of which depend on the values of the meteorological elements (pressure, temperature, and humidity of the air), and signals corresponding to the pauses between the working signals.

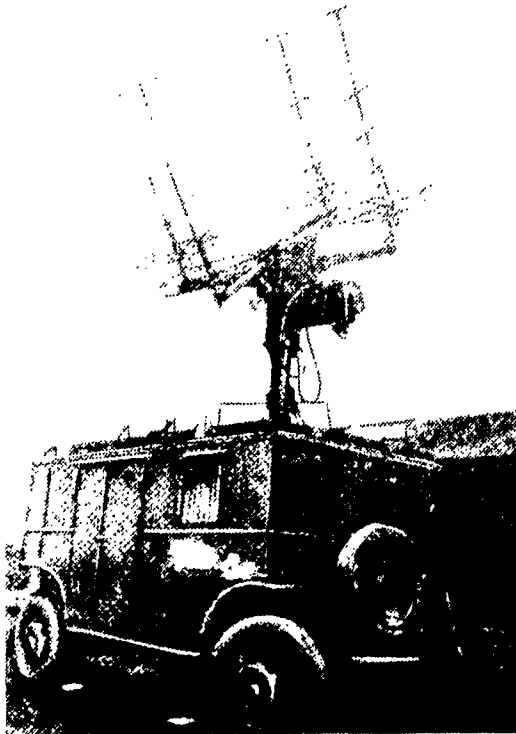


Fig. 51. Over-all view of "Mala-khit" radio theodolite.

These signals are fed to the receiver antenna unit of the radio theodolite, which consists of four individual antennas of the "wave channel" type, bounded on a common rotating frame, in the four corners of a square, one of the diagonals of which is always horizontal. The antennas located on the ends of the horizontal diagonal of the square are used to determine the azimuth of the radiosonde, while the antennas located on the ends of the vertical diagonal are used to determine the elevation angle.

By means of a phasing system and an antenna commutator, a jump-like displacement is imparted to the directivity pattern in space,

such that the pattern occupies extreme positions in the following sequence: left, top, right, bottom.

The direction to the target is determined by the straight line passing through the initial point of the directivity pattern and the point of intersection of the directivity patterns in the other extreme positions. Inasmuch as the directivity patterns have large slopes at the points of intersection, the use of the equal-signal zone principle guarantees high direction-finding sensitivity and accuracy in the determination of the angular coordinates.

The maximum error in the determination of the angular coordinates of the direction finding transmitter is not more than  $1.75^{\circ}$  in the following ranges:  $16$  to  $75^{\circ}$  in elevation and  $0$  to  $360^{\circ}$  in azimuth. The probable random error under these conditions does not exceed  $0.3^{\circ}$ .

The signals of the direction-finding transmitter are received by the radio theodolite receiver, are transformed in the receiver, and are used in two separate channels: the angle-coordinate indicator channel (direction finding channel) and the channel for audio reception of the radiosonde signals (sound channel).

The indicator of the elevation angle and of the azimuth operates with a circuit that provides an amplitude display of the bearing of the target. The indication of the two angle coordinates is combined on the screen of a single cathode-ray tube.

The screen of the tube displays two pairs of pulses of different amplitude. With the aid of the azimuth and elevation cranks, the operator sets the antenna in such a way that the pulses of each pair have identical amplitudes. These correspond to the "bearing" positions for each angle coordinate. The azimuth and the elevation are read against scales mounted on the shafts of selsyn receivers in the precision reading block. The selsyn receivers are electrically coupled with

selsyn transmitters. The latter are connected through a system of gears to the axes of the antenna rotation in azimuth and in elevation. The fine selsyn transmitters are coupled to their axes through gears with a 1:36 ratio.

For approximate (coarse) measurement of the angular coordinates of the radiosonde, two coarse-reading selsyn receivers are used, which have electric coupling to the corresponding selsyn transmitters.

The coarse-reading system is used by the operator who determines the bearing, and the fine system is used by a second operator, who records the coordinates of the radiosonde at definite instants of time. A third operator receives by ear the signals from the radiosonde over the sound channel of the radio theodolite receiver. At the output of this channel is connected a filter, which separates the first harmonic of the low pulse repetition frequency (600 cps) and suppresses the first harmonic of the high pulse repetition frequency. Thus, only signals with frequency of 600 cps are fed to the earphones, with a duration that is determined by the time during which the grid circuit of the direction finding transmitter is closed by the radiosonde commutator. Subsequently, after the signals are processed, the values of the atmospheric pressure, temperature, and humidity of the air are obtained as a function of the altitude.

Having the values of the altitude, determined from the pressure and temperature signals, and the angular coordinates of the radiosonde, it is possible to obtain also the velocity and the direction of the wind at different altitudes.

## 2. RADAR METHOD OF DETERMINING THE WIND VELOCITY AND DIRECTION

The gist of this method is to carry out with the aid of a radar station observations of a specially prepared reflecting target, lifted with a hydrogen-filled rubber envelope. When such a reflector is struck

by the measuring pulse, the reflector becomes a secondary radiator, which sends electromagnetic energy of the same frequency in various directions, including the direction of the radar receiver. In aerology, such a passive target together with its envelope is called a radiopilot.

During the observations one determines the angular coordinates of the radiopilot and the slant range to it. These data yield after processing the velocity and direction of the wind in the free atmosphere.

Inasmuch as a more accurate determination of the wind calls for a high accuracy in determination of the radiopilot coordinates, not all types of radar can be used for wind sounding. The requirements imposed are satisfied only by radars which make it possible to determine the angular coordinates of the radiopilot with an error of several minutes, and the slant range with an error of 10-20 meters.

In the radar method of wind determination, an important factor is the effective reflecting area of the radiopilot target. The size of this area depends on the dimensions and shape of the target, on its orientation relative to the direction to the radar and the plane of polarization of the incident energy. The concept "effective area" is convenient for the comparison of various reflecting surfaces having complicated geometrical forms. The effective area is equal to the cross-section area of an ideal reflecting sphere, which reflects the same amount of electromagnetic energy in the direction of the radar receiver antenna as does the actual reflecting area of the target.

Calculation of the effective area of the radiopilot target using centimeter-band radars is carried out with the aid of the fundamental radar equation for a single target (10), solved with respect to T,

$$T = \frac{9 \cdot R^2 P_{r, \min}}{P_t A_p^2 k} \quad (70)$$

where T is the effective area of the target for a specified range to

the radiopilot R.

For reliable determination of the bearing, it is assumed that the received signal is equal to  $2P_{r \min}$ .

The maximum distance to the radiopilot is limited to the effective radius of the radar which for certain types of radars does not exceed 50 km. Taking the values of R and  $\lambda$  in meters,  $A_p$  in  $m^2$ , and  $P_t$  and  $P_{r \min}$  in watts, we determine T in  $m^2$ . Knowing the effective reflecting area of the target, we calculate the geometrical parameters of the real targets which are suspended from the rubber envelope filled with the hydrogen. The values of the effective reflecting area can be obtained from the data given in Table 14.


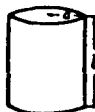


If centimeter-band radars are used for radar measurements of the wind, then the targets are most frequently corner reflectors. The simplest corner reflector represents three metallic planes, forming three mutually perpendicular faces. It has the property that, over a sufficiently wide interval of angles of incidence, the reflection of the electromagnetic waves is strictly in the opposite direction. It must be noted that this property is satisfactorily fulfilled only if the faces are perpendicular to one another with a sufficiently high degree of accuracy. The effective area of a trihedral reflector depends on the foreshortening at which it is seen. This area is sufficiently large almost over the entire space of a solid angle equal to  $\pi/4$ .

The maximum value of the scattering in triple reflection lies in the direction of the symmetry axis of the corner reflector. As the direction of the beam deviates from this axis, the effective reflecting area decreases.

An even larger effective reflecting area is possessed by a corner reflector with square faces. However, this corner has a sharper directivity pattern. For equal values of the sides  $a$ , the square corner

TABLE 14

## Effective Areas of Radiopilot Targets

1 Название мишени	2 Форма мишени	3 Расчетные формулы
4 Металлический шар		$T = \pi a^2 \quad (1')$
5 Металлический цилиндр		$T = 2\pi a \frac{l}{\lambda} \quad (2')$
6 Угловой отражатель		$T_{\text{max}} = \frac{4}{3} \pi \frac{a^4}{\lambda^2} \quad (3')$
7 Полуволновой вибратор		$T_{\text{max}} = 12\pi \frac{a^4}{\lambda^2} \quad (4')$ $T = 0,86 \lambda^2 \cos^4 \theta \quad (5')$

Remark. Formula (1') is valid when  $a/\lambda \geq 1.6$  and Formula (2') when  $a$  and  $l \gg \lambda$ .

1) Name of target; 2) form of target; 3) theoretical formulas; 4) metal sphere; 5) metal cylinder; 6) corner reflector; 7) half-wave dipole.

has nine times more reflecting area than the triangular corner.

Under real lifting conditions, the target may swing and rotate, and it is therefore made in the form of a complicated corner reflector so as to obtain a powerful and sufficiently stable reflected pulse.

This reflector usually consists of four corner reflectors.

Corner reflectors for radiopilots are usually made of metallized cardboard or of cardboard on which unannealed aluminum foil, metal screen, or tinfoil with holes of 10-20 mm are glued.

If meter-band radar is used for the measurement of the wind, then the reflecting target is made of two metallic half-wave dipoles of copper, brass, or aluminum wire 2-3 mm in diameter. The dipoles are in-

serted at right angles to each other into a piece of heavy cardboard so that they do not touch each other. The target is then suspended in horizontal position from the stub of the envelope with the aid of twine fastened to the corners of the cardboard.

An attractive possibility is the use of the envelopes themselves as reflecting targets, by making them conductive. Inasmuch as the effective reflecting area of a sphere is relatively small compared with the area of a corner reflector, this idea has remained unrealized to this time. However, the use of metallized envelopes No. 50 has permitted even now to decrease the dimensions and weight of the corner reflector, and consequently to increase in this manner the vertical speed of the radiopilot and the upper limit of the wind sounding.

Another shortcoming of the radar method is the impossibility of measuring the wind within the radius of the minimum detection range, which for the radars employed usually is equal to 800-1000 m. As a result of this, for a reliable determination of the radiopilot coordinates the latter must be launched at a distance not smaller than the minimum radius of the radar. The launching place is then usually chosen to be on the side in the direction where the wind blows.

Sometimes when there is no possibility of launching the radiopilot at a distance from the radar, an optical theodolite installed alongside the radar station is used for the determination of the coordinates of the radiopilot in the minimum operating radius.

In those cases when along with the wind data it is necessary to have information on the temperature, humidity, and pressure of the air, the corner reflector is suspended together with a RZ-049 or A-22-III radiosonde on a rubber envelope No. 100 or 150, filled with hydrogen. Then the radar is used to determine the coordinates of the launched radiosonde, and a receiver of suitable wavelength coverage is used to

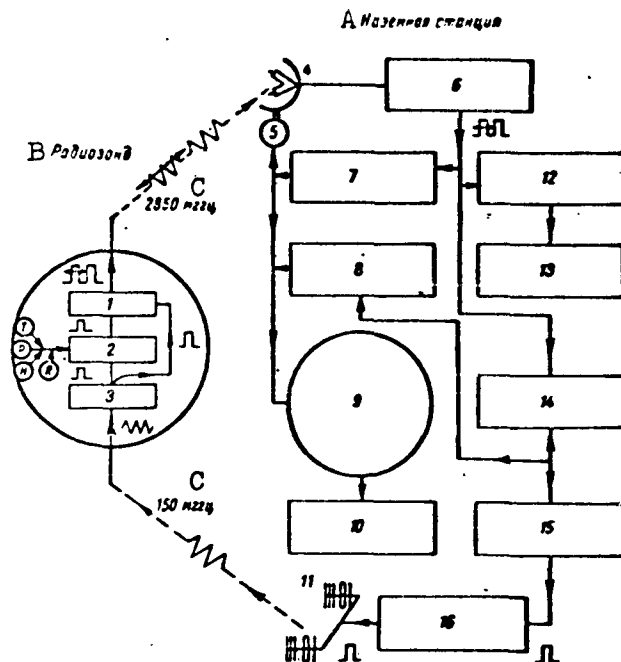


Fig. 52. Diagram of British radio theodolite, operating with a radiosonde responder. 1) Transmitter; 2) delay line; 3) receiver; 4) dipole; 5) azimuth and elevation motors; 6) receiver; 7) automatic adjustment; 8) automatic range finder; 9) computer units for the determination of the wind; 10) automatic wind recorder; 11) transmitting antenna; 12) telemetry apparatus; 13) radiosonde automatic recorder; 14) indicator; 15) calibrator; 16) transmitter. A) Ground station; B) radiosonde; C) megacycles.

receive the sound signals of the radiosonde.

It was pointed out above that a shortcoming of the radar method of measuring wind is the low upper limit of wind sounding. An advantage of this method is the high accuracy of wind determination, compared with the accuracy of base-organized pilot balloon observations. The above-mentioned shortcoming can be eliminated by replacing the passive reflector with a special responder radiotransmitter; apparatus of this type will be considered in Chapter 7 below.

A block diagram of the Mullard apparatus,\* containing a ground



station and a radiosonde with responder transmitter is shown in Fig. 52, which shows the principal blocks of the apparatus.

Circuits and the construction of radiosondes of the relay type will be described in Chapter 7 below.

### 3. ORGANIZATION OF RADIO DIRECTION FINDING AND RADAR WIND MEASUREMENTS

Before carrying out radiometric wind measurements, particular attention is paid to leveling, orientation, and adjustment of the station. Before leveling the radio theodolite, two supporting beams are placed under each plate of the jacks of the truck. The correctness of the leveling is checked against control levels and is regarded as satisfactory if for any rotation of the antenna the bubbles of the control levels do not shift relative to the hairlines.

In orienting the radiotheodolite relative to the points of the compass, the setting is such that when the antenna system points to the north the reading on the azimuth selsyn scales is  $0^{\circ}$ . Of great importance here is the choice of a target, which can be any object located not closer than 500 m. The azimuth of the target is usually determined with an aerological theodolite, which is located 200 m away from the radio theodolite in the direction of the target. Three operators are needed for this purpose: the first is at the radio theodolite (at the optical site), the second inside the cabin, and the third at the theodolite. Together they see to it that the radio theodolite, the theodolite, and the target are all in line. After the coarse setting of the theodolite; one proceeds to its fine setting in line between the target and the radio theodolite. For this purpose the theodolite is aimed first on the target and then on the optical site of the radio theodolite, the difference in the reading of the horizontal angles should then be  $180^{\circ}$  and if it is different from  $180^{\circ}$  it becomes necessary to reinstall the theodolite such that the difference becomes

equal to  $180^{\circ} \pm 0.3^{\circ}$ .

To prevent random errors, the measurements are carried out three times, after which the average of three readings is calculated with accuracy  $0.1^{\circ}$ . The antenna system is then aimed with the aid of the sight at the target, the azimuth of the target is set on the selsyn scales, and the scales are left in this position.

The elevation-angle selsyns are correctly set in an analogous manner. In this case the optical theodolite is mounted on the roof of the radio theodolite cabin. The scales of the elevation-angle selsyns of the radio theodolite are set in accordance with the elevation of the optical theodolite.

After the orientation is complete, one proceeds to correct the radio theodolite so as to align the electrical and geometrical axes of the antenna system. The correction is with the aid of adjusters. The following method of correction is quite effective. A transmitter tuned to 216 Mc (without a radiosonde) is launched in flight, and when the sphere reaches the layer of stable wind, the operator, looking through the sight, records, on command of the operator who takes the bearing, the displacement of the transmitter away from the center of the site. Fifteen to twenty readings of this type are made within as short a period as possible. The correction is completed when the average deviation of the transmitter from the center does not exceed one small division of the sightscale.

#### 4. ACCURACY OF WIND MEASUREMENT

In measuring the wind with the aid of the "Malakhit" radio theodolite and a direction-finding radiosonde, it is necessary to measure accurately not only the angular coordinates, but also the air pressure and temperature. The reason for it is that the values of these meteorological elements are used to determine the height of the radiosonde.

If the error in the measurement of air pressure does not exceed 2 mb and the temperature error does not exceed  $2^{\circ}$ , then the relative error in the determination of the height from the data of the direction finding radiosonde will be of the order of 2% up to heights of 20-25 km. This error becomes acceptable at large altitudes. Above 25 km, in order to determine the height with an error of 1%, the temperature must be measured with an error not more than  $1^{\circ}$  and the pressure error must not exceed 0.5 mb. Such a relatively high measurement accuracy cannot be guaranteed by the comb-type radiosonde RZ-049. However, one of the most recent domestic radiosondes, A-22-III, and some models of foreign radiosondes, make it possible to determine the temperature and the pressure of the air with the above-indicated accuracy.

The nature of the processing of pilot balloon and radiopilot measurements is such that the error in the determination of the wind depends in final analysis on the error in the determination of the horizontal distances of the pilot balloon or the radiosonde. The maximum value of this relative error can be calculated from the formula

$$\frac{\Delta L}{L} = \frac{\Delta H}{H} + \frac{2\Delta\delta}{\sin 2\delta},$$

where H is the height of the radiosonde,  $\Delta H$  the relative error in the determination of the height,  $\delta$  the vertical angle, and  $\Delta\delta$  the error in the measurement of the vertical angle.

An analysis of this expression shows that for specified  $\Delta H$  and  $\Delta\delta$  the relative error in the determination of the horizontal distance will be a minimum at  $\delta = 45^{\circ}$ . The most probable values of the vertical angles  $\delta$  in radiopilot measurements lie in the interval 20-25 $^{\circ}$ . Then the maximum value of  $\Delta L/L$  for  $\Delta H/H = 2\%$  and  $\Delta\delta = 0.3^{\circ}$  will be 4%. For smaller values of the vertical angle, which frequently can correspond to large heights of the radiosonde, the error in the determination of

the horizontal distances will be larger.

To reduce these errors, and consequently the errors in the measurement of the wind, which do not exceed  $\pm 2$  m/sec, it is recommended that the measurements made up to a height on the order of 10 km with values of  $\delta$  larger than  $10^\circ$  be processed every four minutes. If the heights are larger and the angles  $\delta$  exceed  $15^\circ$ , the processing should be carried out every six minutes.

To illustrate the errors in the measurement of the wind with the aid of the "Malakhit" radio theodolite, let us use the experimental data published in the paper by P.L. Yefimov and A.M. Khachatryan [22].

To estimate the accuracy in the determination of the velocity and direction of the wind, use was made of data obtained by comparative measurements of the wind with the aid of the "Malakhit" radio theodolite and optical theodolite at six aerological stations. In addition, parallel observations of a single radiosonde made with two radio theodolites and an optical theodolite were used. Using their measurement materials, the authors calculated the frequencies of occurrence (in percent) of the differences in the wind velocity and direction (Tables 15 and 16).

TABLE 15

	1 Разность (м/сек.)					
	0	1-3	4-6	7-9	10-12	12-15
2 По радиотеодолиту и оптическому теодолиту . . . . .	33	56	8,3	2,3	0,4	0
3 По двум радиотеодолитам . . . . .	23,2	58,7	13,7	3,0	1,9	0,4

1) Difference (m/sec); 2) using a radio theodolite and an optical theodolite; 3) using two radio theodolites.

It is seen from the tables that the difference in the direction and velocity of the wind as obtained using two radio theodolites is

TABLE 16

	1 Разность (град.)					
	0	1-5	6-15	16-25	26-35	36-60
2 По радиотеодолиту и оптическому теодолиту . . . . .	9,0	73,0	13,4	3,8	0,6	1,0
3 По двум радиотеодолитам . . . . .	9,1	56,5	26,8	6,1	1,0	0,4

1) Difference (degrees); 2) using a radio theodolite and an optical theodolite; 3) using two radio theodolites.

somewhat larger than using an optical theodolite and a radio theodolite. This can be attributed to the lower accuracy with which the angle coordinates are determined by radio theodolites.

Most frequently the random errors in the determination of the wind velocity with the aid of the "Malakhit" radio theodolite range from 0 to 3 m/sec, while the errors in the determination of the wind direction are from 0 to  $10^{\circ}$  (frequency on the order of 80%).

The sequence with which radio direction finding and radar measurements of the wind is the same in pilot balloon observations. At the instant of reading the radiosonde or the radiopilot should be exactly in bearing. The rotation of the antenna-drive cranks is stopped during that time. The height is determined after processing the radiosounding data. Then, using the height corresponding to each reading of the angle coordinates, the wind velocity and direction are determined with the aid of the Molchanov circle.

Manu-  
script  
Page  
No.

[Footnote]

172

Tested at the Crowlee observatory.

Manu-  
script  
Page  
No.

[List of Transliterated Symbols]

163	2C3A = 2S3A [tube designation]
163	Др = Dr = drossel' = choke
163	и = i = impul's = pulse
170	макс = maks = maksimal'nyy = maximum

## Chapter 6

### REVIEW OF RADAR METHODS

#### 1. DETERMINATION OF DISTANCE

Radar methods for measurement of distance are based on time measurement. In accordance with the classification of radar methods given in Chapter 1, into systems with continuous and pulsed radiation, different methods are considered for the measurement of time and consequently distance.

Pulsed methods, which guarantee sufficiently high accuracy in the determination of the range (on the order of 10-15 meters) with perfectly satisfactory resolution, are the most widely used. The basis of the determination of the time is the direct relationship between the distance  $\Delta R$  and the time  $\Delta t$ , during which the electromagnetic wave propagates over the indicated distance

$$\Delta R = c\Delta t,$$

where the coefficient of proportionality  $c$  is the velocity of light (in general, of electromagnetic waves).

The time  $\Delta t$  is measured by observing the variation of the voltage  $\Delta U$  during the time interval  $\Delta t$ .

If

$$U = kt$$

the quantity  $\Delta U$  serves as a measure of the range. Inasmuch as in the indicators the motion of the light spot over the screen is under the influence of a variation of the voltage  $\Delta U$ , this measure of range can be determined by visual means.

In systems with continuous radiation, the method of measuring distances is based on the determination of one of the parameters, either the phase or the frequency of the oscillations during the time  $\Delta t$ . A thorough review of the methods was presented by A.F. Bogomolov [28]; the technical solutions are treated in the specialized literature [29].

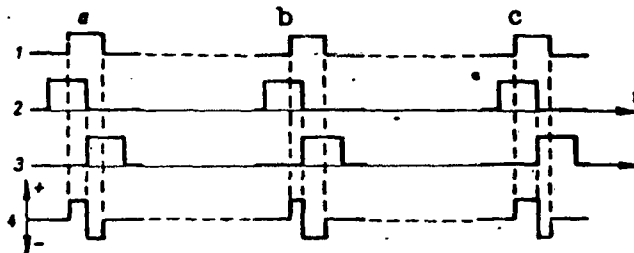


Fig. 53. Formation of "error signal" in automatic control system.

Modern radar technology is equipped with methods for automatic range determination. The advantages of these methods lie in the possibility of obtaining greater accuracy and speed of determination of the data with elimination of individual operator errors. In this case it is possible to track in range automatically and continuously. The time of operation of the automatic system fluctuates between 0.5 and 0.1 second, which is much faster than the speed attainable by manual control, since experience has shown that, depending on his skill and fatigue, an average operator has a "time constant" on the order of one second.

The use of automatic range finders is less justified when working under conditions with low signal/noise ratios and when the signal strength decreases, so that loss of the target is possible. In such cases it is advantageous to use "memory" systems, which maintain automatic tracking in accordance with data preceding those that have dropped out.



The operating principle of automatic devices of this type is based on the following.

The circuit includes a generator which generates a local voltage. In addition to this voltage, the circuit receives a voltage formed by the reflected pulses. As a result of a comparison of these two voltages in the circuit, their relative agreement or disagreement is established. In the latter case the circuit generates an "error signal," which acts through a control system on the local-voltage generator to make the latter correspond to the voltage produced by the reflected pulses.

The foregoing can be explained by the plots shown in Fig. 53.

The pulses reflected from the target have on a type-A indicator screen a form as shown in the figure (marked by the number 1). The circuit generates two similar pulses, which are shifted in time, as shown on axes 2 and 3; these pulses can be shifted simultaneously, by means of a special unit, along the time axis. The addition of the pulses designated on the figure by the numbers 1, 2, and 3 occurs in the circuit; the results of the addition are shown in the figure on the axis 4, with three possible cases, a, b, and c shown. The resultant voltage which is formed at the output of the circuit under the influence of the pulses 4 can be equal to 0 (case a), or can have a negative (case b) or positive (case c) polarity.

The output voltage produced under the influence of pulses 4 is the error signal. It is fed to the regulating mechanism and depending on whether the voltage has positive or negative polarity, the pulses 2 and 3 are shifted and the net result is an elimination of the error, in other words a situation corresponding to case a on Fig. 53 is obtained.

## 2. MEASUREMENT OF ANGULAR COORDINATES

The angular coordinates of the object M (see Fig. 1) in space are:

1) the azimuth angle  $\beta$ , measured (in clockwise direction) from the azimuthal direction to north or, in individual cases, from some arbitrarily assigned direction (for example, the course line of a ship or airplane, etc.);

2) elevation angle  $\epsilon$  reckoned in a vertical plane from the horizon line to the direction to the object.

To determine the angular coordinates, as was already mentioned in Chapter 2, directional transmission and reception are used, in other words, use is made of the directional properties of the antennas.

The simplest method is to make such use of the directional action of the antennas, by which the target (object) is on the bisector of the aperture angle of the directivity pattern or, what is the same, in the direction of maximum radiation. This method is called direction finding on the basis of the maximum. However, as illustrated in Fig. 54, in this method the changes in the radiation field intensity are very small in the vicinities of the direction of maximum radiation (radius  $R_0$ ), and the value of  $\Delta R$  shown in the figure is very small. Consequently, the sensitivity of this system with respect to changes in the angular position of the antenna near the maximum of radiation is quite small.

The method of equal-signal zone has appreciable advantages with respect to increasing the sensitivity; this method consists in the following.

Two lobes of the directivity pattern of the antenna, shown in Fig. 55, make it possible to carry out a comparative measurement of the direction by using alternately the directional action of two antennas. Such a two-lobe diagram is the joint radiation from two directional

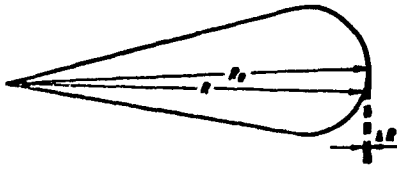


Fig. 54. Illustrating the determination of the sensitivity when direction finding on the basis of the maximum.

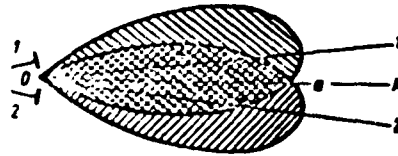


Fig. 55. Double-lobe radiation pattern of antenna.

antennas; such a diagram can also be obtained by using a single antenna but switching alternately its feed. As can be seen from Fig. 55, on the direction OM there is a point a which belongs to both diagrams and corresponds to equal values on both indicators pertaining to antennas 1 and 2. In practice, when both antennas 1 and 2 move simultaneously, they are oriented in such a way that the target is in the direction OM. This will be detected from the equality of the readings of both indicators, i.e., from the quality of the two signals, and this is why this method is called the method of the equal-signal zone.

The advantage of this method lies in the fact that its sensitivity compared with the direction finding based on the maximum is much higher. As can be seen from the figure, the point a is on a steeper part of the diagram than the portion of the diagram corresponding to the direction of maximum radiation; it is clearly seen in Fig. 55 that the central doubly hatched area has at the point a a sharper portion than the directivity pattern of antennas 1 and 2 taken separately.

The establishment of the point a by moving the antenna system is facilitated further in this case by the fact that on the right and left of the direction OM the difference in the signals corresponding to diagrams 1 and 2 increases rapidly; the sign of this difference indicates the direction relative to the equal-signal-zone axis at which the target is located.

Along with advantages, this method has a shortcoming compared with the method of direction finding based on maximum, in that the power utilization coefficient is small for the different stations. V.S. Nelepets has shown [23] that this coefficient ranges from 25 to 72%. This circumstance is capable of reducing the operating range of the radar station using the equal-signal-zone method.

In the determination of directions (angular coordinates), automatic tracking can be used.

The antenna of the station referred to produces radiation in the form of a cone. To carry out determinations in a given system of angular coordinates (i.e., for a simultaneous determination of the elevation and azimuth angles), conical lobing is used (see Section 3).

Automatic tracking is based on the following. The directivity pattern of the antenna is made to rotate in such a way that the principal radiation maximum describes 25-30 times a second a cone in space, with a solid angle at the vertex of approximately  $2.5^\circ$ . Such a diagram is symmetrical and has in transverse section the form of a regular circle. When the target is on the geometrical axis of this cone, it is subjected to uniform irradiation by the main pulses with constant intensity.

During reception, the following takes place. The pulses reflected from the target form in the receiving system a constant voltage and have a constant amplitude on the indicator screen.

As soon as the target changes its position in space and moves relative to the radiation cone, the irradiation of the target becomes asymmetrical. Consequently, an error voltage will begin to be generated in the receiving system, and this will be fed to the control system which effects the displacement of the antenna reflector (see Section 3). Under the influence of the error voltage the antenna will

be aimed automatically on the target until it lies on the axis of the cone, and then the error voltage drops to zero.

The sensitivity of this automatic system is so high that it responds to a target deviation of only several hundredths of a degree from the geometrical axis of the radiation cone. However, owing to the unavoidable inertia of the servomechanism, the output accuracy with which the angles are determined in automatic tracking is much lower and is practically a quantity on the order of tenths of a degree.

Systems of automatic range tracking are also in existence.

### 3. METHODS OF SCANNING THE SPACE

In order to observe a particular region in space, it is necessary to displace the radio beam in space, which is equivalent to displacing the directivity pattern of the antenna. Such a displacement can be the result of mechanical motion (rotation, rocking, etc.) of the antenna, or can be accomplished by specially feeding the antenna. The displacement of the radio beam in space is called space lobing.

Depending on the tasks, space lobing can assume various forms.

Circular lobing (Fig. 56) is obtained by moving the beam along a circle in a horizontal plane; the slant angle  $\Theta$  of the beam does not change.

Helical lobing is a further development of circular lobing in which the value of the angle  $\Theta$  changes after each revolution. Because of this, the beam describes a helical line in space (Fig. 57). After each complete revolution in the horizontal plane, the beam rises a distance equal to half the width of the beam, and this results in higher reliability in the scanning of the space.

In conical lobing (Fig. 58) the directivity pattern formed by the parabolic reflector is shifted relative to the paraboloid axis and rotates continuously about this axis with high speed. As a result, any

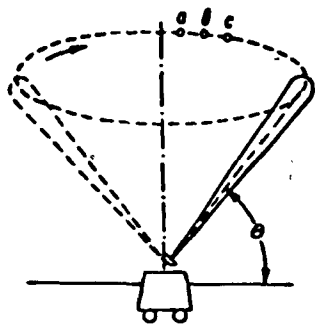


Fig. 56. Circular three-dimensional lobing. The beam passes successively through the points a, b, c, etc.

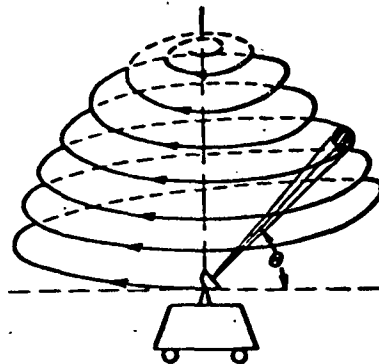


Fig. 57. Helical three-dimensional lobing.

point of the beam describes in space a circle which is the base of a cone, and the axis of the beam serves as a generatrix of the cone.

Such a form of radiation pattern is obtained by using a special radia-

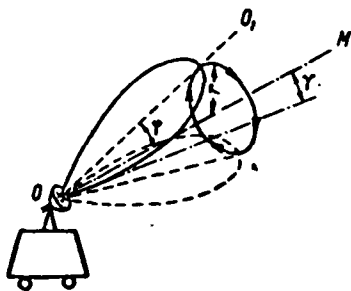


Fig. 58. Conical three-dimensional lobing.

tor construction. The radiator is offset relative to the focus of the paraboloid and is continuously rotating. During the rotation, the directivity pattern formed by the paraboloid generates a cone, and the lobes of the directivity pattern mutually overlap on opposite sides of the cone. Conical lobing is used for simultaneous determination

of the directions in the vertical and horizontal planes, and this guarantees high accuracy, as was already noted in the preceding section.

There exist also other forms of three-dimensional lobing, for example such as sawtooth, etc., but they are less widely used. For cases when a rapid survey of a certain volume in space is required (for example, within a sector of  $20^\circ$ ) or when a rapidly moving target is tracked, high-speed three-dimensional lobing is used. By displacing (mechanically or electrically) the radiator that feeds the parabolic

reflector in relation to this reflector, the sector indicated above is scanned within a fraction of a second, so that the survey is effected not less than ten times a second.

#### 4. INDICATION METHODS AND INDICATOR SYSTEMS.

In radar technology, indication is the final process, which completes the detection of the target and its tracking. The task of indication includes the transformation of the received signals reflected from the objects of observation (targets) into an information form which can be perceived visually or acoustically. Such information duplicates the coordinates of the target in accordance with the three-dimensional lobing system employed in the given radar station, and generally contains data on the space position of the object in the observation zone, and in some cases also on their dimensions, form, and character.

Thus, there is concentrated in the indicator unambiguous and continuously supplemented information, which is represented to the operator (the observer). The reflected signal must be duplicated here in such a way, that the indicator can be used for easy and rapid orientation.

In radar technology there are several known indicators; in practice the indicators are frequently called displays. Among the large number of indication methods we can mention the acoustic method, the method using pointer and vibrating-reed instruments, and also cathode-ray tubes, which, as already indicated above, is the most widely used. There exist some 20 modifications of indicators of this type, the most frequently employed being four types called A, B, C, and P. The type A and P indicators used in meteorological radars (circular-scan indicators) were shown in Fig. 11. In indicators of this type, in order to read short time intervals, which are counted in milliseconds and micro-

seconds, time sweep of the beam is used and this is the most highly perfected and most accurate method of measuring such short time intervals.

The advantages of indicators with cathode-ray tubes are based both on their operating features and on the optical-physiological properties of these indicators, as shown in [3]. In the indicators under consideration one makes use of the fact that the human visual apparatus is an economical system, where the increase in the signal/noise ratio obtained as a result of time accumulation (averaging) leads to an increase in the carrying capacity of the system.

An operationally advantageous fact is that it is possible to represent on the screen of such an indicator, in symbolic form, all three coordinates of the target. The main favorable aspect of the cathode-ray indicator is the practical freedom from inertia in the displacement of the electron beam over the screen. Among the shortcomings is the impossibility of duplicating on a flat screen the three-dimensional pattern of the real picture of the target.

Compared with other indicator systems, the cathode-ray indicator under consideration has advantages which guarantee high operating speeds with maximum accuracy and simplicity of operation.

Structurally these indicators, as used in radar stations, comprise a combination of the cathode-ray tube proper with its sweep device, which applies a sweep voltage on the tube so as to displace the bright spot over the screen. Usually all these elements are combined in a station into a single block called the indicator.

The external view and the construction of cathode-ray tubes is explained in Fig. 59.

The operation of a cathode-ray tube is based on the principle that a light image is formed on a fluorescent screen by a sharply fo-



cused electron beam.

All cathode-ray tubes are divided into two types depending on the method used to focus and deflect the ray (the electron beam): a) electrostatic, in which the ray is controlled by an electric field resulting from a potential difference introduced in the tube, and b) magnetic, in which the control is by using a magnetic field formed by current flowing in a coil placed on the neck of the tube. In some cases tubes with electrostatic focusing and electromagnetic control are used.

Depending on the methods used to obtain the image (marker) on the screen, cathode-ray indicators are divided into those with amplitude markers and those with brightness markers.

In the former, the marker is produced by displacement of the beam over the screen, as is the case for example in a type-A sweep (see Fig. 11b), and the deflection is proportional in this case to the amplitude of the received signal. A brightness marker is obtained by applying to a special electrode of the tube a voltage which is controlled by the magnitude of the signal and which determines the brightness of the light spot which appears at that time on the screen.

The screens of circular-scan cathode-ray tubes are made somewhat different than other screens, say those for the type-A indicator. In circular-scan indicators, where images of pulses reflected from the object are seen to be moving over the screen, it is necessary to "remember" the displacement of these images over the screen.

The inertia of the human eye is insufficient in this case, so that special screens are used in tubes with brightness marker, in which the fluorescent coatings (the phosphors) have an inertia, which leads to the property of integration or averaging. Such coatings are called phosphorescent, and screens of this type are called screens with persistence. Depending on the requirements and on the chosen type

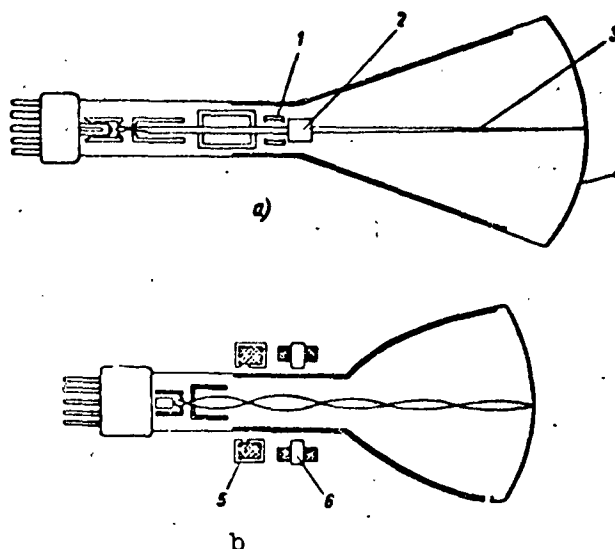


Fig. 59. Arrangement of cathode-ray tubes. a) Electrostatic; b) magnetic; 1) vertical deflecting plates; 2) horizontal deflecting plates; 3) beam; 4) screen; 5) focusing coil; 6) deflecting coil.

of phosphor, the persistence effect ranges from several microseconds to many minutes.

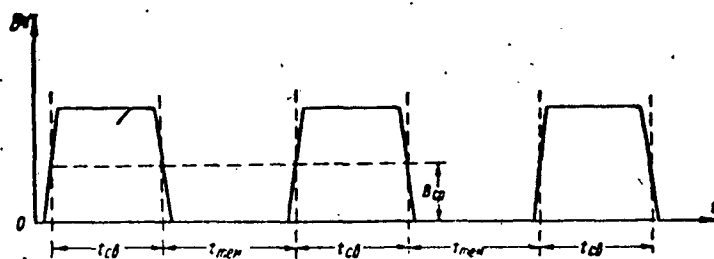


Fig. 60. Periodic sequence of light pulses. Illustrating the determination of the brightness on the indicator screen.

To increase the contrast of the image, colored optical filters with suitable spectral transmission are placed in front of the screens. For screens with afterglow, yellow-orange optical filters are used.

In the general case the degree with which the marker can be distinguished depends on the brightness, which in turn is proportional to

the specific power of the electron beam incident on the given point of the screen; it is inversely proportional to the rate of displacement of the beam over the screen, i.e., in final analysis, to the sweep velocity.

In the reception of pulse signals, as is the case in the majority of practical applications, it is necessary to take into account certain additional specific conditions.

Assuming for a pulsed mode that the brightness of the marker on the screen, under the influence of the reflected pulses, is a function of the time

$$B = \varphi(t),$$

we represent this function graphically (Fig. 60). The average time values used here are:  $t_{sv}$  - the illumination time and  $t_{tem}$  - the dark time. The average values of the brightness shown in the figure are given by

$$B_{cp} = \frac{1}{T} \int_0^T \varphi(t) dt.$$

However, for a correct estimate of the effect of the signal under consideration on the central vision apparatus it is necessary to recall Talbot's law. According to this law, the light sensation produced by a series of individual light pulses can be equated to the light sensation produced under continuous illumination. For this purpose it is necessary that the repetition frequency of the light pulses be sufficiently high and that the eye be incapable of distinguishing individual pulses. It is also necessary that the amount of light energy fed to the retina of the eye per unit time be the same in both compared cases.

In a work devoted to the analysis of the brightness of a flickering source of light as perceived by the eye, Academician S.I. Vavilov [24] indicates that the "subjectively perceived brightness of a flick-

ering source of light is less than the true brightness of the source." This premise, extended to include the action of cathode-ray indicators of radar pulse signals, states that in the reception of pulse signals the requirements concerning the brightness of the signals duplicated on the indicator screen should be related not only (as is the usual case) with the duration of the pulses, but also with their repetition frequency.

These premises and problems associated with them concerning the operation of cathode-ray indicators, are considered in the work of V.S. Nelepets [3].

The purpose of the sweep unit is to produce a voltage with the aid of which the light spot is regularly displaced over the screen of the tube and forms the "time axis," called the sweep line. The character of the sweep is determined by the law governing the variation of the voltage on the deflecting plates in the tubes using electrostatic control, or the law governing the variation of the current in the deflecting coils in tubes with magnetic control.

A type-A sweep is in most cases linear, uniform, and forms a uniform time scale (and consequently distance scale).

The form of the type-A sweep voltage has a sawtooth character. The slow increase in the sweep voltage causes the beam to move over the screen from left to right, this being called the forward trace. After reaching the extreme right position, the beam must return very rapidly (the return trace) to the initial position. For this purpose the sweep voltage, on reaching the "tooth" of the sawtooth, must decrease rapidly, after which the next forward trace cycle begins.

In the A-type indicator one uses cathode-ray tubes with electrostatic control and sweep.

In a circular-scan indicator, the sweep employed causes the beam

to move rapidly radially away from the center toward the outer edge of the screen, this being effected by a magnetic deflecting system; the magnetic field is produced by a sawtooth current flowing through the deflecting coil. In this indicator brightness markers are used: when the signal reflected from the target is received, the brightness of the corresponding portions of the radius increases.

The deflecting system (Fig. 59) is rotated with the aid of gears around the neck of the tube, so that the aforementioned radius, visible on the screen, rotates about the center of the screen. This rotation of the deflecting system is in synchronism and in phase with the azimuthal displacement of the antenna system. If the antenna is not being displaced, but the radiation is swept in space, then the displacement of the aforementioned radius (beam) over the screen is in accord with the rotation of the radiation in space. Synchronous and in-phase matching is attained by using synchronous servomechanisms, which will be mentioned later on in Section 4 [sic].

Sometimes in radar operation (including also the observation of meteorological objects), the following phenomenon is noticed: at ranges located directly behind the object whose reflection is being observed, one sees a peculiar type of "comb" on the indicator screen (for example type-A indicator). The signal reflected from the object masks, as it were, everything that occurs behind the reflecting object, and the larger the intensity of the observed signal, the more noticeable this phenomenon.

The explanation of such a phenomenon must be sought in the peculiar type of reduction in the sensitivity of the receiving circuit resulting from the effect of the powerful reflected pulse, and not in defects of the indicator and certainly not in any peculiarities of the observed objects.

Manu-  
script  
Page  
No.

[List of Transliterated Symbols]

189	cb = sv = svecheniye = brightness
189	tem = tem = (za)temneniye = darkness
189	cp = sr = sredniy = average

## Chapter 7

### RADAR APPARATUS

#### 1. INTERROGATOR-RESPONDER SYSTEMS

The action of radar is based, as is well known, on the use of reflection of radio waves from objects which serve as passive reflectors. In order to improve the efficiency of the system, it is possible to replace the passive reflectors by active "electronic" reflectors. Systems with active responders are based on the principle of using such reflectors.

Such systems include, first, a transmitter which transmits interrogation pulses (the communication channel over which the interrogation is carried out is called the interrogation channel), and second a transceiver, and the individual communication channel employed by the latter is called the response channel.

After the interrogation pulse is received by the responder, the antenna of the latter radiates response pulses. The entire character of the response of the active responders has many features distinguishing them from the character of the signals formed by a passive reflector.

The intensity of the response pulse does not depend on the intensity of the interrogation signal; it is assumed that the power of the latter is sufficient to trigger the responder. The carrier frequency at which the response pulse is transmitted does not depend on the frequency of the interrogation signal; in most practical cases these two frequencies (wavelengths) do not coincide.

The form (the number and duration of the pulses and pauses) of the response signal is not connected with the form of the interrogation signal. Between the instant of arrival of the interrogation and the transmission of the response there occurs an unavoidable time loss (delay), i.e., certain retardation takes place.

Systems of this type include radiosondes of the relay type. There are several known radiosonde systems of this type, but because of the appreciable complexity of the apparatus and the relatively large weight, these systems have not found systematic application.

Recently superregenerative responder transmitters have come into use, and their construction is much simpler than that of the relay type.

By superregenerative is usually meant a radio receiver whose circuit is maintained in a near self-oscillating (regeneration) mode in order to maintain as large a sensitivity as possible. This is accomplished by varying periodically in time one of the parameters influencing the self-excitation. The frequency of this variation is much lower than the frequency making up the spectrum of the received oscillations. The presence of the natural oscillations in the superregenerator tank circuit determines the possibility of using it as a transmitter.

By suitable choice of the mode and of the circuit elements for the radiation of the superregenerative system used as a radiosonde transmitter, it is possible to cover distances on the order of 100-150 km. At the same time, the system, as already noted above, maintains high sensitivity to the signals it receives from the outside. Usually the frequency of the latter should coincide approximately with the natural frequency of the superregenerator tank circuit. The response of the system to the incoming signal is expressed in clearly distin-



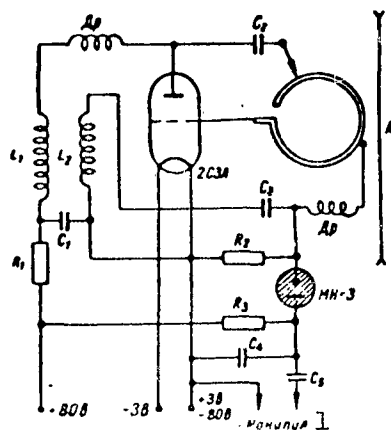


Fig. 61. Schematic diagram of responder transmitter type A-35. A) Receive-transmit antenna; L<sub>1</sub>) coil "universal" PELShO 0.1, 300 turns, L<sub>2</sub>) coil "universal" PELShO 0.1, 200 turns. C<sub>1</sub>) KSO capacitor (200 pF); C<sub>2</sub>) KSO capacitor (100 pF); C<sub>3</sub>) KSO capacitor (100 pF); C<sub>4</sub>) KSO capacitor (1500 pF); C<sub>5</sub>) KSO capacitor (5600 pF). R<sub>1</sub>) Resistance VS-0.25 (24 kilohms); R<sub>2</sub>) resistance VS-0.25 (470 kilohms); 2C3A) radio tube; MN-3) neon lamp; Dr) chokes PE 0.7 (20 turns, 6 mm in diameter). 1) Manipulator.

wire and the interelectrode capacitances of the 2C3A tube is made to oscillate at a frequency  $f = 216$  Mc. The antenna A is excited at this frequency.

The frequency of the oscillations generated by the circuit can be varied by means of a wiper which joins the inductance of the tank circuit through the capacitor C<sub>2</sub> to the plate of the tube. This makes it possible to tune the oscillation frequency at the nominal frequency of

guishable changes in the natural-radiation mode.

Figure 61 shows the diagram of the transponder receiver type A-35, developed at the TsAO, as used with the "Malakhit" radio theodolite, which has been supplemented with a special interrogation and range finding attachment. The attachment includes a pulsed interrogator-transmitter with a pulsed power of approximately 40 kw. The transmitter has a "wave-channel" type directional antenna; a radio range finder is also part of the outfit. The transmitting antenna is mounted in the center of the frame carrying the receiving antennas of the radio theodolite, which has thus been transformed from a radio direction finding to a radar setup.

The responder-transmitter A-35 operates in the following fashion. The tank circuit made up of a turn of thick

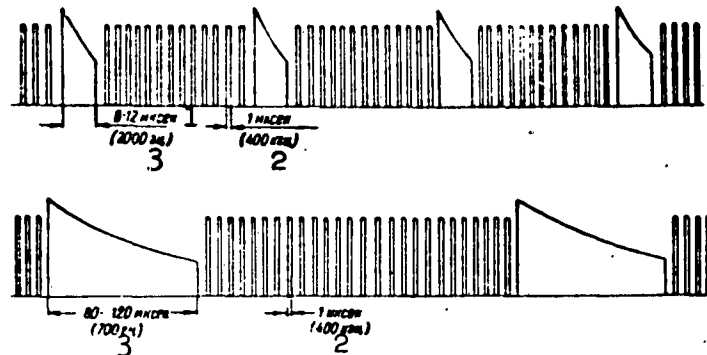


Fig. 62. Envelopes of radio pulses radiated by the responder transmitter A-35. 1)  $\mu\text{sec}$ ; 2) kc; 3) cycles.

the radio theodolite, namely 212 Mc.

The microwave oscillations are modulated twice: owing to the strong feedback between coils  $L_1$  and  $L_2$ , deep self-modulation is produced at a frequency of about 400 kc, which is periodically quenched by the neon lamp MN-3, which forms a modulator oscillator controlled by the manipulation circuits of the radiosonde, whereas the microwave oscillations continue to exist. The neon oscillator generates modulation pulses with a repetition frequency of 700 cps, when the code signals of the radiosonde are transmitted; during the interval between the latter, the repetition frequency is 2000 cps. This structure of the signals from the A-35 transmitter is illustrated in Fig. 62, which shows the envelopes of the radio pulses corresponding to the instants of signal transmission (below) and pauses in the radiosonde signals (above). This figure does not show the 216-Mc carrier of all these pulses.

Figure 63 shows the signal on the screen of the radio range keeper indicator as observed during the process of range measurement.

The response signal is similar in form to the signal reflected from a target and observed on a type-A indicator, to which reference was made above. It has the character of a clearly pronounced pip above

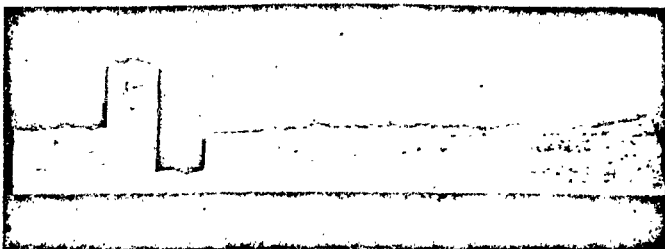


Fig. 63. Picture of the response signal on the screen of the range finder indicator.

a sweep line, produced by the radiation of the superregenerator, and a clearly seen trough following the pip, called the "response pause."

The distances to the responder are best measured relative to the leading front of the response signal, since measurement referred to other portions of the response image call for the introduction of corrections for the width (duration) of the response pulse.

Preliminary experience gained at the TsAO in the use of responder transmitters of the regenerative type, according to data by V.S. Khakhlin, confirm the advantage of introducing such responder transmitters on a large scale, since the data on the slant range greatly improve the measurement of the wind and the pressure, particularly at altitudes of 25-30 km and above.

The foreign literature contains the following data [76] on the interrogator-responder system.

The radiosonde equipped with a responder is launched in free flight and makes it possible to determine, first, the velocity and direction of the air streams, and second, reports data on temperatures from  $-65$  to  $43.5^{\circ}$ , on the relative humidity from 0 to 100%, and on pressure in a range of 30-300 mb. The accuracy attained is  $\pm 0.2^{\circ}$  for the temperature,  $\pm 10\%$  for the relative humidity, and  $\pm 2$  mb for the pressure.

In the system described, the antenna of the ground station radi-

ates an interrogation at a frequency  $f = 152.5$  Mc in the form of radio pulses of duration  $\tau_1 = 2$   $\mu$ sec at a power  $p_1 = 50$  kw. After receiving the interrogation of the ground station, the responder produces a pulse transmission at a frequency  $f = 2850$  Mc, width-coded in accordance with the measured data; the latter are continuously switched with the aid of a small motor. In addition, the responder transmits periodically a standard voltage signal.

The ground apparatus includes a device for automatically tracking the radiosonde as it moves in space. The radiosonde signals are received on the ground with a parabolic antenna 1.5 meter in diameter.

The range to the responder is determined by usual radar methods by measuring the time, while the height is determined by radio direction finding methods using the elevation angle of the antenna in the vertical plane. The ground installation is provided with a unit for automatically recording the data and with a computer.

The transmission cycle from the responder lasts 15 seconds, and consequently the periodicity with which data are received from the responder is a time slightly exceeding this interval. Inasmuch as the responder signals are recorded automatically, it becomes possible to transmit the interrogation from the ground installation up to three times a minute.

After reaching the limiting height, the envelope of the balloon bursts and a parachute opens automatically, permitting a slow drop of the responder. The responder continues to answer the interrogations during its descent.

General problems connected with the construction of such systems with active response are considered in the work by Harris [77].

## 2. RADAR STATIONS FOR TEMPERATURE-WIND SOUNDING

Aerological observations by measurement of wind currents at high

altitudes, as indicated in Chapter 5, are carried out with radar methods of observing radio pilots using passive targets, and by radio direction finding methods using active targets. Both methods can be realized using half-wave meter-wavelength targets using a weapons-aiming station.

The outfit of such a station contains two cabins, one for transmission and one for reception.

The transmitter antenna radiates sounding (main) pulses of duration on the order of  $1 \mu\text{sec}$ , the number of which ranges from 1000 to 2200 per second. The entire control of the transmitter is concentrated on the front panel of the cabinet. The tank circuits and the remaining apparatus are located inside the cabins.

Simultaneously with transmitting the main pulse, a synchronizing pulse is transmitted from the transmitter cabin to the receiver cabin by cable and triggers the indicator sweeps.

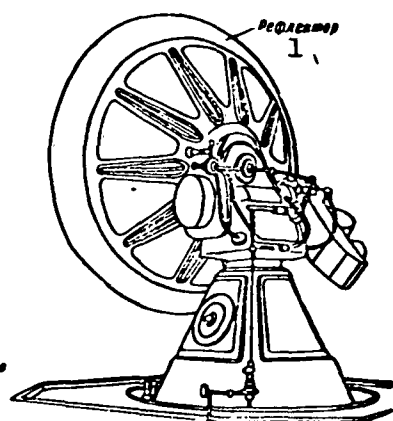


Fig. 64. Radar antenna for the centimeter band.  
1) Reflector.

Chapter 6. The gain of such an antenna is 1200, the beam width ranges between  $4^\circ$  and  $6^\circ$ , and the range available for search and tracking amounts to 75 km or somewhat more.

Improvements in radar technology during the war years have led to

the appearance of centimeter radar stations; at this wavelength radar has many advantages, major among which is the higher accuracy in measurement of the angular coordinates.

When it comes to general tactical and technical data and to accuracy of the determination of the coordinates, the SCR-584 radar is suitable for radio-wind observations. We present a brief description of the station. Under mobile conditions it is placed in a trailer which is pulled by a motor vehicle.

On the roof of the trailer is the antenna, the general appearance of which is shown in Fig. 64. The station operates at a wavelength  $\lambda = 10\text{-}11$  cm (frequency 4700-2900 Mc) with a pulse duration  $\tau_n = 0.8$   $\mu\text{sec}$  at a repetition frequency of 307 cps. The pulse power  $P_{\text{imp}}$  equals 300 kw.

For meteorological observations the station can also be used in stationary position; the antenna is then mounted in an open space, permitting an unobstructed survey.

The antenna of the station is used for both transmission and reception. Structurally the antenna system is made in the form of a parabolic reflector 1.8 meters in diameter, and a radiating dipole mounted in the focus of the paraboloid and rotating at 1800 rpm. The line feeding this dipole is made in the form of hollow tubes; the latter are filled with dry air under pressure, to protect against moisture, since moisture increases the attenuation of the high-frequency energy.

In connection with the fact that the rotating dipole is asymmetrical with respect to the rotation axis, the center of its radiation is offset somewhat relative to the focus of the paraboloid, so that the antenna beam is deflected from the antenna by approximately  $1.25^\circ$ . Rotation of the dipole leads to the formation by the beam of a conical surface, the solid angle of which is  $2.5^\circ$ . The nature and characteris-

tic features of such three-dimensional lobing were described in Section 3 of Chapter 4. The antenna gain is 1200. The beam width produced by the antenna system under consideration is  $4^{\circ}$  without rotation and reaches  $6.5^{\circ}$  upon rotation. One can also note that helical sweep is used during search and conical sweep during tracking. The search is carried out at ranges up to approximately 75 km while tracking is up to ranges exceeding somewhat 30 km. The sensitivity in the determination of the coordinates is about 2 meters in range and  $0.06^{\circ}$  in angle.

As noted earlier, this station employs a system for automatic target tracking. The operating principle of such a system was considered in Section 1 of Chapter 6 (Fig. 53). The two produced error voltages (azimuth and elevation signals) are fed to amplidynes (magnetic amplifiers) which control the rotation of the antenna in azimuth and in elevation.

Connected to the output of the receiver is a system of range indicators, containing two cathode-ray tubes, one for coarse and the other for fine reading of the range.

The automatically generated target coordinates are fed to a data-transmission channel. In addition, there is a circular-scan indicator used during the search for the target.

### 3. RADAR STATION FOR THE OBSERVATION OF PRECIPITATION ZONES AND ATMOSPHERIC FORMATIONS

The H2X radar is a typical centimeter-band installation. It contains a magnetron transmitter, receiving and amplifying units, two circular-scan indicators, an antenna unit with parabolic reflector, a high-voltage supply block, a control panel, selsyns, and auxiliary blocks.

The antenna unit can be aimed at any point forward in space, for which purpose the installation is provided with an electric motor which

turns the entire unit in azimuth; a second motor inclines the antenna in a range from 10 to 30°. Selsyns provide a sweep that is synchronized with the azimuthal rotation of the antenna.

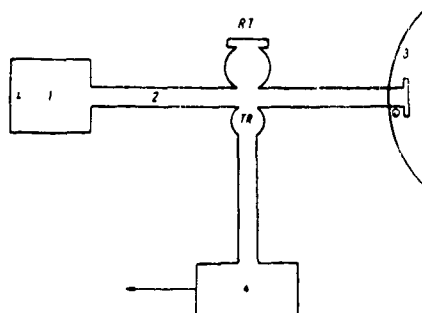


Fig. 65. High-frequency channel of the radar station. 1) Transmitter; 2) waveguide; 3) paraboloid; 4) receiver.

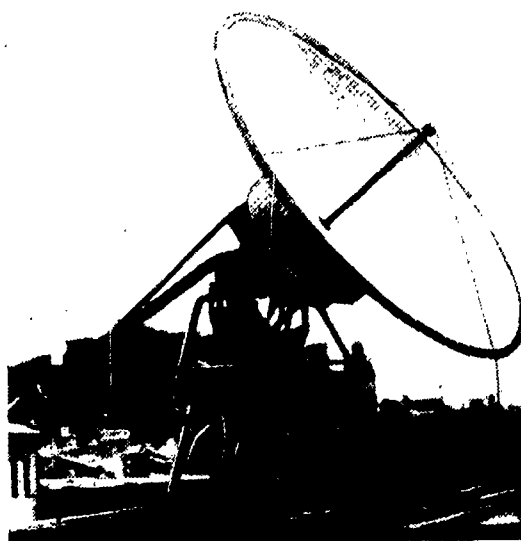


Fig. 66. Antenna unit of the radar station.

With the aid of a waveguide transmission channel, shown schematically in Fig. 65, the antenna is coupled to the magnetron of the transmitter part during the time of transmission, and to the input of the receiver during the time of reception. Two chambers, RT and TR, with gas-filled arrester, are placed in the high-frequency path in the



waveguide and protect the receiver during the time of radiation of the main pulse and during the transmission of the reflected pulses from the antenna to the receiver, with a minimum of attenuation.

The image produced on the indicator screens has a character similar to that shown in Figs. 23-29. A distinguishing feature of the sweep is that the operator can choose at his convenience one of five range intervals within the limits from 20 to 200 km for which purpose suitable scales are installed. At small ranges (8-40 km) it is possible to vary the scale of the image continuously, so that the radius of the screen corresponds to any chosen range from 8 to 40 km.

Range markers (circles) are produced on the screen electrically (see Fig. 11a); in the radar station under consideration, the distance between the calibration circles can be set to be either 2 or 10 km.

The various types of radars used for meteorological observations were modified in individual cases; in particular, the antenna was modernized (Fig. 66). It was pointed out earlier (in Section 4 of Chapter 2) that the efficiency of the directional antenna depends on the diameter of the radiator.

#### 4. AUXILIARY EQUIPMENT

##### Measuring Apparatus

To service radar equipment, a large number of various measuring devices and instruments are used. Among the domestic equipment, these include the type 35IM resonant wavemeter and the more complicated 44I heterodyne wavemeter, which employs the beats of the measured oscillations with a definite harmonic of an internal generator; the operation of the instrument is based on this principle. The reading is by setting the beats to zero with the aid of an earphone. The same group of instruments includes also the waveguide measuring line 33I for measuring the traveling-wave coefficient KBV, the automatic measuring

line 53I and others.

To test and verify the operation of a radar station for the centimeter band, and also to measure the power of the reflected signals, extensive use is made of a universal testing instrument 31IM, also called a radar tester. Its diagram is shown in Fig. 67. It is divided into four parts: the thermistor section, the resonant wavemeter, the attenuator, and the detector section. This instrument combines the functions of a power meter, a wave meter, and a standard signal generator. In addition, it makes it possible to measure the restoration time of the sensitivity of the receiving channel after the action of the main pulse; the radar tester can be used to tune the high-frequency elements of the radar station and to carry out many measurements of research nature.

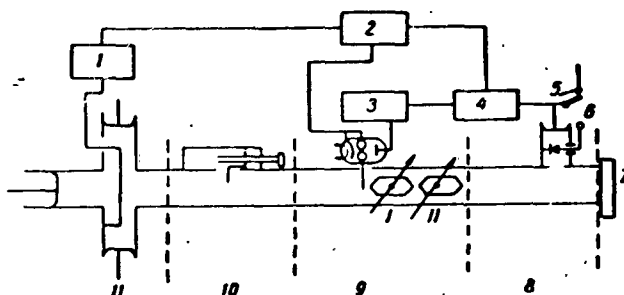


Fig. 67. Universal testing instrument 31IM. 1) Thermistor bridge; 2) power supply; 3) manipulator; 4) synchronizer; 5) low-frequency synchronizer; 6) high-frequency synchronizer; 7) output flange of the instrument; 8) detector section; 9) attenuator; 10) wavemeter; 11) thermistor section.

The radar tester has a frequency range of 8700-9700 Mc, an operating temperature range  $\pm 40^{\circ}$ , a maximum permissible relative humidity 95-98% at a temperature of  $20^{\circ}$ .

When the radar tester is used as a resonant wavemeter, a klystron oscillator is in operation in it; in this case one half of the power

is fed to the thermistor power meter, and the other to the output. There are two graduated attenuators, which together provide an attenuation on the order of 72 db.

The power-measurement range was 0.1- 2.0 mw (the average power).

The accuracy of the absolute measurements is  $\pm 1.5$  db in power and  $\pm 4$  Mc in frequency. The accuracy of the difference (relative) measurements is  $\pm 0.8$  db and  $\pm 1$  Mc, respectively. The maximum power at which measurements can be carried out is 2 watts average and 200 watts in pulse. The traveling wave coefficient in the high-frequency channel exceeds 0.8. The following types of internal modulation are provided: AM, FM, and PM in meander form (a pulse having a special wavy form) and others. Provision is made for modulation from an external source.

By using the radar tester as an equivalent of a transmitter, it is possible to tune the heterodyne in the radar receiver. The radar tester can be used to measure the sensitivity of radar receivers, and also to measure various types of mutual attenuation, for example mutual attenuation between antennas, attenuation of a cable or of a waveguide-coaxial transition. It is possible to use the 31IM to plot the directivity pattern of the radar antenna.

#### Servomechanisms with Selsyns

In modern radar stations, including those mentioned above, certain problems in remote control (including control of high degree of accuracy) are solved with the aid of devices that belong to the class of synchronous servomechanism units. These include synchronous (and in-phase) rotation of the deflection system in a cathode-ray indicator (Section 4 of Chapter 6) with the rotation of the radar-system antenna. One can include here equally well the devices used in automatic tracking systems mentioned in Section 2.

In most cases the basis of the synchronous servomechanisms is a device called a selsyn. A selsyn is an electromechanical unit with the aid of which it is possible, by transmitting voltages over wires, to transmit angular data or positions (displacements) and torques over a distance.

Circuit wires, selsyns are rotating transformers. The control power of such a device can range from milliwatts to a kilowatt, and the torque from milligram-millimeters to kilogram-meters.

The construction of a selsyn is similar to that of an ordinary low-power three-phase generator or AC motor, and it has stator and rotor windings placed in slots of a core of sheet steel.

There exist several types of selsyns. Most frequently employed is a combination of a selsyn transmitter and a single selsyn receiver. These selsyns are interconnected with electric wires as shown in Fig. 68. On the end A of the system a single phase AC voltage is applied to the rotor winding of the selsyn transmitter, and this gives rise to a magnetic field. This field links with the stator (secondary) windings which are arranged  $120^{\circ}$  relative to one another and star-connected; a secondary voltage is induced in this winding, the magnitude and phase of which depends on the angular position of the rotor relative to the stator winding.

The currents produced in the windings on the B end produce at the center of the stator of the receiver selsyn a resultant field, under the influence of which a torque is produced.

The operation of the entire unit is thus based on the conversion of the mechanical rotation of the rotor in A into a rotation of a magnetic field and a change in the magnitudes and phases of the resultant voltage in the wires of the three-phase system, as a result of which the rotation of the rotor in A results in a similar rotation of the

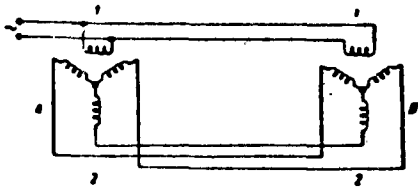


Fig. 68. Diagram showing the connection of a selsyn transmitter to a selsyn receiver. 1) Rotor; 2) stator.

rotor in B. This essentially is the nature of the transmission of angular quantities over electrical wires with the aid of selsyns.

Owing to friction in the bearings and the brushes, the discrepancy between the selsyn transmitter and the selsyn

receiver reaches  $2-3^{\circ}$  if the rotor of the selsyn receiver is not excessively loaded (for example, if it is used only to turn the pointer of an instrument). When the selsyn rotor actuates some mechanical system, the error angle may turn out to be larger than that.

The diagram shown in Fig. 68 is intended only to explain the operating principle of the selsyn system. Practical circuits contain also additional elements. It is possible to connect the selsyn transmitter to the receiver using only three wires.

The class of instruments considered includes also the already mentioned computer units which are used in some radar instruments.

#### CONCLUSION

Further development of radar methods for meteorological observations, particularly methods for the detection and investigation of clouds, precipitation, inversions, turbulent and convective formations in the atmosphere, as can be readily visualized, should follow primarily the path of increasing the reliability of observation. Indeed, the presently existing storm-warning radars have a relatively low efficiency for the detection of thunderstorms and showers, starting with distances of 100-150 km, while zones of continuous precipitation are observed only within a radius of several times ten kilometers. This shortcoming pertains also to cloud measuring radars, in which the reliability of detection of the clouds, inversions, or convective and

turbulent formations of the atmosphere is still insufficiently high.

This lack of sensitivity is frequently due to the prevailing small values of the reflected signal from the atmospheric formations, when this signal remains smaller than the internal noise of the receiving channel of the radar station. Consequently, it is necessary to construct special meteorological radars, in the design of which the primary technical problem would be an increase in the signal/noise ratio. This problem can be solved relatively easily for storm-warning radars, where this ratio must be increased by 10-20 times, but when it comes to radars intended for the detection of clouds and dielectric inhomogeneities in the troposphere, this problem becomes much more complicated, since the signal/noise ratio for this equipment would have to be increased by several hundred times. However, its solution is made appreciably easier by such singularities of atmospheric formations as their large geometrical dimensions and small rate of displacement. Starting from these singularities, many authors [46, 50] are already proposing the following technically feasible methods for increasing the signal/noise ratio, and consequently also the efficiency of radar detection of atmospheric formations: increase the antenna aperture, use storage devices at the output of the radar receiver, or increase the power of the main (sounding) pulses.

For cloud-measuring radars, in which the radiation is produced upward at an elevation angle close to  $90^{\circ}$ , it is possible to use all three of the indicated methods. In the detection of thunderstorms and showers, it is more convenient to employ the second and third methods.

Along with increasing the efficiency of detection, a very urgent problem is that of improving methods of indication and registration of atmospheric formations. Each radar used for meteorological purposes should have a circular-scan or sector-scan indicator, a "height-range"

indicator, and an indicator with amplitude marker. Taking into account the need for quantitative measurements of atmospheric formations, it is convenient to employ indicators with large screens and to make provision in the constructions of the stations for the possibility of measuring the power of the reflected signals. The accuracy with which range is determined for storm-warning radar stations should be on the order of  $\pm 500$  m, while that of cloud-measuring radars should be  $\pm 20$  m. It is sufficient to determine the angular coordinate accurate to  $\pm 1^\circ$ .

Photoregistration of the radio echoes and methods of data reduction should be automatized.

Along with improvements in the techniques and procedure of radar observations, it is necessary to develop further a network of radar stations for meteorological use. This is important primarily for meteorological information and weather forecasting. The number and placement of the storm-warning radars should be such that the space covered by them should be without gaps not only for thunderstorms and showers, but also for weak precipitation.

Data on precipitation, supplemented with results of observation and measurement of the heights of the cloud layers, their water contents, the icing zones, the turbulent and convective formations in the atmosphere, will greatly improve the meteorological service to aviation. An analysis of these data makes it possible to clarify the space-time variability of the indicated most important meteorological elements and phenomena, and to investigate to a deeper extent the processes of cloud formation and precipitation on scales of such synoptic objects as cyclones, anticyclones, and atmospheric fronts. As a result, the weather forecasts will become more reliable and new possibilities will be uncovered for effective action on the weather.

As regards further development of radar methods of all-inclusive

temperature-wind sounding of the atmosphere, it should follow the direction of increasing the accuracy in the determination of the radiosonde coordinates and obtaining more accurate values for the main meteorological elements, increasing the sounding height, and introduction of automatic servomechanisms and computer devices. In this respect, the most promising is a radar method using responder radiosondes.

At the present time the sounding ceiling amounts to approximately 30 km. Even a few years ago such a ceiling was more or less satisfactory for practical use. However, in our age of rocket technology, when it became possible and necessary to carry out direct meteorological measurements as high as the upper atmosphere, the value of radar methods of wind measurements becomes even more important and the problem of increasing the sounding ceiling has become very acute.

The problems covered by modern physics of the atmosphere include measurements of pressure and density, temperature, and the composition of the earth's atmosphere at high altitudes.

It can be assumed that with the launching of artificial earth satellites and research rockets in the Soviet Union the arsenal of research means for the study of the properties of the upper layers of the atmosphere has greatly increased, and we have gained the possibility of studying phenomena which heretofore could be observed from earth only by indirect methods. For all the urgency of this problem, it could not be considered in the present book.

The giant progress of Soviet science and technology in recent years, which has found its embodiment in the launching of artificial earth satellites, cosmic rockets and ships, will undoubtedly find its reflection in other branches of research work and will bring about further improvement in radar methods of meteorological observations.



Manu-  
script  
Page  
No.

[List of Transliterated Symbols]

198	и = i = impul's = pulse
200	н = n = nominal'nyy = rated, nominal
200	имп = imp = impul's = pulse

#### REFERENCES

1. Vysokovskiy, D.M., Pogloshcheniye mikroradiovoln v atmosferykh obrazovaniyakh i radiolokatsiya [Absorption of Microwaves in Atmospheric Formations and Radar], Uspekhi fizicheskikh nauk [Progress in the Physical Sciences], XLVII, 1952.
2. Vysokovskiy, D.M., Ob uchete mnogokratnogo rasseyaniya pri diffuznom rasprostraneniі UKV v troposfere [Accounting for Multiple Scattering in Diffusive Propagation of USW in the Troposphere], Radiotekhnika i elektronika [Radioengineering and Electronics], Vol. II, No. 6, 1957.
3. Nelepets, V.S. and Nelepets, V.V., Impul'snyye rezhimy v radio-tekhnicheskikh tsepyakh [Pulse Modes in Radio-Engineering Circuits], Voenizdat [Military Publishing House], Moscow, 1960.
4. Nelepets, V.S., Antenny metrovykh voln [Meter-Wave Antennas], Voenizdat, Moscow, 1957.
5. Beketov, V.I., Antenny sverkhvysokikh chastot [Ultra-High Frequency Antennas], Voenizdat, Moscow, 1957.
6. Gorelik, A.G., Kostarev, V.V. and Chernikov, A.A., Radiolokatsionnoye izmereniye turbulentnykh dvizheniy v oblakakh [Radar Measurements of Turbulent Motions in Clouds], Meteorologiya i gidrologiya [Meteorology and Hydrology], No. 5, 1958.
7. Shifrin, K.S., K teorii opticheskikh metodov issledovaniya kolloidnykh sistem [Toward a Theory of Optical Methods in the Investigation of Colloidal Systems], Trudy vsesoyuznogo zaochnogo lesotekhnicheskogo instituta [Trans. of All-Union Correspondence Forest-Engineering Institute], No. 1, 1955.
8. Stepanenko, V.D., Uluchsheniye effektivnosti obnaruzheniya meteorologicheskikh tseley radiolokatorom "Kobal't" [Improving the Effectiveness of Detecting Meteorological Targets with the

- "Cobalt" Radar], Trudy TsAO [Trans. of the Central Astronomical Observatory], No. 20, 1958.
9. Kostarev, V.V., Opyt radiolokatsionnogo zondirovaniya atmosfery [Experience in Radar Sounding of Atmosphere], Trudy TsAO [Trans. of the Central Astronomical Observatory], No. 20, 1958.
  10. Kotov, N.F. and Nikolayev, P.N., Metod radiolokatsionnykh nablyudeniy livney i groz [Method of Radar Observations of Showers and Storms], Trudy TsAO [Trans. of the Central Astronomical Observatory], No. 20, 1958.
  11. Sal'man, Ye.M., Radiolokatsionnyye issledovaniya struktury livney i groz [Radar Investigation of the Structure of Showers and Storms], Trudy GGO [Trans. of the Main Geophysical Observatory], No. 72, 1957.
  12. Materialy konferentsii po voprosam dal'nego rasprostraneniya UKB v yanvare 1957 g. [Data of Conference on the Problems of the Long-Distance Propagation of USW in January of 1957], Radiotekhnika i elektronika [Radio Engineering and Electronics], No. 5, 1957.
  13. Troitskiy, V.N., Otrazheniye UKV ot sloistyykh neodnorodnostey troposfery [Reflection of USW From the Stratified Discontinuities in the Troposphere], Radiotekhnika [Radio Engineering], No. 1, 1956.
  14. Krasnushkin, P.Ye., O volnovodnykh svoystvakh odnorodnykh sred [The Waveguide Properties of Homogeneous Media], Zhurn. tekhnich. fiziki [Journal of Technical Physics], No. 4, 1948.
  15. Fok, V.A., Otrazheniye Frenelya i zakony difraktsii [Fresnel Reflections and the Laws of Diffraction], Uspekhi fizich. nauk [Progress in the Physical Sciences], Vol. 36, 1948.
  16. Popov, A.S., O pribore registriruyushchem napryazheniye elek-

- tricheskogo polya atmosfery dlya sharov, zondov i zmeyev [An Instrument Which Registers the Strength of Atmospheric Electric Field for Balloon, Sonde and Kite], Zhurn. Russkogo fiziko-khimicheskogo ob-va [Journal of Russian Physicochemical Society], Vol. 34, 1902.
17. Stepanenko, V.D., O kolichestvennoy otsenke obledeneniya samoletov s pomoshch'yu radiolokatsionnykh stantsii [The Quantitative Evaluation of Aircraft Icing with Radar Stations], Trudy LKVVIA im. A.F. Mozhayskogo [Trans. of the Leningrad "Red Banner" Air Force Engineering Society], No. 348, 1960.
  18. Shupyatskiy, A.B., Radiolokatsionnoye izmereniye intensivnosti i nekotorykh drugikh kharakteristik osadkov [Radar Measurement of the Intensity and Certain Other Characteristics of Precipitation], Gidrometeoizdat [Hydrometeorology Publishing House], Moscow, 1960.
  19. Muchnik, M., Opredeleniye grozovogo i livnevogo polozheniya radiolokatorom Shtormopovescheniya [The Determination of Storm and Shower Positions by Storm-Forecasting Radar], Trudy TsaO [Trans. of the Central Astronomical Observatory], No. 20, 1958.
  20. Imyanitov, I.M., Kulik, M.M., and Chuvayev, A.P., Opyt issledovaniya grozovykh zon v yuzhnykh rayonakh Yevropeyskoy territorii Soyuza SSR i v Zakavkaze [Experience in Investigating Storm Zones in the Southern Regions of the European Part of the Union of Soviet Socialist Republics and in Transcaucasia, Trudy GGO, No. 67, 1957.
  21. Mazin, I.P., Fizicheskiye osnovy obledeneniya samoletov [Physical Bases of Aircraft Icing], Gidrometeoizdat [Hydrometeorology Publishing House], Leningrad, 1957.

22. Yefimov, P.L. and Khachatryan, A.M., Tochnost' opredeleniya napravleniya i skorosti vetra na vysotakh radioteodolitom [Accuracy in the Determination of the Direction and Velocity of Wind and Altitude by Radio Theodolites], No. 31, 1959.
23. Nelepets, V.S. et al., Osnovy radiolokatsii [Fundamentals of Radar], Part 2, Oborongiz [State Publishing House of the Defense Industry], Moscow, 1954.
24. Vavilov, S.I., Optika v voyennom dele [Optics in War], Vol. 1, Izd. AN SSSR [Publishing House of the Acad. Sci. USSR, Moscow-Leningrad, 1945.
25. Kessenikh, V.N., Rasprostraneniye radiovoln [The Propagation of Radio Waves], GITTL [State Publishing House of Technical and Theoretical Literature], Moscow, 1952.
26. Arenberg, A.G., Rasprostraneniye detsimetrovykh i santimetrovykh voln [The Propagation of Decimeter and Centimeter Waves], Izd. "Sovetskoye radio" [Publishing House of Soviet Radio], Moscow, 1957.
27. Shchelkunov, S.I. and Friis, G. Antenny [Antennas], Translation from the English, Izd. "Sovetskoye radio," Moscow, 1955.
28. Bogomolov, A.F., Osnovy radiolokatsii [Fundamentals of Radar], Izd. "Sovetskoye radio," Moscow, 1954.
29. Lampovyye skhemy dlya izmereniya vremeni [Tube Circuits for Time Measurement], Trans. from the English, Edited by A.Ya. Breyntbart, Izd. "Sovetskoye radio," Moscow, 1951.
30. Shifrin, K.S., Rasseyaniye sveta v mutnoy srede [Scattering of Light in a Turbid Medium], Gostekhzdat [State Publishing House of Theoretical and Technical Literature], Moscow, 1951.
31. Rasprostraneniye ul'trakorotkikh radiovoln [The Propagation of Ultrashort Radio Waves], Translation from the English Edited by

- B.A. Shillerov, Izd. "Sovetskoye radio," Moscow, 1954.
32. Gol'dshteyn, L.D. and Zernovm, N.V., Elektromagnitnyye polya i volny [Electromagnetic Fields and Waves], Izd. "Sovetskoye radio," Moscow, 1956.
  33. Kratkiye osnovy radiolokatsii [Concise Fundamentals of Radar], Edited by Breytbart, A.Ya., Izd. "Sovetskoye radio," Moscow, 1951.
  34. Bonch-Bruyevich, M.A., Korotkiye volny [Short Waves], Gos. izd. po tekhnike svyazi [State Publishing House for Communications Engineering], Moscow, 1932.
  35. Khakhalin, V.S., Radiotekhnika v aerologii [Radio Engineering in Aerology], Gidrometeoizdat, Leningrad, 1957.
  36. Nazemnyye amerikanskiye i angliyskiye radiolokatsionnyye stantsii [American and English Ground Radar Stations], Voenizdat MVS SSSR [Military Publishing House, Ministry of the Armed Forces USSR], Moscow, 1947.
  37. Khichfel'd, V. and Marshall, D., Vliyaniye zatukhaniya na vybor dliny volny dlya radiolokatora nablyudeniya za sostoyaniyem pogody [The Influence of Damping on the Choice of Wave Lengths for Weather Radar], Proceedings of the JEE, July, 1954.
  38. Primeneniye radiolokatora dlya izmereniya kolichestva vypadayushchikh dozhdey [The Use of Radar for Measurement of Quantity of Falling Rain], Vestnik informatsii [Information Herald], No. 18, 1953.
  39. Sheppard. Radiometeorology, Nature, Vol. 157, No. 4000, June, 1946.
  40. Booker, A.G., Elements of radiometeorology, The Journal of the Institute of Electr. Engineers, Vol. 93, Part III, A, Radiolocation, No. 1, 1946.

41. Andrew W. Clement, Seacoast Artillery Radar, Coast Artillery Journal, May-June, 1948.
42. Perlat, A., Voge, I., Attenuation des ondes, centimetriques et millimetriques dans l'atmosphere [Attenuation of centimeter and millimeter waves in the atmosphere], Annales des Telecommunications [Annals of Telecommunications], No. 12, December, 1953.
43. Hooper, E.V., Kippax, A.A., Radar echoes from meteorological precipitation. Proc. 1, R, E, Vol. 97, No. 105, May, 1950.
44. Weiller, P.G., The radar equation, Electronics, Apr. 1945.
45. Appleton, Edw., Extra-tropospheric Influences on Ultra-Short Wave Radar Operation, J.I.E.E., part III, Vol. 93.
46. John F. Bachman, M.T.J. in Radar Systems and the Doppler Myth. Tele-Tech. and Electronic Industries, April, 1953.
47. Electronics Covers the Weather, Electronics, July, 1954.
48. Proc. of Conference on Radio Meteorology, Nov., 1953.
49. Air Force Times, Sept, 1951.
50. Cloud Base and Top Indicators, Electronics, Vol. 23, Dec., 1950.
51. Inter-Avia, Sept., 1955.
52. Ibid, July, 1953.
53. Ibid, Dec., 1950.
54. Amer. Aviation Daily, 25 July, 1955.
55. Wheelon Alb. D., Relation of Radio Measurements to the Spectrum of Tropospheric Dielectric Fluctuations. Journal of Applied Physics, Vol. 28, No. 6, June, 1957.
56. Tolbert, C.W., Straiton, Deformation Measurements with Centimeter Radio Waves, Proc. of Soc. for Experimental Stress Analyzers, Vol. 11, No. 2, 1954.
57. Iamada, R., On the wave propagation in a stratified atmosphere,

- Journ. Phys. Soc. Japan, Vol. 12, No. 9, IX, 1957.
58. Kitchen, F.A., Richmond, I.J., Some Characteristics of Ion Distance Scatter Transmission via tropospheric Scatter., Brit. Communications and Electronics, Vol. 4, No. 3, III, 1957.
  59. Saxton, J., Kreilsheimer, K.S., Luscombe, G.W., Measurement of Height-Gain at Wavelength. Electronics and Radio Eng., Vol. 34, No. 3, 1957.
  60. Gordon, W., Radio Scattering in the Troposphere Scatter in an atmosphere containing a turbulent layer by elevated turbul. layers, Proc. I.R.E., Vol. 38, Apr. 1950, ibid No. 1, 1955.
  61. Atlas, D., Banks, H., The interpretation of microwave reflections from rainfall. Journal of Meteorology, Vol. 8, No. 5, 1951.
  62. Donaldson, R.I., The measurement of liquid water content by radar, Journal of Meteorology, Vol. 12, No. 3, 1955.
  63. Hitschfeld, W., Bordan, I., Errors inherent in the radar measurement of rainfall at attenuating wavelengths, Journal of Meteorology, Vol. 11, No. 1, 1954.
  64. Fannin, B.M., Jech, K.H., A study of radar errors. Transactions of the Instit. of Radio Engineers - Professional Group on Antennas and Propagat., Vol. A.P. 5, No. 1, 1957.
  65. Twersky, Victor, On Scattering and Reflection Electromagnetic Waves by Rough Surfaces. - ibid.
  66. Plank, V.G., Atlas, D., Paulsen, W.H., The nature and detectability of clouds and precipitation as determined by 1.25 centimeter radar, Journ. of Meteorology, Vol. 12, No. 4, 1955.
  67. Ligda, M., Radar Storm Observation. Compendium of Meteorology, 1951.
  68. Marshall, I., Langill, R., Palmer, W., The measurement of rainfall by radar, Journ. of Meteorology, Vol. 4, 1947.



69. Wexler, R., Swingly, D.M., Radar storm detection, Bulletin of the American Meteorology Society, April, 1947.
70. Wexler, R., Theory and Observation of Radar Storm Detection. Compendium of Meteorology, 1951.
71. Macfarlane, G.G., Application of a Variational Method to the Calculation of Radio Wave Propagation Curves for an Arbitrary Refractive Index Profile in the Atmosphere, Proc. Physical Soc. 61, No. 343, 1948.
72. Stickland, A., Meteorolog. Factors in Radio Wave Propagation. Report of a Conference at the Royal Meteorological Society, London, April, 1946.
73. Sexton, J.A., The dielectric Properties of Water Vapor at Very High Radio Frequencies, *ibid.*
74. Sharpless, W.M., Measurement of the Angle of Arrival of Microwaves, Proc. I.R.E., Vol. 34, No. 11, Nov., 1946.
75. Ryde, J.W., Meteorolog. Factors in Radio-Wave Propagation and Radar. Echoes Produced at Centimeter Wavelengths by Various Meteorological Phenomena, London, Physical Society, 1947.
76. Radar in Meteorology, "Research" Vol. 6, No. 11, 1953.
77. Harris, K.E., Some problems of secondary surveillance radar systems, Journ of the Brit. Instit. of Radio Eng., Vol. 16, No. 7, 1956.
78. Mentzer, J.R., Scattering and diffraction of radio waves, R. Pergamon Press, London and New York, 1955.
79. Battan, L.I., Radar Meteorology. The University of Chicago Press, 1959.
80. Atlas, D., The Estimation of Cloud Parameters by Radar, Journ. of Meteorology, Vol. 11, No. 4, August, 1954.
81. Keigler, J.E. and Krawitz, L., Weather Radar Observations from an

Earth Satellite. Journ. of Geophysical Research, Vol. 65, No. 9,  
September, 1960.

82. Amerikakanskiye i angliyskiye radionavigatsionnyye sistemy  
[American and English Radar Navigation Systems], Translated from  
the English and Edited by A.A. Tankov, Voenizdat MVS SSSR,  
Moscow, 1948.

# DISTRIBUTION LIST

DEPARTMENT OF DEFENSE	Nr. Copies	MAJOR AIR COMMANDS	Nr. Copies
		AFSC	
		SCFDD	1
		DDC	25
HEADQUARTERS USAF		TDBTL	5
		TDRDP	6
AFCIN-3D2	1	AEDC (AEY)	1
ARL (ARB)	1	SSD (SSF)	2
		APGC (PGF)	1
		ESD (ESY)	1
OTHER AGENCIES		RADC (RAY)	1
		AFSWC (SWF)	1
CIA	1	ASD (ASYIM)	1
NSA	6	AFMTC (MTW)	1
DIA	9		
AID	2		
OTS	2		
AEC	2		
PWS	1		
NASA	1		
ARMY (FSTC)	3		
NAVY	3		
NAFEC	1		
RAND	1		
SPECTRUM	1		